Acyl-CoA Dehydrogenases: Mechanistic studies on Medium Chain Acyl-CoA Dehydrogenase

Dissertation

zur Erlangung des akademischen Grades des
Doktors der Naturwissenschaften
(Dr. rer. nat.)
an der Universität Konstanz
(Fachbereich Biologie)

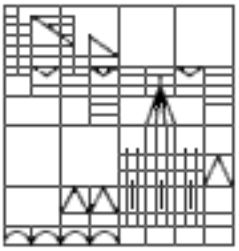

vorgelegt von
Vasile Robert Gradinaru
Konstanz, im Juni 2005

Tag der mündlichen Prüfung : 9. November 2005

Referent: Prof. Dr. Sandro Ghisla

Referent: Prof. Dr. Peter Macheroux

Acknowledgements

I am greatly indebted to my supervisor, Prof. Dr. Sandro Ghisla, for his advice and support. He has been an excellent supervisor providing insightful comments and constructive criticism throughout this PhD project.

I would also like to thank my colleagues in the Universities of Konstanz and Iasi for their advice, encouragement and friendship, without which I would certainly not have completed this thesis. In particular, I would like to thank Prof. Dr. Richard Schowen, Prof. Dr. Peter Macheroux, Prof. Dr. Colin Thorpe, Prof. Dr. Jung-Ja. Kim, Prof. Dr. Tatiana Nicolaescu, Prof. Dr. Constantin Ciugureanu, Prof. Dr. Robert Bach, Dr. Olga Dmitrenko, Susanne Feindler-Boeckh, Gudrun Vogt, Elmi Leisner, Karl Janko, Lili Smau, Nasser Ibrahim, Phaneeswara Rao Kommoju, Sudarshan Rao Ande, Lakshminarayana Kaza, Cosmin Pocanschi, Paula Bulieris for their active interest during the course of this project. My gratitude also goes to Prof. Alexandru Cecal for encouraging me to embark on this PhD.

I express my loving thanks to my wife Luiza whose love, support, patience and understanding made this work easier.

Above all, I wish to express my sincerest gratitude to my parents, who made my studies possible and who have always encouraged me.

This study was financiarlly supported by the Deutsche Forschungsgemeinschaft (Gh 2/6-4).

Parts of this study are to be published or have been published:

1 **Gradinaru, R.***,* Kieweg, V., Küchler, B. & Ghisla, S. (2002) On the role of the 376-functional group in catalysis by medium chain acyl-CoA-dehydrogenase. In *Flavins and Flavoproteins.* Proceedings of the 14th International Symposium, Cambridge, UK (Chapman, S., Perham, R., Scrutton, N., eds.), Agency for Scientific Publishers, Berlin, pp.193-198.

2 ***Gradinaru*, R.**, Dmitrenko, O., Lakshmi Narayana, K., Bach, R. D. & Ghisla, S. (2005) Role of the active center Thr168-flavinN(5) H-bond in MCAD catalysis, In *Flavins and Flavoproteins.* Proceedings of the 15th International Symposium (17-25 April, Shonan-Japan) in press.

3 **Gradinaru, R.**, Kieweg, V., Schowen, R. & Ghisla, S. (2005) Human Medium-Chain Acyl-CoA Dehydrogenase, Proton Inventory Studies on the Dehydrogenation Mechanism of the Glu376Gln Mutant (Biochemistry).

4 **Gradinaru, R.***,* Dmitrenko, O., Bach, R. D. & Ghisla, S. (2005) Mechanisms and properties of medium-chain acyl-CoA dehydrogenase: Role of the active center Thr168-flavinN(5) H-bond in catalysis (Biochemistry).

5 **Gradinaru, R.***,* Dmitrenko, O., Bach, R. D. & Ghisla, S. Mechanisms and properties of medium-chain acyl-CoA dehydrogenase: Role of the active center Thr136-flavinN(1) H-bond in catalysis (manuscript under preparation).

ABBREVIATIONS

ACADs	Acyl-CoA dehydrogenases
ATP	Adenosine triphosphate
bp	Basepairs
BSA	Bovine serum albumine
CoA	Coenzyme A
C_4CoA	Butyryl-CoA
C_6CoA	Hexanoyl-CoA
C_8CoA	Octanoyl-CoA
C_{10}CoA	Decanoyl-CoA
C_{12}CoA	Lauroyl-CoA
C_{14}CoA	Myristoyl-CoA
C_{16}CoA	Palmitoyl-CoA
C_{18}CoA	Stearoyl-CoA
C_{20}CoA	Arachidoyl-CoA
CPT I	Carnitine palmityol transferase I
DAAO	D-Amino-Acid Oxidase
ε	Extinction coefficient
ETF	Electron transfer flavoprotein
ETF:QO	ETF:coenzyme Q oxidoreductase
FAD	Flavinadenindinucleotide
FcPF6	Ferriceniumhexafluorphosphate
FMN	Flavinmononucleotide
FPLC	Fast protein liquid chromatography
HPLC	High performance liquid chromatography
IPTG	Isopropyl-β-D-1-Thiogalactopyranoside
LCAD	Long Chain Acyl-CoA Dehydrogenase
K_a	Acidity constant
$K_{d,\,app}$	Apparent dissociation constant
KDa	Kilo Dalton
KPi	Potassium phosphate buffer
K_m	Michaelis-Menten constant
MW	Molecular weight
MCAD	Medium Chain Acyl-CoA Dehydrogenase
MCADD	Medium Chain Acyl-CoA Dehydrogenase Deficiency
PCR	Polymerase chain reaction
SCAD	Short Chain Acyl-CoA Dehydrogenase
SIDS	Sudden Infant Death Syndrome
SDS	Sodium Dodecyl Sulfate
SDS-PAGE	SDS Polyacrylamide Gel Electrophoresis
TO	Turnover Number
VLCAD	Very Long Chain Acyl-CoA Dehydrogenase
V_{max}	Maximum velocity

SHORT HAND SYMBOLS FOR AMINO ACIDS

One letter	Three letter	Amino Acid
A	Ala	Alanine
R	Arg	Arginine
N	Asn	Asparagine
D	Asp	Aspartic acid
B	Asx	Asn or Asp
C	Cys	Cysteine
Q	Gln	Glutamine
E	Glu	Glutamic acid
Z	Glx	Gln or Glu
G	Gly	Glycine
H	His	Histidine
I	Ile	Isoleucine
L	Leu	Leucine
K	Lys	Lysine
M	Met	Methionine
F	Phe	Phenylalanine
P	Pro	Proline
S	Ser	Serine
T	Thr	Threonine
W	Trp	Tryptophan
Y	Tyr	Tyrosine
V	Val	Valine

ZUSAMMENFASSUNG

Acyl-CoA Dehydrogenasen bilden eine Familie von Flavoproteinen, welche die α,β-Dehydrogenierung von Fettsäure-CoA Thioester. Die sogenannte "Medium Chain Acyl-CoA Dehydrogenase (MCAD) ist eines der am besten untersuchten Mitglieder dieser Familie. Die α,β-Dehydrogenierung beinhaltet die konzertierte Spaltung der α- und β-C-H Bindunges des Substrates. Dies geschieht indem eine Base am Aktivzentrum, Glu376-COO^-, das α-H als Proton abspaltet. Damit gekoppelt ist die Übertragung eines Hydrids aus der Substrat β-Stellung auf die Flavin N(5) Funktion. In meiner Dissertation habe ich verschiedene Aspekte der Katalyse durch die MCAD untersucht. Hierzu wurde u.A. auch eine Mutante der MCAD erzeugt, die am C-Terminus einen sog. "His Tag" trägt. Dies erleichtert die Reinigung von heterolog exprimiertem Protein. Zur Untersuchung des Mechanismus wurden vor allem Mutanten der E376- und der E99-Funktionen eingesetzt. Letztere befindet sich "am Boden" des Aktivzentrums und es wurde davon ausgegangen, dass es Ionisationsvorgänge innerhalb des Aktivzentrums beeeinflusst. Ein wesentlicher Teil der Studien betraf die E376Q-MCAD Mutation. Diese Mutante sollte eigentlich "tod" sein, denn das Glutamin hat keine basische Funktionen. Allerdings zeigt sie eine "residual "activity" im Bereiche von 1/100000 verglichen mit wtMCAD. Dies ist zwar ein kleiner Wert, ist jedoch um eine gleiche Grössenordnung grösser als die unkatalysierte Reaktion. Zum Studium des Mechanismus der Reaktion, die durch diese Mutante katalysiert wird, wurde die sog. "proton inventory technique" eingesetzt. Zudem wurde ermittelt, dass die Geschwindigkeit dieser Reaktion linear mit dem pH zunimmt. Dies legt eine Beteiligung von HO^- nahe. Eine Vergleichbare Abhängigkeit wurde mit der Glu376Gln+Glu99Gly-MCAD Mutante beobachtet. Dies schliesst eine Beteiligung von Glu99 bei der Reaktion aus. Die E376Q-MCAD Mutante zeigt einen aussergewöhnlich grossen Lösungsmittelisotopeneffekt ≈ 8.5. Dies wird der Versänderung mehrerer H-Brücken im Verlaufe des Schrittes zugeschrieben.

Eine weitere Untersuchung betrifft die Rolle einer “speziellen” Wasserstoff-brückenbindung zwischen N(5) des Flavinkofaktors und Thr168-OH. Eine funktionelle Gruppe, die eine ähnliche H-Brücke ausbilden kann ist inerhalb der ACAD-Familie konserviert (Thr oder Ser). Mit der T168A-MCAD Mutante, bei der diese H-Brücke nicht ausgebildet werden kann, sind zwei Arten von Effekt beobachtet worden: a) Einen Einfluss auf die Aktivierung des Substrates und auf das Redoxpotential des Flavins sowie b) eine Rolle bei der Optimierung der Orientierung zwischen substrat und Flavin. Ein weiteres Threonin (Thr136) moduliert das Redoxpotential des Flavins (≈ -30 mV im Vergleich zu wtMCAD =>1.4 $Kcal \cdot M^{-1}$). So wird z.B. bei der Thr136Ala Mutante der Kofaktor nur noch teilweise reduziert, was auf die Erniedrigung des Redoxpotentials zurückgeführt wird. Diese Experimente wurden durch theoretische Berechnungen unterstützt, die durch die Gruppe um Prof. R. Bach (Univ. Delaware, USA) durchgeführt wurden.

SUMMARY

Acyl-CoA dehydrogenases constitute a family of flavoproteins that catalyze the α,β-dehydrogenation of fatty acid acyl-CoA thioesters. Medium chain acyl-CoA dehydrogenase (MCAD) is one of the best-studied members of this family. The α,β-dehydrogenation reaction involves the concerted C-H bonds cleavage of the substrate. First, the active site base, Glu376-COO^-, removes a proton by and then a hydride is transferred to the flavin N(5) position of FAD. In my thesis MCAD several mechanistic details of the dehydrogenation reaction for MCAD were investigated. For this, among other things, a mutant of MCAD was created, which carries a C-terminal "His Tag". Addition of affinity His Tag facilitates purification of recombinant MCAD. For the investigation of the mechanism above several E376- or/and E99-MCAD mutants were used. Last one received an earlier attention since the Glu99 is located underneath of the active site of MCAD. This residue affects ionizations inside the active center cavity. Many studies were focused on E376Q-MCAD mutant. This mutant was highly inactive, because the glutamine does not play the role of the base. However its residual "activity" is 1/100000 of that of wtMCAD. This is a small value, but has the same order of magnitude as those found in non-catalyzed reactions. Proton inventory technique was suitable for mechanistic study of this mutant. Apart from this, it was observed that the log of rates of dehydrogenation increases linearly with the pH suggesting HO^- as a reactant. A similar dependence was observed with Glu376Gln+Glu99Gly-MCAD. Thus, activity and reduction studies exclude Glu99 as a candidate for proton abstraction in the first step of dehydrogenation. E376Q-MCAD mutant reflected a large unexpected solvent isotope effect of ≈ 8.5. The large isotope effects resulted from proton inventory experiments are attributed to the change in state of several H-bonds that occur during the process.

A further investigation concerns the role of a "special" H-bond between N(5) of the flavin cofactor and Thr168-OH. However, an amino acid functional group that forms such a

H-bond is strictly conserved in the ACAD familily (Thr or Ser). In the absence of this H-bond (T168A-MCAD) two effects could be observed: a) electronic – influence on the substrate activation as well as on the redox potential of the flavin; b) steric - this H-bond is involved in the fine-tuning of the orientation of the flavin cofactor and ligand. Another threonine residue (Thr136) modulates the redox potential of the flavin (≈ -30 mV compared to wtMCAD 1.4 Kcal·M^{-1}). Thus e.g. with the Thr136Ala mutant the cofactor was partially reduced by the substrate, which is attributed to decrease of the redox potential. These experiments were supported by theoretical calculations, which were accomplished by Olga Dmitrenko working at Univ. of Delaware (USA) in Prof. R. Bach group.

TABLE OF CONTENTS

1. INTRODUCTION

1.1. General introduction

1.1.1 Fatty acid synthesis and use

Fatty acid synthesis takes place in the cytoplasm of cells (compared to ß-oxidation, which occurs inside the mitochondria). The process begins with acetyl-CoA and cyclic reactions add two-carbon units to the growing fatty acid chain. Completion of the synthesis and the formation of unsaturated fatty acids are complex. The role of fatty acid synthesis is to supply the body's needs for particular fatty acids not supplied in the diet and to convert excess dietary glucose to fatty acids for storage. Glucose is converted to pyruvate (glycolysis), then to acetyl-CoA for which ATP is required, is oxidized in the citric acid cycle. If the glucose intake exceeds the body's energy needs (and after saturation of glycogen stores) the acetyl-CoA can be used for fatty acid synthesis (in the liver) and storage as triglyceride in the adipose tissue. Triglycerides make up about 70 % of the body's energy reserve; they yield a large amount of energy when they are oxidized (40 kJ/g triglyceride). Fatty acids are an important metabolic fuel particularly for muscle tissue. They are used by all tissues (except the brain) under normal dietary circumstances and are used exclusively by some tissues under altered dietary conditions such as starvation.

1.1.2. Storage and mobilisation of fatty acids

Dietary fat (which is digested and then resynthetized into triglycerides) is non-polar and must be transported in form of lipoproteins. The protein molecules provide a polar coat for the non-polar lipid and thus enable transportation in the polar (water based) bloodstream. Chylomicrons are assembled in the intestinal mucosa as a means to transport dietary cholesterol and triacylglycerols to the rest of the body. Storage in the adipose tissue is catalysed by the lipoprotein lipase, the activity of which is stimulated by insulin, the same hormone that stimulates storage of glucose as glycogen. Free fatty acids promote insulin secretion in an acute phase (G-protein coupled receptor, GPR40, which is

abundantly expressed in the pancreas, function as a receptor for long chain free fatty acids) (Itoh et al., 2003). Human serum albumin (HSA) is an abundant plasma protein that is responsible for the transport of fatty acids (Bhattacharya et al., 2000) to various tissues and then oxidized.

1.1.3. Mammalian mitochondrial ß-oxidation

ß-Oxidation is the major process by which fatty acids are oxidized, thus providing a source of energy for heart and skeletal muscle (Felig & Wahren, 1975). Hepatic ß-oxidation serves a different role by providing ketone bodies (acetoacetate and ß-hydroxybutyrate) to the peripheral circulation.

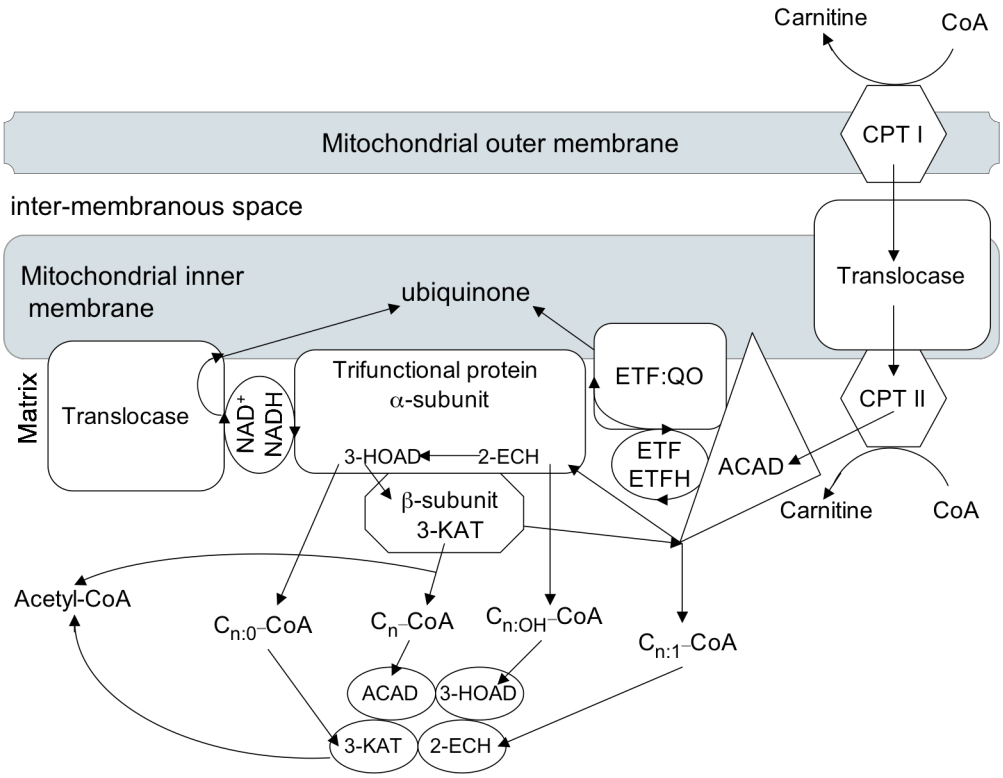

Scheme 1. Enzymes of mitochondrial ß-oxidation (Adapted from (Zhang et al., 2002)). C_n, refers to number of carbon atoms; 2,3-enoyl-CoA esters are indicated by the $C_{n:1}$; 3-hydroxy-acyl-CoA esters are indicated by $C_{n:OH}$ and 3-oxoacyl-CoA esters by the $C_{n:O}$, 2-ECH refers to 2-enoyl-CoA hydratase; 3-HOAD refers to 3-hydroxyacyl-CoA dehydrogenase; 3-KAT refers to 3-oxoacyl-CoA thiolase.

Ketone bodies are an important fuel for extra-hepatic organs, especially the brain, when blood glucose levels are low. For this reason, ß-oxidation is stimulated when glucose

levels are low, for instance during starvation or endurance exercise, essentially as postulated in the Randle cycle.

The enzymes of ß-oxidation all act on CoA esters (Scheme 1), so a prerequisite to ß-oxidation is the ATP-dependent formation of fatty acyl-CoA esters that is catalysed by acyl-CoA synthase. Several acyl-CoA synthases are associated with mammalian mitochondria. Of these, the short-chain acyl-CoA synthases are found within the matrix and are important in ruminants (Bergman et al., 1965). Two medium-chain acyl-CoA synthases are also found in the mitochondrial matrix (Mahler et al., 1953; Killenberg et al., 1971). Long-chain acyl-CoA synthase activity is found in the mitochondrial outer membrane and it appears to be a transmembrane protein with at least the CoA-binding domain on the cytosolic face (Hesler et al., 1990).

Hepatic CPT I (the outer CPT) has been purified and immunologically characterized as distinct from CPT II (the inner CPT) (Kolodziej et al., 1992) and has been cloned and sequenced, allowing expression in yeast and demonstration of malonyl-CoA binding by the catalytic polypeptide (Brown et al., 1994). Carnitine/acylcarnitine translocase has the capacity for unidirectional transport of carnitine (Indiveri et al., 1991).

There are multiple enzymes for each of the constituent steps of the pathway, which vary in their chain-length specificity. In the case of acyl-CoA dehydrogenation there are five enzymes: short-chain acyl-CoA dehydrogenase (SCAD, active with C_4 and C_6), medium-chain acyl-CoA dehydrogenase (MCAD, active with C_4 to C_{12}), long-chain acyl-CoA dehydrogenase (LCAD, active with C_8 to C_{20}) and two very-long-chain acyl-CoA dehydrogenases (vLCAD, active with C_{12} to C_{24}). Each of these enzymes catalyses the formation of 2-enoyl-CoA from the corresponding saturated ester. SCAD, MCAD and LCAD are homotetramers located in the matrix. VLCAD, however, is a homodimer and is located in the inner mitochondrial membrane. Until recently it had been assumed that there are only three ACADs involved in mitochondrial ß-oxidation: SCAD, MCAD and LCAD. However, the isolation and purification of vLCAD (Izai et al., 1992), and the demonstration that patients previously thought to have inherited deficiencies of LCAD were in fact suffering from vLCAD deficiency, has shown that there are in fact five enzymes. Recently, another gene, ACAD-9 encoding a protein with dehydrogenase activity on palmitoyl-CoA, has been reported (Zhang et al., 2002). Additional

dehydrogenases with homology to MCAD are isovaleryl-CoA dehydrogenase (iVD), 2-methyl branched-chain acyl-CoA dehydrogenase (i2VD) (Andresen et al., 2000; Gibson et al., 2000), and isobutyryl-CoA dehydrogenase (iBD) (Nguyen et al., 2002).

MCAD is the best-characterized member of the ACAD family. The mechanism of the action of this group of flavoproteins appears to be very similar, with the concerted removal of the pro-R-α-hydrogen from the acyl-CoA as a proton and elimination of the corresponding pro-R-ß-hydrogen to the N-5 position of the flavin as a hydride equivalent (Scheme 3).

Reoxidation of the FAD prosthetic group of the ACADs requires a matrix FAD-linked protein, the ETF (Hauge et al., 1956) which in turn passes reducing equivalents to ETF:ubiquinone oxidoreductase (ETF:QO) (Ruzicka & Beinert, 1977) and thence to the mitochondrial respiratory chain at the level of ubiquinone. ETF contains 1 mol of bound FAD per mol of dimer (Furuta et al., 1981), and ETF:QO is a 68 kDa iron-sulphur flavoprotein of the inner membrane (Ruzicka & Beinert, 1977; Beckmann & Frerman, 1985). There are four 2-enoyl-CoA hydratases: very long-, long-, medium-, short-chain-2-enoyl-CoA (crotonase is a homohexamer and most active towards C4 substrates).

Third step of the pathway is the oxidation of L-3-hydroxyacyl-CoA by NAD^+, catalysed by two enzymes (L-3-hydroxyacyl-CoA dehydrogenases) with overlapping chain-length specificities. The short-chain enzyme is a soluble matrix enzyme, which will act on substrates of chain-length C_4 to C_{16} although. A long-chain 3-hydroxyacyl-CoA dehydrogenase is firmly associated with the inner mitochondrial membrane and is active with medium- and long-chain substrates bigger than C_{16}.

The final step of the β-oxidation cycle is catalyzed by three enzymes, which create acetyl-CoA and an acyl-CoA chain shortened by two carbon atoms. Two soluble activities have been identified. One is specific for acetoacetyl-CoA and 2-methyl-acetoacetyl-CoA. The second is active with all substrates from C_6 to C_{16} to an approximately equal extent (Staack et al., 1978). The third is trifunctional enzyme, which also comprises the long-chain 2-enoyl-CoA hydratase and long-chain 3-hydroxyacyl-CoA dehydrogenase activities.

The trifunctional protein complex, a heterooctamer made up of four α-units with long-chain-enoyl-CoA hydratase and 3-hydroxyacyl-CoA dehydrogenase activities and

4 ß-units with long-chain 3-oxothiolase activity, is closely associated with the inner mitochondrial membrane (Uchida et al., 1992).

1.1.4. Intramitochondrial control of ß-oxidation

As mitochondrial ß-oxidation consists of several enzymes of overlapping chain-length-specificities, some of which are membrane bound (the trifunctional protein and VLCAD) and transferring equivalents to the respiratory chain, the possibility of supramolecular organization of the ß-oxidation enzymes and auxiliary systems should be considered. The ACADs appear to have by far the lowest activity of the enzymes of ß-oxidation in rat and human tissues (Melde et al., 1991).

The ACADs have a high affinity for their acyl-CoA substrates and for their enoyl-CoA products, resulting in product inhibition (Powell et al., 1987). In addition, short-, medium- and long-chain ACADs respectively 3-hydroxyacyl-CoA dehydrogenases are inhibited by 3-oxoacyl-CoA esters. The inhibition of 3-oxoacyl-CoA thiolase by acetyl-CoA is a point of potential control of ß-oxidation by the acylation state of mitochondrial CoA. Gerland et al. (Gerland et al., 1965) found that 95 % of intramitochondrial CoA was acylated during maximal ß-oxidation flux, so that a small amount of free CoA is sufficient to sustain ß-oxidation. ß-Oxidation is linked to the respiratory chain at two stages: one is 3-hydroxyacyl-CoA dehydrogenase via complex I via NAD^+/NADH, and the second at the level of the ACADs via ubiquinone, ETF and its oxidoreductase. Inhibition at these stages leads to inhibition of ß-oxidation. ETF-semiquinone, a partially reduced form of ETF, can accumulate when the ubiquinone pool is reduced, but disproportionates to the fully oxidized and reduced forms in a reaction catalysed by ETF:QO. Hence the activity of ACADs could be responsive to the redox state of the ubiquinone pool via ETF and ETF-semiquinone or by complex I and accumulation of 3-hydroxyacyl-CoA esters (which will lead to accumulation of 2-enoyl-CoA esters and inhibition of the ACADs) (Beckmann et al., 1981).

1.2. Flavoproteins

1.2.1. Introduction and history

Old yellow enzyme was isolated from brewer's bottom yeast by Warburg and Christian (1932) during attempts to elucidate the nature of biological oxidations. Glucose 6-phosphate was oxidized by methylene blue in presence of two components of erythrocytes, an enzyme and a small, heat-stable „co-ferment". Following this, Warburg identified a yellow enzyme that permitted the system to form a complete respiratory chain-reacting with molecular oxygen. Following the isolation of the second yellow enzyme from yeast by Haas (1938), Warburg's enzyme was termed „Old Yellow Enzyme" (OYE), a name that has persisted to this day. OYE was purified by Theorell in 1935 (Theorell, 1935), and shown to consist of a colourless apoprotein and a yellow dye (riboflavin 5'-phosphate or FMN), both essential for enzyme activity. OYE has been characterized in detail by Vincent Massey's laboratory (Matthews et al., 1975). The physiological reductant of OYE is assumed to be NADPH and substrates capable of reoxydizing OYE include methylene blue, Fe^{3+}, quinones, cytochrome c and ferricyanide. Reoxidation can be brought about by molecular oxygen to yield hydrogen peroxide and superoxide. Only □,ß-unsaturated aldehydes and ketones (cyclic enones) are substrates (acids, esters and amides did not react). The crystal structures of the oxidized and reduced forms of OYE, and for the complex with the phenolic inhibitor p-hydroxy-benzaldehyde were solved at 2 Å (Fox & Karpus, 1994).

Flavoproteins commonly contain one of two prosthetic groups, FMN or FAD. The FMN is non-covalently bound in all known cases. FAD may be non-covalently bound (*e.g.* in dihydrolipoamide dehydrogenase (NADH), EC 1.8.1.4 and MCAD) or covalently bound to the flavin moiety via an amino acid residue, such as cysteine, histidine or tyrosine, (*e.g.* succinate dehydrogenase, EC 1.3.99.1). 8-Hydroxy-pyrimidino[4,5-*b*]quinoline-2,4-dione (8-hydroxy-5-deazaflavin) functions as prosthetic group in methanogens and in deoxyribodipyrimidine photolyase (EC 4.1.99.3). Apart from a few exceptions where the role of the flavin is not clear, *e.g.* tartronate-semialdehyde synthase (EC 4.1.1.47), flavoproteins carry out oxidation-reduction reactions, in which one substrate is oxidized and a second is reduced. For all these enzymes each catalytic cycle

consists of two distinct processes, the acceptance of redox equivalents from a reducing substrate and the transfer of these equivalents to an oxidized acceptor. Accordingly, the catalysed reactions consist of two separate half-reactions: a reductive half-reaction in which the flavin is reduced and an oxidative half-reaction, in which the reduced flavin is reoxidized. The nature of the substrate involved in the two separate half-reactions has been used as the basis for a scheme in which five broad classes of flavoenzymes are defined (Hemmerich et al., 1972):

a) Transhydrogenase, where two-electron equivalents are transferred, along with the appropriate hydrogen ions, from one organic substrate to another.

b) Dehydrogenase-oxidase, where two-electron equivalents are transferred to the flavin from an organic substrate, where molecular oxygen is the oxidizing substrate, being reduced to H_2O_2.

c) Dehydrogenase-monooxygenase, where the flavin is reduced, generally by a reduced pyridine nucleotide, and where in oxidation with O_2 in the presence of a cosubstrate one atom of oxygen is inserted into the cosubstrate, while the other is reduced to H_2O.

d) Dehydrogenase-electron transferase, where the flavin is reduced by 2-electron transfer from a reduced substrate and then reoxidized in sequential single electron transfers to acceptors, such as cytochromes and iron-sulfur proteins. An example is the NADPH cytochrome-*b*5 reductase (EC 1.6.2.2). This class might be further subdivided to distinguish those enzymes which are functioning in the reverse sense, *i.e.*, those which receive electrons one at a time and then transmit them in a two-electron step in the reduction of a pyridine nucleotide. An example is ferredoxin NADP+ reductase (EC 1.18.1.2).

e) Electron transferase, where the flavin is reduced and reoxidized in 1-electron steps. There are two examples. The first is the so-called electron-transfer flavoprotein that catalyses the transfer of electrons from another enzyme, namely butyryl-CoA dehydrogenase (EC 1.3.99.2), acyl-CoA dehydrogenase (EC 1.3.99.3), sarcosine dehydrogenase (EC 1.5.99.1) or dimethylglycine dehydrogenase (EC 1.5.99.2), to the respiratory chain. The second is flavodoxin, a group of flavoproteins of low potential that catalyse electron transfer between two other redox proteins as part of photosynthetic, nitrogen- or sulfate-reducing or hydrogen-evolving systems.

1.2.2. Acyl-CoA dehydrogenases

The first representatives of this family of enzymes were discovered in the 1950s in the course of the elucidation of the pathway of ß-oxidation of long-chain fatty acids by the group of Lynen in Munich, respectively Lardy and Green at Madison (Wisconsin). This pathway progressively breaks down C18 and C16 fatty acyl chains, 2 carbon units at a time.

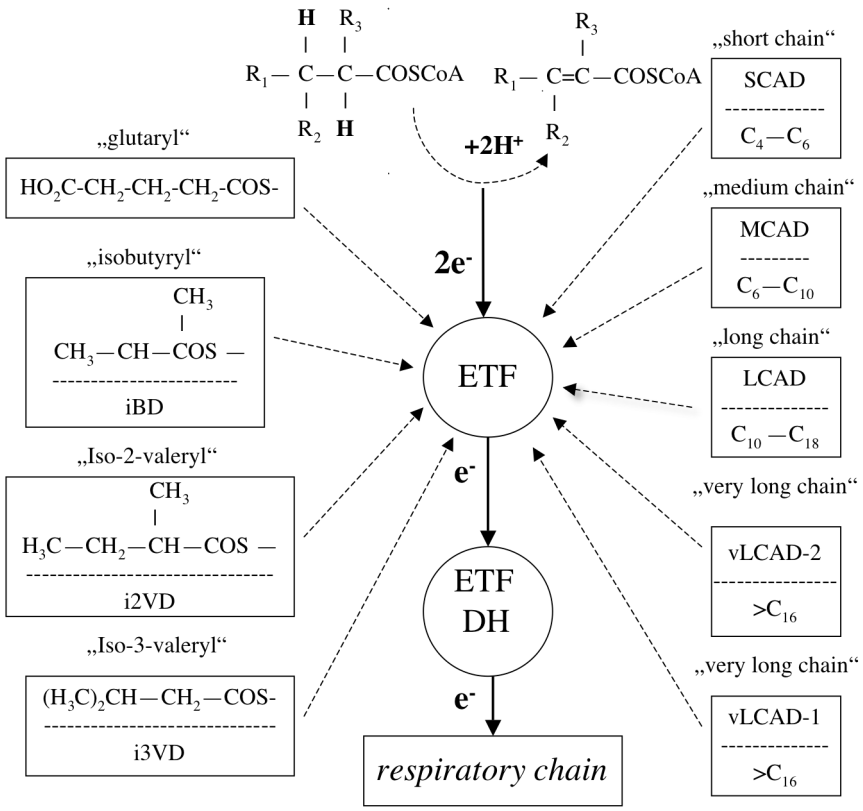

Scheme 2. Reoxidation of Acyl-CoA-Dehydrogenases. ETF is the electron acceptor for nine primary dehydrogenases. Adapted from (Thorpe, 1990).

Several acyl-CoA dehydrogenases have been described: very long (two members), long, medium, short and branched short-chain acyl-CoA dehydrogenases (iso-2- and iso-3-valeryl, isobutyryl and glutaryl). The first five catalyze the initial reaction in the ß-oxidation of fatty acids, while the last category catalyzes the dehydrogenation of branched short-chain acyl-CoAs in the metabolism of branched-chain amino acids. The oxidant in the forward reaction is ETF (electron transferring flavoprotein; Scheme 2) (Toogood et al., 2004). In the mitochondrial ß-oxidation this protein (ETF) in turn feeds

reducing equivalents to a further flavoprotein, which contains an iron-sulfur cluster. This is ETF-dehydrogenase (or ETF-CoQ reductase) which is an integral part of the respiratory chain (Goodman et al., 1994).

1.2.2.1. Mechanisms of reaction

The reductive half-reaction in acyl-dehydrogenases involves abstraction of the *pro*-R-α-proton of bound acyl-CoA thioester with elimination of the *pro*-R-ß-hydrogen as a hydride equivalent and its transfer to the N-5 position of the flavin (the reaction is concerted, Scheme 3) (Pohl et al., 1986; Schopfer et al., 1988; Ghisla & Massey, 1989; Ghisla et al., 1993).

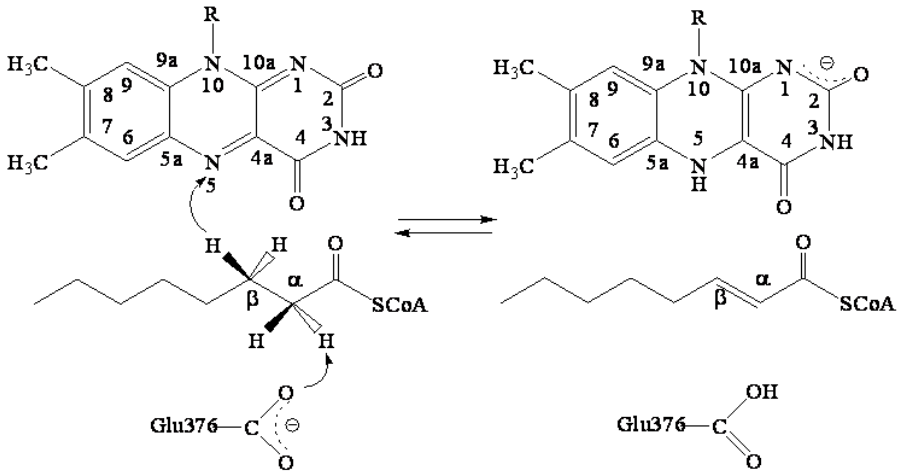

Scheme 3. Chemical mechanism and stereochemistry of acyl-CoA dehydrogenation by acyl-CoA dehydrogenases (Ghisla & Thorpe, 2004)

The transition state for the dehydrogenation reaction has an appreciable enolate character as negative charge migrates from the carboxylate base through the thioester to the flavin prosthetic group (Scheme 4) (Thorpe & Kim, 1988; Engel, 1992; Ghisla et al., 1993; Johnson et al., 1995; Trievel et al., 1995).

An example of the enzyme's ability to stabilize enolates is provided by the intense green complexes observed upon addition of trans-3-enoyl-CoA analogs (Powell et al., 1987) or 3-S-acyl-CoA thioesters (Lau & Thorpe, 1988) to the oxidized dehydrogenase.

The isolation of an active-site peptide from pig kidney Medium Chain Acyl-CoA Dehydrogenase labelled with [1-^{14}C]-2-octynoyl-CoA did suggest that a glutamate (Glu

401) is the base that abstracts the α-proton during dehydrogenation of normal substrates (Powell & Thorpe, 1988). One similar case was inactivation of *M. elsdenii* butyryl-CoA dehydrogenase by 3-pentenoyl-CoA witch leads to derivatization of glutamate residue (the inactivation proceed through enzyme-catalyzed rearrangement of the acetylene to an allene, followed by nucleophilic addition of the carboxylate to the allene) identified by amino acid analysis after reduction with borohydride (Fendrich & Abeles, 1982).

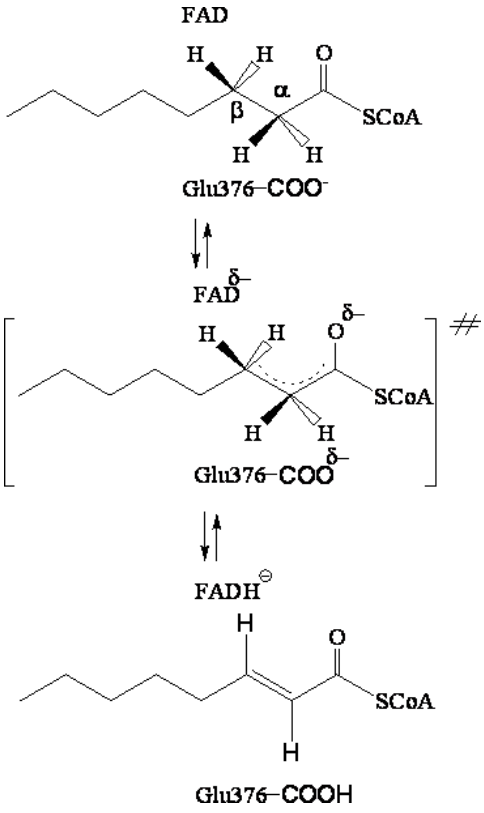

Scheme 4. Acyl-CoA dehydrogenation-transition state (negative charge migrates from the carboxylate base through the thioester to the flavin prosthetic group)

When Glu was mutated to Gln the activity of the purified protein was less than 0.01% that of wild type. The flavin reduction rate of the mutant with the normal substrate (C_8CoA) was five orders of magnitude lower in comparison with wild-type enzyme. This proves that Glu 376 plays an important role in the initial step of dehydrogenation (Bross et al., 1990). A second glutamate group (Glu 99 situated at the bottom of the active site of MCAD) affects the behavior of the ligands and might affect ionizations inside the active center cavity (Küchler et al., 1999).

A crucial step in the dehydrogenation reaction of acyl-CoA dehydrogenase is the mode and extent of activation of αC-H. For efficient catalysis, current concepts assume that microscopic pK_a values of two partners involved in the transfer of one H_3O^+ between them have similar values (Gerlt & Gassman, 1993; Schan et al., 1996). The microscopic pK_a of Glu 376-COO^- has been determined as ≈ 6 in uncomplexed enzyme and 8-9 in complexed enzyme (Ghisla et al., 1994; Vock et al., 1998). The microscopic pK_a of the substrate αC-H should be lowered from an estimated value of ≈ 20 toward ≈ 9 (Amyes & Richard, 1992; Ghisla et al., 1994).

These large effects are induced by two tight H-bonds to the ligand thioester carbonyl oxygen (one with 2'-OH of the ribityl chain of FAD and another with main-chain amide nitrogen atom of Glu376). Polarisation of the specific ligands, due to transfer of charge toward thioester carbonyl group has been deduced using UV-Vis (Engst et al., 1991; Johnson et al., 1992; Trievel et al., 1995) and Raman spectroscopy (Nishina et al., 1992; Nishina et al., 1995; Hazekawa et al., 1997).

1.2.2.2. Three-dimensional structure of MCAD

The three-dimensional structure of MCAD from pig liver mitochondria was solved by Kim and Wu in 1988 at 3 Å resolution an five years later at 2.4 Å resolution (Kim & Wu, 1988; Kim et al., 1993). The MCAD is a dimer of dimers with an overall diameter of about 90 Å (Figure 1).

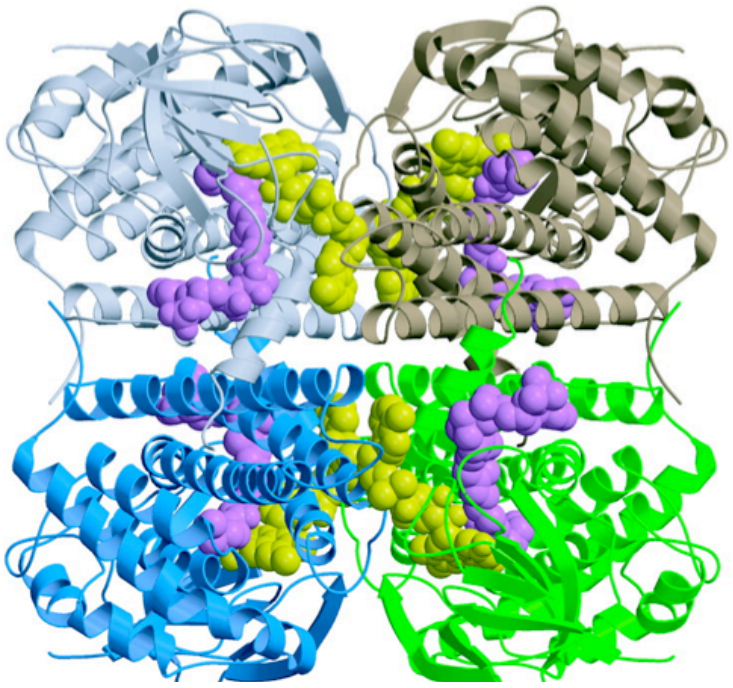

Figure 1. Ribbon diagram of MCAD structure (tetramer) with bound C_8CoA (purple) (Kim & Miura, 2004)

The interface between 2 monomers is extensive and involves the FAD binding sites, whereas contacts between dimers are much more limited (the interactions between the dimers are mainly helix to helix on the equatorial plane). The monomers are folded into three domains of approximately equal size. The N-terminal and C-terminal domains

are mainly □-helices packed together forming the core of the tetrameric molecule, whereas the middle domain is composed of two orthogonal □-sheets. The FAD has an extended conformation. The flavin ring is buried in the crevice between the two □-helical domains and the □-sheet domain of one subunit. The adenosine pyrophosphate moiety is stretched into the subunit junction with a neighbouring subunit, composed of two C-terminal domains.

The pyrimidine portion of the isoalloxazine ring is surrounded by the residues from the loops between the ß-strands and forms hydrogen bonds with polar side chains as well as with the main-chain atoms of the peptide. The dimethyl benzene portion of the ring is surrounded by the loop between the H- and G-helices of the neighbouring subunit and its sinister (*si*) face is partially covered by Trp-166 and Met-165. The substrate associates with the rectus (*re*) face of the flavin, so ETF must interact with the dehydrogenase through the si side of the flavin. Trp-166 and Met-165 might play a role in the transfer of the electrons between the two flavoproteins. There are many polar residues (Arg-210, Glu-212, Arg-223, Arg-164, and Glu-136) lying at the surface of the MCAD molecule around Trp-166 where ETF might bind the enzyme through electrostatic interactions (Beckman & Frerman, 1983).

The adenosine moiety of the FAD makes contacts with the other subunit of the dimer and lies at the surface of the tetrameric molecule. Arg-281 and Gly-353 of the neighbouring subunit make hydrogen bonds with the oxygen atoms of the pyrophosphate, and Thr-263 and Gln-349 make hydrogen bonds with N7 of the adenine ring and 3□-hydroxyl group of the ribose, respectively. The resulting map shows tubular electron densities near the FAD ring and between the ß-sheet domain and the two □-helix domains.

The alkyl chain of the acyl-CoA ligand in the MCAD structure is deeply buried inside the protein, at the *re* side of the flavin, confirming the stereochemistry proposed by Pai and coworkers (Manstein et al., 1986). The binding cavity for the fatty acyl moiety is located between helices E and G (Figure 1) and is lined with the side chains of Glu-376, Tyr-375, Val-259, Thr-168, Leu-103, and Ala-100. Glu-99 and Thr-96 form the bottom of the deep hole where the end of the alkyl chain lies. The $C_{\square}$-$C_{\square}$ bond of the bound ligand molecule is sandwiched between the carboxylate of Glu-376 and the flavin ring, with

distances 4.2-4.6 Å from the C_{α} to the carboxyl oxygens of Glu-376 and ≈ 3.3 Å between the C_{α} and N_5 of the FAD ring.

The binding mode of the CoA moiety to the enzyme is somewhat similar to those observed in citrate synthase (Remington et al., 1982) and in chloramphenicol acetyltransferase (Leslie et al., 1988) in that the pantetheine portion of the molecule is shielded from the bulk solvent, whereas the phosphates lie at the surface of the molecule. The „adenine binding loop“ described in the structure of citrate synthase is not observed in MCAD.

The carboxylate of Glu-376 swings toward the C_{α} atom of the substrate, ready to abstract its proton. Tyr-375 is conserved in all acyl-CoA dehydrogenases sequenced (Matsubara et al., 1989) and the plane of the phenolic side chain is tilted to face rather than to be edge on to the alkyl chain of the substrate. The most pronounced side-chain movement upon binding of the ligand is that of Glu-99, which turns almost 90° making the substrate binding „hole“ deeper. Side chains of Leu-103, Val-259, and Gln-95, which surround the alkyl chain, move away from the bound ligand to make more room. In the native enzyme structure, the active site cavity is filled with a string of well-ordered water molecules. The ribityl 2‑hydroxyl group of FAD is hydrogen bonded to water W-1; waters W-1, W-2, W-3, and W-4, carboxylate oxygens of Glu-99, and water W-5 are connected in series via hydrogen bonds. In the complexed enzyme structure, the string of water beads is broken and W-1 through W-4 are replaced by the fatty acyl thioester moiety of the ligand. The positioning of the ligand is such that the carbonyl oxygen of the thioester occupies roughly the same position that W-1 does in the native structure, Glu-99 moves away to make enough room for the tail end of the fatty acyl chain, and W-5 remains and bonds tightly to the hydroxyl groups of Tyr-372, Tyr-375, and the ‑amide group of Gln-95.

The tight binding of the fatty acyl chain in the active site hole is likely to prevent molecular oxygen from approaching the flavin ring (Kim & Miura, 2004). The displacement of water molecules in the fatty acyl cavity upon substrate binding is in agreement with the hypothesis of Wang and Thorpe (Wang & Thorpe, 1991) who proposed that the protection of the reduced enzyme from molecular oxygen is due to the desolvation of the active site and consequent destabilization of the superoxide anion

formed during reoxidation of the flavin. Since thioethers give 10^{-2} to 10^{-3} times the protection of thioesters, it would be interesting to see whether any water molecule, particularly W-1, remains in the active site when thioether analogues bind to the enzyme. It is tempting to speculate that some of the water „beads“ serve as nucleophiles in the intrinsic hydratase activity of MCAD that is observed with substrates shorter than C_8CoA (Lau et al., 1986).

1.2.2.3. Effect of the Lys304 mutation on oligomer assembly

The prevalent mutation found in patients with MCAD deficiency is a point mutation, A → G, at nucleotide 985 in the MCAD gene, which results in the Lys-304 → Glu substitution (Kelly et al., 1990; Matsubara et al., 1990; Yokota et al., 1990). Lys-304 is located in the middle of the H-helix, forming a hydrogen bond with the δ-carbonyl oxygen of Gln-342 that lies in the I-helix. It lays ≈ 20 Å away from the active site and is not involved in binding of the substrate or FAD. Glu-304 in the mutant protein is also capable of forming a hydrogen bond with the δ-amido-NH_2 of Gln-342. There are two other acidic residues, Asp-300 and Asp-346, within 6 Å of the δ-carboxylate of Glu-304. Furthermore, these residues lie at the dimer-dimer interface of the tetramer. This concentration of negative charge could affect the polypeptide folding and the tetramer formation and result in instability of the enzyme (Bross et al., 1995).

1.2.2.4. Evolution of the acyl-CoA dehydrogenase family

Acyl-CoA dehydrogenases have most likely originated from one ancestral gene (Tanaka & Indo, 1992) and their overall structures are essentially the same. However, the active site of each enzyme has evolved for optimal catalysis of ist specific substrate, while retaining the basic chemical and structural elements (all contain glutamate as an active base) (Kim & Paschke 1999).

1.2.2.5. Interaction of ETF with MCAD

Roberts and others have modelled the docking of ETF to MCAD. In this model, the surface area of interaction between the two proteins is maximized (≈ 3400 $Å^2$), while the flavin-flavin distance is maximized (≈ 19.5 Å). There are at least 13 salt bridges and

several hydrogen bonds formed between ETF molecule and MCAD dimer and the distance between the two FADs could be decrease as much as 3-4 Å. From this model, electrons would pass from MCAD at the *si* side of the FAD ring, since the acyl-CoA ligand is „blocking“ the *re* side (some kinetic studies also demonstrate that enoyl-CoA product is present when MCAD binds ETF) (Roberts et al., 1996). Parker and Engel have suggested that mammalian ETF forms stable, soluble complexes with its partner dehydrogenase. These complexes are present also within the mitochondria where ETF is a component of the electron transport chain (Parker & Engel, 2002).

1.3. Medium-Chain Acyl-CoA Dehydrogenase Deficiency (MCADD)

There are many fatty acid oxidation disorders that can be assigned to the following families:

A. Disorders of Plasma Membrane Functions
- long-chain fatty acid transport/binding defect
- carnitine uptake defect

B. Disorders of Mitochondrial Fatty Acid Transport
- carnitine palmitoyltransferase deficiency
- acylcarnitine translocase deficiency
- carnitine palmitoyltransferase II deficiency

C. Disorders of Long-Chain Fatty Acid ß-Oxidation
- very-long-chain acyl-CoA dehydrogenase deficiency
- trifunctional protein deficiency and isolated long-chain L-3-hydroxy-acyl-CoA dehydrogenase deficiency

D. Disorders of Medium-Chain Fatty Acid ß-Oxidation
- medium chain acyl-CoA dehydrogenase deficiency
- medium- and short-chain L-3-hydroxyacyl-CoA dehydrogenase deficiency
- medium chain 3-ketoacyl-CoA thiolase deficiency

E. Disorders of Short-Chain Fatty Acid ß-Oxidation

F. Further fatty acid oxidation disorders

F.1. Disorders of Ketogenesis

- 3-hydroxy-3-methylglutaryl-CoA synthase deficiency
- 3-hydroxy-3-methylglutaryl-CoA lyase deficiency

F.2. Primary Disorders of Respiration Effecting fatty acids oxidation

- glutaric acidemia type 2 has been linked to mutations in three genes, two coding for ETF-α and β and one for ETF-Q

Since the initial clinical and biochemical reports that date back almost 20 years, MCAD deficiency has emerged as the most frequently encountered disorder of the fatty acids oxidation pathway and overall as one of the most recognizable inborn errors of metabolism.

Fatty acid oxidation fuels hepatic ketogenesis, a major source of energy for peripheral tissues once glycogen stores become depleted during prolonged fasting and periods of higher energy demands. In a typical clinical scenario, a previously healthy child presents with hypoketotic hypoglycaemia, lethargy, seizures, and coma triggered by a common illness. Hepatomegaly and acute liver disease are often present, leading in some cases to a diagnosis of Reye syndrome (characterized by acute non-inflammatory encephalopathy with hyperammonemia, liver dysfunction, and fatty infiltration of the liver). The first acute episode usually occurs before two years of age, but affected individuals may present at any age including adulthood (Raymond et al., 1999). Sudden and unexplained death is often the first manifestation of MCAD deficiency (Iafolla et al., 1994). Rapid clinical deterioration that is disproportionate in the setting of a common and generally benign infection should raise the suspicion of MCAD deficiency or other fatty acid ß-oxidation disorders, and should prompt administration of intravenous glucose and the collection of urine and blood samples for metabolic testing.

A defect of the MCAD enzyme leads to accumulation of medium-chain fatty acids, which are further metabolized to glycine- and carnitine-esters and to dicarboxylic acids. These metabolites are detectable in body fluids (blood, urine, bile) by gas chromatography/mass spectrometry and tandem mass spectrometry. MCAD deficiency meets existing newborn screening criteria (Chace et al., 1997; Charrow et al., 2000). Since the early 1990s, tandem mass spectrometry (MS/MS) has been applied to the analysis of newborn screening blood spots. Today, several states and countries have introduced this technology into their newborn screening programs (Matern, 2002). The

biochemical diagnosis of MCAD deficiency can be confirmed by measurement of the activity of the MCAD enzyme in fibroblasts and other tissues and by molecular genetic testing of the *ACADM* gene (chromosomal locus 1p31).

The K304E (985A—>G) mutation (located in exon 11) of the *ACADM* gene (*ACADM* is a nuclear gene consists of 12 exons that span more than 44 kb and encode a precursor monomer of 421 amino acids) was independently described by four groups (Kelly et al., 1990; Matsubara et al., 1990; Yokota et al., 1990; Gregersen et al., 1991). It is the only prevalent mutation in Caucasians, and is likely due to a founder effect (Tanaka 1997).

Table 1. Frequency by country of homozygosity for Lys329Glu (G985A) MCAD allelic variant

Country of origin	Frequency	Country of origin	Frequency
UK (Birmingham)	1:6,400	Poland	1:38,000
Finland	1:10,000	Germany	1:53,000
Netherlands	1:16,000	Turkey	1:186,000
France (Paris)	1:19,000	Scotland	1:304,000
Russia	1:27,000	Italy	1/442,000
US (Pennsylvania)	1:28,400	Japan	0

Early estimates of the frequency of K304E, based on retrospective clinical studies, were close to 90 % of all alleles investigated (Tanaka et al., 1992; Carpenter et al., 2001; Zytkovicz et al., 2001; Chace et al., 2002). This allele frequency has been confirmed by newborn screening for MCAD deficiency in Northern Europe (Sander et al., 2001).

The first large-scale prospective newborn screening study in the USA shows that the K304E mutation occurs in only 72 % of the alleles (13/18) (Ziadeh et al., 1995). However, less than 1% of sudden infant death cases have this mutation.

Further expansion of newborn screening for MCAD deficiency in diverse populations revealed an allele frequency of 76 % (120/158) and homozygosity for the K304E mutation in 54 % (43/79) of identified patients. Thirty additional mutant alleles, for the most part family-specific mutations, are usually present only in heterozygous form. Testing for non-K304E mutations is presently available only in a limited number of clinical laboratories. The incidence for the K304E mutation of the ACADM gene is described in Table 1 (Wang et al., 1999).

Lys-304 is positioned at the interface between the homotetramer-forming subunits of the enzyme (helix H) and for this reason the folding and tetramer assembly are affected. Tanaka et al. have found seven new mutations (Tanaka et al., 1992). MCAD deficiency is a disease that is prevalent in Caucasians, especially those of Northern European descent. The carrier frequency for the K304E mutation of the *ACADM* gene is between 1:40 and 1:100 (See table 1). The overall frequency of the disease has been estimated to range between 1:4900 to 1:17000, a variability related to the ethnic background of the population studied, only a few African-American and Native-American patients have been reported (no cases confirmed by molecular analysis have been identified in the Asian population).

Andersen et al. have found seven new mutations (Andersen et al., 1997). One of these is a point mutation (A577G) resulting in the replacement of a threonine residue with alanine at position 168 in the amino acid sequence of the mature protein. The T168A mutation constitutes the first case of a modification within the active site of MCAD. Thr-168 is located in contact with the FAD cofactor and forms a hydrogen-bond with the flavin N(5) position (Küchler et al., 1999). Further point mutations (G267R, I375Y, C244R, M149I, C91Y, Y133X, M301T, S331R, R324X, Y327C, G170R, R28C) have been reported for MCAD.

Patients with MCAD deficiency appear normal at birth and usually present between three and 24 months of age in response to either prolonged fasting (e.g., weaning the infant from night time feedings) or intercurrent and common infections (e.g., viral gastrointestinal or upper respiratory tract infections), which typically cause loss of appetite and increased energy requirements when fever is present. Later presentation in adulthood is also possible (Duran et al., 1986). Such instances of metabolic stress lead to vomiting and lethargy, which may quickly progress to coma and death. The episodes may also begin with or be accompanied by seizures. Hepatomegaly is usually present during acute decompensation, which is also characterized by hypoketotic (not necessarily non-ketotic) hypoglycaemia, increased anion gap, hyperuricemia, elevated liver transaminases, and mild hyperammonemia.

Discriminating features of the longer-chain fatty acid ß-oxidation disorders include cardiomyopathy and rhabdomyolysis, neither of which is typically observed in

MCAD deficiency. Ketogenesis defects, urea cycle disorders, organic acidurias, respiratory chain defects, and inborn errors of carbohydrate metabolism (e.g., hereditary fructose intolerance) may also present with a Reye-like syndrome. Biochemically, the same diagnostic markers seen in MCAD deficiency are also elevated in glutaric acidemia type 2, but the presence of several additional organic acids (glutaric acid, 2-hydroxy glutaric acid, ethyl malonic acid), C4 and C5 carnitine and glycine esters (Millington et al., 1992), and the normal excretion of phenylpropionylglycine (Rinaldo et al., 1988) are important elements for the differential diagnosis.

Recently, Filiano and Kinney have been proposed a triple risk model for the occurrence of SIDS in which the syndrome occurs during a critical developmental period in vulnerable infants subjected to an exogenous stressor (Kinney et al., 2003). Sleeping face down is considered one such a stressor. Another risk factors include mother's smoking and alcohol consumption during pregnancy. It has been found that the number of serotonin receptors is lower than normal in the brains of SIDS victims, leading to conclusion that the development of an abnormal serotonergic system may put an infant at increased risk of developing the disorder (Kinney et al., 2003). Richerson thinks that a large subset of SIDS is due to defects in carbon dioxide homeostasis. Normally, blood carbon dioxide levels are regulated to within a narrow range, with just a change from pH 7.4 to 7.2 resulting in a fourfold change in the firing rate of neurons (maybe the serotonergic neurons' primary role is to control pH) (Nattie et al., 2004). While Lauder (she is investigating how prenatal exposure to drugs or environmental agents might damage the serotonin system) asserts that is "not certain how SIDS might be prevented, since we know little about ist etiology " (Buznikov et al., 2001).

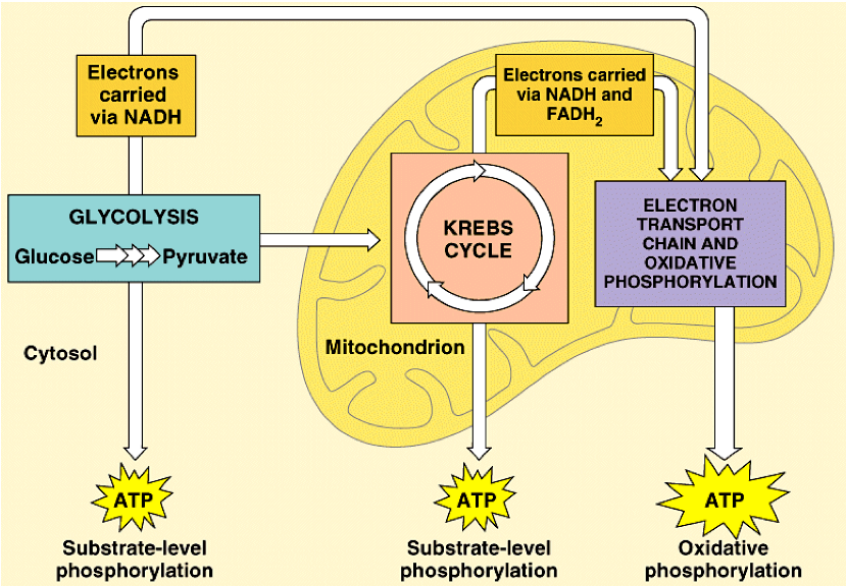

Scheme 5. Catabolism of glucose, picture taken from Campbell, N.A. & Reece, J. B. (2003) Biologie (6 Aufl.), Heidelberg; Berlin, Spektrum Akad. Verl. , pp 190.

The mainstay in the treatment of MCAD deficiency is avoidance of fasting for more than 12 hours. Infants require frequent feedings. It is recommended that toddlers receive 2 g/kg of uncooked cornstarch as a source of complex carbohydrates at bedtime to ensure sufficient glucose supply overnight (source of ATP; see scheme 5).

2. MATERIALS & METHODS

2.1. Materials

2.1.1. Tools

All UV-VIS absorption spectra were recorded using Kontron UVIKON 810, 930 and 933 Spectrometers (with thermostatted cell holders). For the UV and VIS-domain quartz cuvettes were used (Helma/Müllheim). Fermentations (high cell density culture of *E.coli*) were carried out in fed-batch mode in a 12 L stirred-tank fermentor (manufactured by B. Braun Biotech International). Centrifugations were performed with Sorvall RC-SB (Du Pont de Nemours/Germany), Heräus Cryofuge 8500i, Eppendorf 8504R and Eppendorf Mini Spin centrifuges (Hamburg) instruments. Transformed cells were disrupted by sonication with a Sonifier Cell Disruptor B-30. Proteins were separated with a FPLC system (Pharmacia / Freiburg) alongside a fractions collector Frac-100, a UV-detector, a UV-1-monitor and a recorder. The purity of the CoA esters was checked with a HPLC system (Kontron DATA SYSTEM 450-MT2/DAD, 2 Pumps Kontron HPLC Pump 420 a Kontron Diode Array Detector 440, a Rheodyne injection valve mod. 7125, Macherey-Nagel Chromcart 25/4 Nucleosil C18 column- diameter 5 µm). Protein electrophoresis in Agarose-Gels and SDS-PAGE Gels were performed with a device from Biometra (Göttingen). Proteins were concentrated with a Centriprep Centrifugal Filter Unit YM-30, YM-50 or Amicon Stirred Ultrafiltration Units (Millipore GmbH-Eschborn, Deutschland).

2.1.2. Chemicals

Aldrich (Steinheim)	Ferricenium-hexafluorophosphate, Chloramphenicol, Poly-(propylene glycol) 2000
BioRad (USA)	Low molecular mass standards for SDS-PAGE
Boehringer (Mannheim)	FAD (flavin adenine dinucleotide)
BioTech Trade (Munich)	IPTG (Isopropyl-ß-D-thiogalactopyranoside)
Difco (USA)	Bactotryptone Bacto^{TM} Yeast Extract

Fluka (Neu-Ulm)	Hydroxylapatite (fast flow)
Euriso-Top (France)	Deuterium oxide
Merck (Darmstadt)	Magnesiumsulfat-heptahydrate, Acetic acid, sodium azide, Trichloroacetic acid
Pierce (Rockford)	BCA Protein Assay Kit
Pharmacia (Freiburg)	Q-Sepharose (fast flow)
Riedel de Häen (Seelze)	Glycerol, di-Potassium hydrogen phosphate, Potassium dihydrogen phosphate, sodium dithionite
Roth (Karlsruhe)	Ampicillin, HEPES, MES, Tricine
Roche (Grenzach-Wyhlen)	Glucose-Oxidase
Serva (Heidelberg)	Coomassie Brilliant Blue G250, Bromophenol blue sodium salt, TEMED, SDS
Sigma (Deisenhofen)	Trizma base

2.1.3. Bacterial strains

Most bacterial strains used in recombinant DNA work are derivatives of *Escherichia coli* strain K-12 (Table 1).

Table 1. Bacterial strains

E. coli strain	**Genotype**	**Reference**
BL 21	*hsd*S, *gal,* (λ*c*I*ts857, indl,* S*am7, nin5,lac*UV5-T7gene1) BF-*ompT hsdS*(r_B-m_B-) *dcm*+ Tet^r *gal* λ	Studier & Moffat, 1986
BL21-CodonPlus (RIL)	(DE3) *endA* Hte [*argU ileY leuW* Cam^r]	Stratagene
Rosetta Blue™ (DE3)	*endA1 hsdR17*(r_{K12}^- m_{K12}^+)*supE44 thi*-1 *recA1gyrA96 relA1 lac (DE3)* [*F'Pro A*$^+$*B*$^+$ *lacI*^{q}*Z*Δ*M15::Tn10*]*pRARE* (*Cam*^{R}, *Tet*^{R})	Novagen
TG1	*sup*E1, *hsd*Δ*5 thi* Δ(*lac-pro* AB) F'(*tra* D36 *pro* AB$^+$ *lacIq lacZ*ΔM15)	Gibson, 1984, Amersham Internat.

2.2. Methods

2.2.1. Introduction of plasmid DNA into cells. Construction of expression plasmid pTrc MCAD

2.2.1.1. Transformation using calcium chloride

Generation of Competent cells

A single colony of *E. coli* was inoculated into 50 mL LB medium. The cells were grown at 37°C with shaking (250 rpm) to an $OD_{580} \approx 0.4$-0.6. The cells were transferred to one 50 mL sterile polypropylene tube and kept on the ice 5-10 min. After centrifugation (7 min at 1600xg, 4 °C) the pellet was resuspended in 10 mL ice-cold $CaCl_2$ solution and the slurry kept on ice 30 min. After a second centrifugation (5 min at 1600xg, 4 °C) the pellet is resuspended gently in 2 mL ice-cold $CaCl_2$ solution. The „competent cells“ are transferred in aliquots (250 µl) and frozen immediately at –70 °C (Sambrook et al., 1989).

Transformation

1 pg - 1 ng of pTrcMCAD was mixed with 100 µL competent cells and incubated 30 min on the ice bath (the tube was shaken every 2-4 min). The cells were heated for 45 min at 42 °C (heat shock). Then 1 mL of LB medium (preheated to 42 °C) was added and the mixture was incubated for 1 h at 37 °C on the roller drum (250 rpm). After incubation 10-100 µL cells were plated on appropriate antibiotic-containing plates, and incubated 12 to 16 h at 37 °C. Transformation efficiency was 10^7 - 10^8 colonies/g DNA (Hanahan et al., 1998).

2.2.1.2. High-efficiency transformation by electroporation

1 µL plasmid (pTrcMCAD) was mixed 100 µL competent cells. The mixture was transferred to a prechilled cuvette. After the pulse cycle (the electroporation apparatus was set to 2.5 kV, 25 µF and the pulse controller to 200) 1 mL LB was added and the medium was transferred into a sterile culture tube and incubated for 30-60 min. After incubation 10 - 100 µL cells were plated on appropriate antibiotic-containing plates, and

incubated 12 to 16 hrs at 37 °C. Transformation efficiency was 10^9 colonies / g DNA (Ausubel et al., 2001).

2.2.1.3. Construction of mutants

Construction of E376Q, E376G and E376Q+E99G mutants

The generation of the system for the expression of E376Q-MCAD and E376G-MCAD was described earlier (Bross et al., 1990; Nandy et al., 1996). E376Q+E99G-MCAD was obtained by mutagenesis starting from the E376Q-MCAD gene (Nandy et al., 1996).

Construction of the T136A mutant

Quick change Site-Directed Mutagenesis Kit, purchased from Stratagene was used for mutagenesis reaction. A set of forward primer, T136A.for (5'-GTG TGC TTA TTG TGT AGC AGA ACC TGG AGC AGG-3') and a reverse primer, T136A.rev (5'-CCT GCT CCA GGT TCT GCT ACA CAA TAA GCA CAC-3') were used to replace the threonine with that of alanine at 136th position in wild type MCAD protein sequence. The plasmid pTrc-WTMCAD was used as template for mutagenesis reaction. Amplification of DNA sequences was performed in a T3 Thermocycler (Biometra) and conditions were denaturation at 95 °C for 1 min, annealing (95 °C for 30 sec, 55 °C for 1 min and 68 °C for 12 min) and extension at 68 °C for 15 min for 20 cycles. Standard reactions were performed in volume of 50 µL contained 5 µL of 10X reaction mix, 10 ng of dsDNA, 125 ng (0,5 µl) each of forward and reverse primers, 1 µL of dNTP mix and 1 µL of *Pfu* DNA polymerase (2.5 U/µl) in double distilled water. The amplified DNA was treated with 1 µL of *Dpn I* (10 U/µl) restriction enzyme for 1 hour at 37 °C to digest the wild type pTrc-WTMCAD plasmid ds DNA template. 5 µL of this DNA was used to transform XL1-Blue competent cells. Plasmid DNA was isolated from a single transformant sequenced. The mutation T136A was verified by sequence alignment.

Construction of T168S and T168V mutants

The wild-type pHis-hMCAD was used as a template for site-directed mutagenesis by PCR with Pfu-Ultra DNA polymerase using a complementary primer method. The following primers were designed using a Stratagene program (QuikChange® Primer Designer): AGCTTTTCCTCCGTT***GCT***TATCCACATCTTCTGAC (T168S, antisense),

CAATTAGCTTTTCCTCCGTT***CAC***TATCCACATCTTCTGACCAT (T168V, anti-sense). The products of PCR were digested with DpnI and the resultant mutant DNA fragments were used to replace the DNA fragment from the wt pHis-MCAD. The result was confirmed with DNA sequencing.

2.2.2. Protein purification and characterization

2.2.2.1. Determination of protein concentration

The most used colorimetric methods are Bradford, Lowry and the Bicinchoninic acid assay. The last one (Bicinchoninic acid reaction) is simple to perform and is less sensitive to interfering substances (Smith et al., 1985).

MCAD is a flavoenzyme containing one noncovalently bound FAD per subunit (Ikeda et al., 1985a). For estimation of λ_{max} of the FAD in the visible range, SDS was added to a final concentration of 1 % (w/v) to a solution of 8-10 µM His-Tag-MCAD in 20 mM sodium phosphate pH 7.8. The resulting spectrum of the flavin was recorded and λ_{max} was calculated on the basis of an ε_{450} of 10.8 $mM^{-1}\cdot cm^{-1}$ for free FAD (Whitby, 1953). The resulting coefficient (ε_{453} 14.2 $mM^{-1}\cdot cm^{-1}$ for His-Tag-MCAD; the native enzyme has an ε_{446} of 14.8 $mM^{-1}\cdot cm^{-1}$ (Kieweg et al., 1997)) was used in all determinations of enzyme concentrations.

2.2.2.2. Western Blotting

Samples were subjected to electrophoresis according to Laemmli using SDS-PAGE (Laemmli, 1970). Western blot analysis were performed according to the method of Towbin et al. (Towbin et al., 1979).

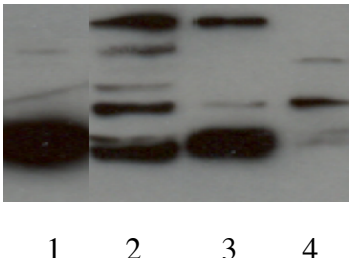

Figure 2. Western Blot of E376Q/E99G-MCAD before and after Q-SepharoseFF separation, where: line 1 corresponds to hMCAD wt (purified protein); lines 2 were protein in crude extract (in TG1) 3 respectively 4 were fractions eluted at separation. The secondary antibody was a Goat Anti-mouse IgG.

The method allows detection of the MCAD, especially active-site mutants having lower activity (E376Q or E376Q/E99G-MCAD).

2.2.2.3. Expression of human wild-type and mutant MCAD in *E. coli*

E coli cells (strain TG1, BL21CP-RIL or RosettaBlue®DE3*) were transformed with human wild-type and E376Q, E376H, E376G, E376Q/E99G, E99G, T168A, T168S*, T168V* and T136A-mutant plasmids (pTrc MCAD or hisMCAD*) and plated on LB-Agar or NZ-Agar containing the appropriate antibiotic (Ausubel et al., 1995). 5 mL LB sterile medium containing appropriate antibiotic was inoculated with a colony picked from the plate and cells were grown for 6-7 hrs. 2L Erlenmeyer flask (with 400 mL LB medium; 1 µg antibiotic / 1 mL medium) was inoculated with 0.4 mL medium from previous step and the overnight culture was transferred aseptically to a 8L (B. Braun Biotech International fed-batch) fermentor. TY2x medium (Ausubel et al., 1995) containing 100 µg of ampicillin (+30 µg of chloramphenicol) / mL at a temperature of 28 °C to avoid inclusion body formation. Polypropylene glycol 2000 (1-2 mL / 8 L) was used (Kleman & Strohl, 1994) as antifoaming agent (to prevent foam formation by a coalescent effect of the micro-bubbles). Expression of MCAD protein was induced at OD_{578} = 1.0 with 0.1 mM IPTG, and the *E.coli* cells were harvested after an induction time of about 6-7 hrs with an OD_{578} of 10-11. Feed back processes have most often been used to obtain high cell-density (ammonium hydroxide 25 % is frequently used as a nitrogen source and as a base; HCl 1 M is used as a acid and glucose 1 M or glycerol 95% as carbon source) (Yee & Blanch, 1992).

The cells were harvested for 20 min (5000 G) with a Heraeus Cryofuge and the wet cell paste (100-200 g) was stored at –20 °C. *E. coli* cell paste (200 g) was thawed and suspended in 600 mL 0.1 M Tris/HCl pH = 7.8. The cell suspension was sonicated three times for 5 min. (50 % pulsed / 10 min break), and the slurry (about 600 ml) was centrifuged for 30 min at 11000 g. The pellet was resuspended in 300 mL 0.1 M Tris and resonicated three times for 5 min. (50 % pulsed) and centrifuged for 30 min at 11000 g (15-20 % of protein was recovered from this pellet).

2.2.2.4. Ammonium sulfate precipitation

The pooled supernatants were precipitated very slowly (2 hrs) with ammonium sulfate (the final concentration was 35 %). The slurry was centrifuged for 10 min at 11000 g. The supernatant was precipitated with the same salt at a final concentration of 85 %. The precipitate was stored overnight at 4 °C.

2.2.2.5. Ion-Exchange Chromatography

The precipitate resulted from the previous step was centrifuged for 10 min at 11000 g. The pellet was dissolved and dialyzed 5 times (every 4 hrs) against 2-3 L of 50 mM Tris/ HCl. The proteins mixture (≈ 300 - 400 mL) was concentrated using an Amicon unit (the cut-off of the membrane was 10 kDa) to approx. 50 mL and then loaded on a Q-Sepharose fast flow column (15 x 280 mm, equilibrated with 50 mL Tris/HCl, flow rate 2 mL/min). MCAD binds as a green/yellow band at the top. After elution of unbound protein, a gradient (0-350 mM NaCl; 6 column volumes, with a flow rate of 17 cm/h) was applied. The protein is eluted at 180 - 210 mM NaCl. The color and ionic strength of elution are conveniently used to locate MCAD protein in the case of inactive mutants.

2.2.2.6. Hydrophobic Interaction Chromatography

The pooled fractions from the previous step were concentrated by precipitation with 85 % ammonium sulfate and the dissolved pellet was dialyzed against 5 mM KP_i pH 7.8. The protein solution ($A_{272/444}$ = 30 ÷ 35) was applied (0.7 mL/min) to a hydroxylapatite (fast flow) column (30 x 140 mm, equilibrated with 5 mM KP_i and a flow rate of 1.5 mL/min). The column was washed with the same buffer and then with 500 mL KP_i 100 mM (flow rate 1ml/min). MCAD was eluted at 200-250 mM KP_i using a linear gradient of 100-500 mM KP_i over 500 min. For E376Q and E376Q/E99G-MCAD the yellow form is eluted before the green one. The yellow form has an $A_{272/444}$ ratio of about 6 and purity more than 90 % (Figure 3).

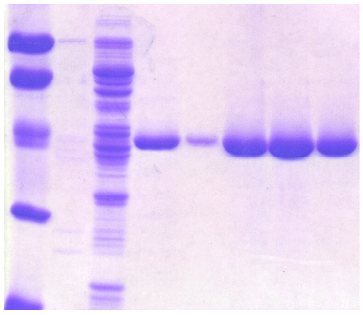

M 1 2 wt 3 4 5 6

Figure 3. SDS-PAGE electrophoresis of T168A-MCAD during HO-Apatite separation, where: M is the marker; lines 1 and 2 are fractions resulted after washing with KPi 5 mM respectively 100 mM KPi (pH = 7.8); wt - hMCAD wt (purified protein); pure mutant (lines 3, 4, 5, 6) was eluted at 200-250 mM KPi.

For degreening (removal of tightly bound CoA-persulfide) 200 µL saturated solution of dithionite (in desired buffer) was added to 800 µL enzyme (concentrated MCAD in the same buffer). The enzyme becomes colorless while is dissolved, and after 1-2 min it is passed through a Sephadex G25M column (3.5 mL), during which process it reoxidizes to yellow form (alternatively a Centriprep YM-30 was used and the buffer was changed 3-4 times) (Steyn-Parve & Beinert, 1958).

2.2.2.7. Purification of histag-MCAD

E.coli RosettaBlue®DE3 cells were used for the expression of His-Tag-MCAD from pwt-MCAD-COOH-his (or its mutant plasmids). Cultures were grown as described before. The bacterial paste (10-20 g) was suspended in 50-100 mL of lysis buffer and sonicated 4 x 3 min (7 min break). The lysate was centrifuged 30 min at 10000 g and resulted supernatant was recentrifuged 15 min at 15000 g. The lysate supernatant resulted from the previous step was loaded onto 1 mL His-Trap column (for large scale purification a 5 mL column has been used; Amersham Biosciences, Germany). The column was washed with (10-12 columns volume) lysis buffer (50 mM NaPi containing 40 mM imidazole, 500 mM NaCl and 10% glycerol at pH 8) at room temperature, then with washing buffer (10-20 columns volume; this buffer contain 65 mM imidazole). The enzyme was eluted (100-110 mM imidazole) using an imidazole gradient (65-350 mM). The purified His-Tag-MCAD was concentrated using a Centricon unit (Centriprep YM-30, Millipore) and thus the excess of imidazole was removed. The purification procedure, from cell disruption to freezing of the purified sample, takes about 7-8 hrs (for the native – non His-Tag - enzyme the hole process takes at least 3-4 days!). Similar procedures were used to purify two mutants of His-Tag-MCAD (T168S and T168V).

2.2.3. Preparation of CoA thioesters and indigo monosulfonate

A variety of methods, including chemical and enzymatic syntheses, are currently available for the preparation of CoA thioesters of fatty acids. Chemical syntheses most frequently employed involve the acid anhydride (C_8CoA, $3SC_8$CoA), the acid chloride (C_{12}CoA-C_{20}CoA), the mixed anhydride of ethyl hydrogen carbonate (C_8enoylCoA) and N-hydroxysuccinimide ester of the fatty acid (most useful for arylacetyl-CoA derivatives)

as the acylating reagent (Al-Arif & Blecher, 1969). In general CoA was dissolved in 30 mL THF/KPi100 mM (pH = 7.8) 2:1 previously degassed for 15 min (with N_2) which contains tributylphosphine (to avoid dimerization of the CoA) and afterwards acylating agent (used in 8-10 fold excess) was slowly added (the pH of the reaction mixture was adjusted at 7.9 - 8.0 with Na_2CO_3). The reaction was carried out at room temperature and pH = 8.0 for 3-7 hrs. At the end the reaction mixture was acidified to pH = 3, extracted with ethyl ether (50 mL x 3) to remove the unreacted fatty acid and the water layer was lyophilized. The powder was resuspended in water and applied on Sep-Pak C_{18} Cartridge. The cartridge was whased with 5 column volumes of water to remove inorganic salts. The esters were eluted using a gradient of methanol and analyzed with a HPLC system. The thioester content of the preparations was determined by measuring the ratio of the 232 and 260 nm absorptions (the extinction coefficients are C_nCoA: ε_{260} 15.4 $mM^{-1}cm^{-1}$, $3SC_8CoA$: ε_{260} 16 $mM^{-1}cm^{-1}$, 4NPA-CoA: ε_{260} 20.8 $mM^{-1}cm^{-1}$).

Indigo monosulfonate was prepared by controlled sulfonation of indigo according to Bloxam (Bloxam, 1906) . The obtained crude mixture of products contains indigo 5,5',7,7'-tetra-, 5,5'-di-, 5- respectively 7-monosulfonate. Indigo 5-monosulfonate was obtained by chromatography on a silica gel column using n-butanol : AcOH : H_2O = 8 : 1 : 2 as eluent. The product yields a single spot on TLC (same eluents) and using indirubin-5-sulfonic acid as standard (Hoessel et al., 1999).

2.2.4. Activity measurements

Acyl-CoA dehydrogenases deliver reducing equivalents to electron transferring flavoprotein witch discharges reducing equivalents to respiratory chain via the third flavoprotein, ETF-QO oxidoreductase (Beckmann & Frerman, 1985; Frerman & Turnbull, 1990). Ferricenium salts ($Fc^+PF_6^-$) are excellent acceptors for acyl-CoA dehydrogenase reacting some 150-fold faster than the phenazine methosulfate (widely employed mediator of acyl-CoA dehydrogenase). Routine assays followed the reduction of 200 µM ferricenium ion (in 10 mM HCl) at 300 or 617 nm (ε_{300} = 4.3 $mM^{-1}\cdot cm^{-1}$ and ε_{617} = 0.41 $mM^{-1}\cdot cm^{-1}$) in 100 mM HEPES or KPi (pH = 7.6), 50 µM C_8CoA and 30 - 300 nM enzyme (depending on the mutant enzyme), at 25 °C (Lehman & Thorpe 1990).

$$\text{Total activity} = \frac{\Delta OD_{300}}{\Delta t(\text{min}) \cdot \varepsilon(\text{l} \cdot \text{mol}^{-1} \cdot \text{cm}^{-1}) \cdot \text{d(cm)} \cdot V_{enz.}} \cdot V_{assay} \cdot V_{total} \cdot 10^6 \left(\frac{\mu\text{mol Ferricenium}}{\text{min}} \right) \quad (1)$$

$$\text{Specific activity} = \frac{\text{Total activity}}{\text{mg total protein}} \left(\frac{\mu\text{mol Ferricenium}}{\text{min} \cdot \text{mg}} \right) \quad (2)$$

$$\text{Turnover} = \frac{\Delta OD_{300}}{\Delta t(\text{min}) \cdot \Delta\varepsilon(\text{l} \cdot \text{mol}^{-1} \cdot \text{cm}^{-1}) \cdot \text{d(cm)} \cdot V_{enz.} \cdot C_{enz}(\text{mol/l})} \cdot V_{assay} \left(\frac{\mu\text{mol Ferricenium}}{\mu\text{mol enzyme} \cdot \text{min}} \right) \quad (3)$$

Equations 1-3: Determination of total and specific activity respectively turnover-number using ferricenium assay

pH-dependence of enzyme activity was determined in 50 mM buffer containing 250 mM KCl (Table 2) and 10 % glycerol. Alternatively, an equimolar mixture (12.5 mM of each component) of HEPES, Tricine, Tris and Glycine (so called "mixed buffer") containing the same concetration of salts was used for this purpose.

Table 2. Buffers used in activity measurement (containing 250 mM KCl)

pH-interval	4.5-5.0	5.0-6.5	6.0-7.0	7.0-8.5	8.5-9.0	9.5-11.0
buffer	Acetate/ HCl	MES/ KOH	HEPES/ KOH	Tricine/ HCl	Tris/ HCl	Glycine/ HCl

The presence of high salt concentration in the cuvette is to ensure that ionic strength remains constant in the reaction mixture.

2.2.5. Stopped-flow technique

The stopped-flow technique was originally developed by Chance et. al (Chance et al., 1964) from the continuous flow technique. Continuous flow was used by Hartridge and Roughton (Hartridge & Roughton, 1923) to study the binding of oxygen to haemoglobin (was very expensive with regard to solution volumes and can only be used where large amounts of reactants are readily available). In the stopped-flow technique, two solutions are rapidly mixed together and at any given point the age of solution were defined by the flow rate and the volume between mixing and observation. However, by the use of a back syringe, the flow of the mixed reactants is suddenly stopped and the reaction is followed in real time with a suitable detection system. Figure 4 shows a typical stopped-flow trace which illustrates the processes occurring in the instrument where the recording device is storing data from 50 ms before the point when flow stops. When the

reactant syringes are driven forward, the new solution displaces the old solution from the observation cell. Then a period of constant signal is seen. Over this time, the reactant solution has a constant age as described for the continuous flow method.

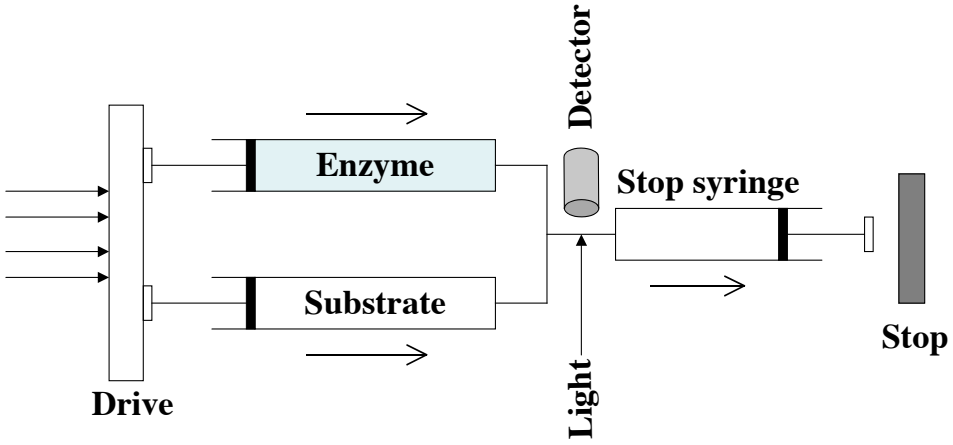

Figure 4. Simplified diagrammatic representation of stopped-flow technique

This age is defined as the "dead-time" of the instrument and is the shortest time from which a reaction can be monitored. Typically the "dead-time" of the instrument is in the region of 1-6 ms. For the determination of the dead-time of instruments operating in the absorption mode, the alkaline hydrolysis of the 2,4-dinitro-phenylacetate can be measured. This has a second-order rate of 45 $M^{-1} \cdot s^{-1}$ corresponding to $t_{1/2}$ = 15.4 ms). When the flow stops, the reaction is followed with time.

In a typical stopped-flow experiment, equal volumes of the enzyme and substrate are mixed. The concentration in the observation cell are therefore half of those in the syringe and it is important to define which concentration is being quoted.

It is important that the solutions are thoroughly mixed when observation commences so that the observed rate of the reaction is the true one and is not limited by the mixing process. Protonation reactions occur with rate constants much faster than the stopped-flow time scale so that if an indicator (for absorption mode experiments phenol red: λ_{max} = 560 nm; ε = 54 $mM^{-1} \cdot cm^{-1}$) at a pH above its pK_a is mixed with buffer below its pK_a, the reaction should be completed within the "dead-time" of the instrument.

Deuterium and quartz halide lamps have lower intensity outputs and are suitable for absorbance measurements, which have a much lower requirement for light intensity. The emitted light is usually detected by a photomultiplier after it has passed through a

suitable optical filter (the WG 320 cut-off filter blocks light in the UV region and passes light at higher wavelengths with 50 % transmission at 320 nm).

The volume of reactants to be mixed should be at least 100-150 µL (stop volume could be determined by adjusting the position of the back-stop of the stopping syringe).

2.2.6. Mathematical fit routines

All Fit routines were executed with the programs KaleidaGraph, BioKine or Specfit. K_m and maximal velocity (V_{max}) were determined from the *Michaelis-Menten* equation (4) using a set of measurements of velocity (V), at different substrate (ligand) concentrations (Fersht, 1985).

$$V = \frac{V_{max} \cdot K_m}{K_m + [S]} \quad (4)$$

The rates of the binding/reduction were measured by the decrease of absorption at 450 nm (reduction of flavin) and fit to a mono or a multi-exponential equation:

$$f(t) = d_1 \exp^{-k_{fast} t} + d_2 \exp^{-k_{slow} t} + \ldots + C \quad (5a)$$

where d_1 and d_2 are the amplitudes of two exponentials with rate constants k_{fast} and k_{slow} (the first step is faster and the second slower) and C is an offset (Nieslanik et al., 1999).

Alternatively, the relaxation time resulted from stop flow measurements were fitted using the *Kohlrausch-Williams-Watts dependency* (Sastry et al., 1998):

$$F_s(k, t) = \exp\left[-\left(\frac{t}{\tau(T)}\right)^{\beta(\tau)}\right] \quad (5b)$$

where F_s (k,t) is space Fourier transform function, $\tau(T)$ is relaxation time and β is the deviation from strict exponential behavior ($0 < \beta < 1$)

Depending on the specific nature of the binding sites and their binding affinity, structurally analogues compound in comparison with the native ligand (substrate) are more or less accepted. They can bind stronger than the substrate or they may have antagonistic effect (blocking the binding site). For the calculation of the dissociation constants for the reaction (I) according to the law of mass action the concentration of the free enzyme, free ligand and enzyme ligand complex under equilibrium conditions must be known.

$$E + L \underset{k_{-1}}{\overset{k_1}{\rightleftharpoons}} EL \quad (I)$$

$$[E]_0 = [E]_{free} + [EL] \quad (6)$$

$$[L]_0 = [L]_{free} + [EL] \quad (7)$$

where $[E]_0$, $[L]_0$ are the total quantities of enzyme and ligand used for the experiment; $[E]_{free}$, $[L]_{free}$ are concentration of the free enzyme, respectively ligand; $[EL]$ is concentration of the complex at equilibrium.

The dissociation constant at equilibrium is described in equation (8). The concentration of the bound ligand is reflected in equation (9) where: n - the number of identical binding sites, Y is saturation function. For the evaluation of spectroscopic titration an asymptote is attached to the curve in the saturation area (Figure 5).

$$K_d = \frac{[E]\,[L]}{[EL]} = \frac{([E]_0 - [EL])\cdot[L]}{[EL]} \quad (8)$$

$$[L]_{bound} = n \cdot [EL] = \frac{n\,[E]_0 \cdot [L]}{K_d + [L]} \quad (9)$$

$$\frac{1}{Y} = \frac{[L]_{bound}}{n \cdot [E]_0} = \frac{[L]}{K_d + [L]} \quad (10)$$

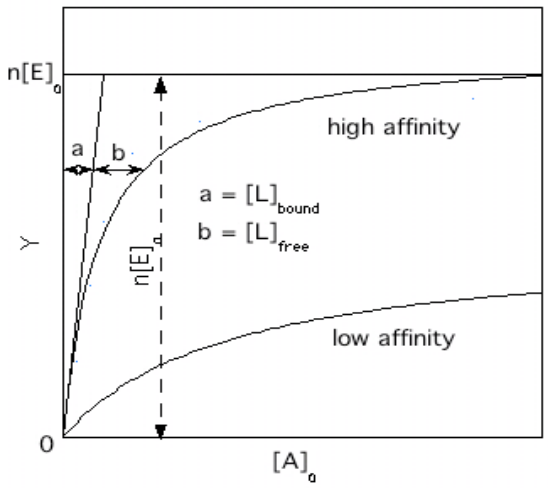

Figure 5. Evaluation of spectroscopic titration While the total distance from the ordinate to a certain measuring point is $[L]_0$, the abscissa section up the source tangent is $[L]_{bound}$, and from there to the measuring point $[L]_{free}$. If all the binding sites are saturated, further ligand can not be present in free form and the binding curve merging with the saturation asymptote (Bisswanger, 1994).

The intercept of the ordinate is $xn[E]_0$ (x = factor dependent on the measurement signal). In spectroscopic titration the amount of ligand free (Bisswanger, 2002) ($[L]_{free}$) is not directly obtained from the measurement. A tangent is laid through the ordinate base to the almost linearly rising valves in the start area at low ligand concentration. The line intersect the saturation function (Y) at the abscissa value $[L]_0 = n[E]_0$.

The pH dependence of the pK_ds for binding of the ligand to wild type enzyme and mutants were plotted according to Dixon equation (Dixon & Webb, 1979):

$$pK = -\log K_L + \log\left(1 + \frac{K_{EL1}}{[H^+]}\right) - \log\left(1 + \frac{K_{E1}}{[H^+]}\right) - \log\left(1 + \frac{K_{E2}}{[H^+]}\right) + \log\left(1 + \frac{K_{EL2}}{[H^+]}\right) \quad (11)$$

Where: K_L is the dissociation constant of neutral ligand (L-H) from the neutral form of the enzyme E-H, pK_{EL1} and pK_{EL2} are ionizations of the enzyme-ligand complex (E~L-H); pK_{E1} and pK_{E2} are ionizations of uncomplexed enzyme (or ligand).

For the simulation pK_{EL1} (resulted from extinction coefficient of the E~L complex versus pH for the wild-type enzyme) and pK_{E2} (resulted from extinction coefficient of the E~L complex versus pH for the mutant enzyme) were fixed.

The activities of many enzymes vary with pH in the same way that simple acids and bases ionize. Although enzymes contain a multitude of ionizing groups, it is usually found that plots of rate against pH take the form of the simple single or double ionization curves (ionizations of groups at the active site can have a major role in catalysis).

The ionization constant K_a for an enzyme is defined by:

$$K_a = \frac{[E^-][H^+]}{[EH]} \quad (12) \qquad [EH] = \frac{[E]_0\,[H^+]}{K_a + [H^+]} \quad (13) \quad \text{and} \quad [E^-] = \frac{[E]_0\,K_a}{K_a + [H^+]} \quad (14)$$

$$\text{where } [E]_0 = [EH] + [E^-] \quad (15)$$

$$V_H\,[E]_0 = V_{EH}[EH] + V_{E^-}[E^-] = \frac{V_{EH}[E]_0\,[H^+]}{K_a + [H^+]} + \frac{V_{E^-}[E]_0\,[H^+]}{K_a + [H^+]} \quad (16a)$$

$$V_H = \frac{V_{EH}\,10^{-pH} + V_{E^-}\,10^{-pKa}}{10^{-pKa} + 10^{-pH}} \quad (16b)$$

The variation of concentration of EH and E^- with the proton concentration is found from rearranging of the equation 12, 13 and 14. The product of the reaction rate V (or TO) and the concentration of a certain species at a particular pH is constant (equation 16), were V_H is the reaction rate or turnover; V_{E^-} and V_{EH} are reactions rate of the enzyme in the protonated and deprotonated forms. The determination of enzyme activity must always

take place under saturating conditions for all substrates at the apparent maximum velocity (V_{app}). For determination of the pK values according to Dixon (Dixon & Webb, 1974) log V_{app} is plotted against the pH value. Molecular pK values are given by the intersection of the asymptotes to the curve (Parkash & Bhatia, 1980). Ionisation constants may also be obtained from secondary plots of the Lineweaver-Burk diagram plotting $1/V_{app}$ against 1/[S] ([S] is the substrate concentration).

Studies of general-catalyzed reactions (including enzymatic reaction) are very commonly conducted in water and occasionally in other protic solvents. The isotope effects for general-catalyzed proton bridging can be measured by isotopic labeling in the catalytic site. The most common experiments are deuterium solvent isotope effects in witch a rate constant measured for H_2O is compared with one for D_2O solution or proton inventories effect by using of mixtures of isotopic solvents. The technique of employing rate measurement in mixture of protium and deuterium oxides to produce an analysis of the number of exchangeable sites contributing to the isotope effect has become known as *proton-inventory method* (Cho et al., 1994; Schowen et al., 2000). The algebraic prediction for proton inventories effects (where protein-structural effects are combined with effects from general-catalytic bridging) is reduced to three simple cases:

(17a) $k_n/ k_0 = 1 + n (\phi - 1)$ no medium/structural effect (linear)

(17b) $1/ k_n = (1 - n+ n\phi) / k_0$

(18) $k_n/ k_0 = Z^n$ medium/structural effect only (exponential)

(19) $k_n/ k_0 = [1 + n (\phi - 1)] Z^n$ both medium/structural and bridging effects

where n is the atom fraction of D in solvent, k_n is the rate constant for mixed solvent containing atom fraction n of D, k_0 is the rate constant for pure H_2O (n = 0) , $1/\phi$ is the isotopic effect for proton bridging, and 1/Z is the medium isotope effect. For our case a limited number of qualitatively different models (two) can be expected to reproduce this kind of curve: (i) a one-step model combining an inverse isotope effect from one site with a normal isotope effect from multiple sites; (ii) a two-step model in which one step generates a multisite normal isotope effect and a second step generates an inverse isotope effect from nucleophilic or general-base participation by hydroxide ion.

One-step model

A one-step model will have the general form,

$$k_n = k_0 \frac{TSC(n)}{RSC(n)} \quad (20) \qquad TSC(n) = 1 - n + n\alpha \quad (21a) \qquad RSC(n) = Z^n \quad (21b)$$

where: TSC -"transition-state contribution" and RSC - "reactant-state contribution"

This model has two characteristics. First, there is an event such as an enzyme conformational change that produces a net loosening of the binding potential at a large number of hydrogenic sites in the structure of the protein and associated waters of solvation, as the reactant state is converted to the transition state.

Two-step model

The expected form of k_n for a two-step reaction can be obtained as follow. The steady-state rate constant k_n for a sequence of two reactions with rate constants k_{an} and k_{bn} will be given by equation (22) whence multiplication by k_0 (rate constant at n = 0) yields

$$\frac{1}{k_n} = \frac{1}{k_{an}} + \frac{1}{k_{bn}} \quad (22)$$

$$\frac{k_0}{k_n} = \frac{k_0}{k_{a0}}\frac{k_{a0}}{k_{an}} + \frac{k_0}{k_{b0}}\frac{k_{b0}}{k_{bn}} \quad (23) \qquad \frac{k_0}{k_{a0}} + \frac{k_0}{k_{b0}} = 1 \quad (24)$$

$$\frac{k_0}{k_{a0}} = w_a \qquad \frac{k_0}{k_{b0}} = 1 - w_a \quad (25) \qquad \frac{k_{a0}}{k_{an}} = \frac{RSCa(n)}{TSCa(n)} \qquad \frac{k_{b0}}{k_{bn}} = \frac{RSCb(n)}{TSCb(n)} \quad (26)$$

$$k_0 / k_n = (1 - w_a)(1 - n + n\alpha) + w_a Z^n \quad (27) \qquad k_0 / k_n = (1 - w_a)(1 - n + n0.5) + w_a 90^n \quad (28)$$

2.2.7. Determination of oxidation / reduction potentials

The redox potentials of wt-MCAD and T136A-MCAD were determined at 25 °C by the dye-equilibration method (Minnaert, 1965) and xanthine/xanthine oxidase reduction system proposed by Massey (Massey, 1991). For this 10 μM enzyme was placed in an anaerobic cuvette in phosphate buffer (pH 8), together with 200 μM xanthine and 5-10 μM of dye (indigo 5,5'-disulfonate was used for wt-MCAD and indigo 5-monosulfonate for threonine mutants). To ensure rapid equilibration of reducing equivalents, 5 μM benzyl viologen was added to the enzyme solution. The cuvette was made anaerobic and the visible spectrum of the anaerobic enzyme was recorded. The

reaction was initiated by adding xanthine oxidase (10–30 nM) from the side arm of the Thunberg cuvette. Then the absorbance spectra were collected until an increase in the ≈ 600 nm peak of the mediator (benzyl viologen) was evident (1-2 hrs). The concentrations of the oxidized and reduced forms of the enzyme and reference dye were determined from the absorbance values at various wavelengths (using an isosbestic point for the different enzyme and dye forms). The redox potentials were calculated according to (Hemmerich et al., 1972). Other dyes either do not possess appropriate redox potentials or do interfere with MCAD.

2.2.8. Computational methods

Approximate density functional theory (DFT) calculations were carried out by Dr. Olga Dmitrenko and Prof. Dr. Robert Bach as previously described (Dmitrenko et al., 2003).

3. RESULTS & DISCUSSION

3.1. Activity measurements: substrate chain length specificity of MCAD, pH dependences and activation energies

3.1.1. Introduction

Several spectrometric assay are being used for assessing the activity of acyl-CoA dehydrogenases in which ETF was replaced by a dye / mediator dye system (dye: DCPI; MB and mediator dye: PMS; INT; PES) (Green et al., 1954; Dommes & Kunau, 1976; Shaw & Engel, 1987; Trievel et al., 1995). We have used the ferricenium assay described by Lehman and Thorpe (1990) for the study of the catalytic activity. The electron transfer properties of ferricenium are closest to those of electron-transferring flavoprotein, the physiological electron acceptor (Lehman & Thorpe, 1990).

Bross et al. have reported first mutagenesis experiment for MCAD and concluded that a glutamate residue is the functional base at the active site (Bross et al., 1990). The position of the catalytic glutamate, identified as Glu376 in MCAD, Glu254 in human isovaleryl-CoA dehydrogenase (iVD), Glu261 in human long chain acyl-CoA dehydrogenase (LCAD) and Glu368 in rat short chain acyl-CoA dehydrogenase has been suggested to affect substrate chain length specificity (Battaile et al., 1996). Similarly, Glu164 (Glu165 in the rat enoyl-CoA isomerase) was confirmed to be essential for the catalytic activity of both the rat 2-enoyl-CoA hydratase-1 and the enoyl-CoA isomerase, suggesting that it is probably involved in the protonation/deprotonation steps (Muller-Newen et al., 1995). Studies with D304 mutants of polyhydroxybutyrate (PHB) synthase (catalyzes the conversion of ß-hydroxybutyryl-CoA to PHB) suggest D302 functions as a general base catalyst in activation of the 3-hydroxyl of HBCoA (Jia et al., 2000).

Nandy et al (1996) (Nandy et al., 1996) have found that the activities of wt-MCAD and T255E-MCAD (in LCAD glutamate residue is found in position 255) are maximal with C_8CoA, while with E376G/T255E-MCAD the maximum is shifted to C_{12} and C_{14}CoA (become close to that of LCAD). Thus, Glu255 has no significant influence on substrate chain length specificity. Küchler et al. have shown that the specific activities of T168A and K304E-MCAD are also shifted to longer substrate chain (Küchler et al.,

1999), but K_m values are decreasing with the substrate chain length (see Figure 1; the K_m value for C_{16}CoA was calculated and has almost the same value with K_m of C_{12}CoA which was reported earlier).

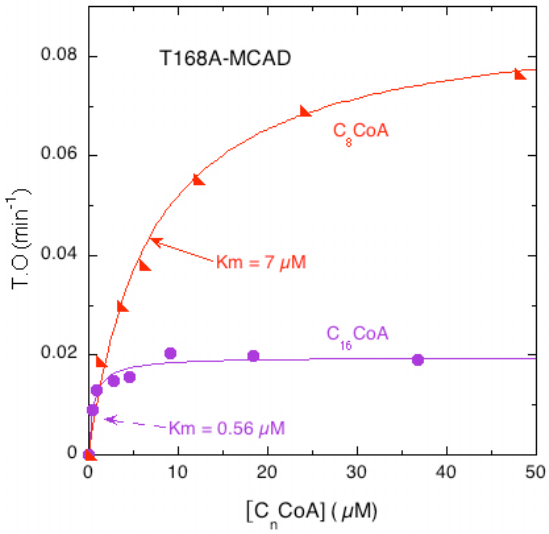

Figure 1. Activity of T168A-MCAD measured with the ferricenium assay using C_8CoA respectively C_{16}CoA. Activity was measured by incubation with C_8 or C_{16}CoA in KPi 100 mM pH = 7.6 and 25 °C. The data points shown are the average of at least three individual determinations. The extrapolated maximum velocities were 27 min^{-1} for C_{16}CoA (T.O. = 0.02 min^{-1}) and 120 min^{-1} for C_8CoA T.O. = 0.088 min^{-1}).

In addition to K304E-MCAD, new human genetic mutations have been found (Andresen et al., 1997). Two of these are point mutations in the amino acid code of the mature protein resulting in the replacement of a cysteine at position 91 to a glycine or a tyrosine. Ghany et al. have purified and characterized C91G-MCAD and C91Y-MCAD (both mutants are unstable; the instability is due to or accompanied by loss of FAD during purification). The chain length/activity profile of C91G-MCAD is shifted towards long chain substrates (Abdel Ghany et al., 1999).

3.1.2. Chain length specificity of wt-, T136A-, E376H- and E376Q-MCAD

3.1.2.1. Effect of E376X substitution on the chain length specificity

In previous studies several E376X mutants have been created and studied in order to assess the role of Glu376 in catalysis (Bross et al., 1990; Kim & Wu, 1988; Powell & Thorpe, 1988; Kim et al., 1993). During these investigations it was observed that the mutants exhibit a different activity vs chain length profile compared to wt-MCAD (Ghisla & Strauss 1994; Peterson 2000). This has now been studied in some detail. First it should be noted that the reaction of E376X mutants with acyl-CoA substrates (influence on the reduction rates of the flavin or T.O.) is much lower compared to wt-MCAD (Bross 1990;

Ghisla et al., 1994; Gradinaru et al., 2002). This allows the direct monitoring of the dehydrogenation reaction by UV-Vis spectroscopy. For this the enzyme, in the present case E376Q-MCAD is incubated under anaerobic conditions in the presence of varying amounts of substrate, and the changes in absorption at 450 nm are recorded. As with wt-MCAD the course of enzyme flavin reduction is biphasic (Fig. 3; Chapter 3.2.2). From exponential analysis of the decay curves two reaction rates can be extracted that are named k_1 (fast) and k_2 (slow). The E376Q-MCAD shows a preference for C_8CoA. Similar results were obtained from activity/substrate chain-length profile of wt-MCAD (Nandy et al., 1996).

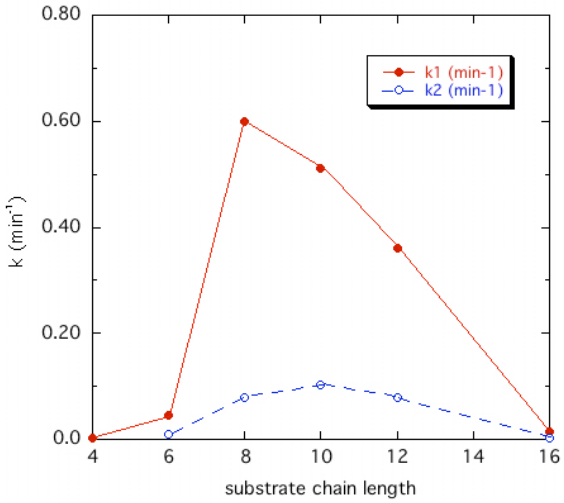

Figure 1. Substrate chain length dependency of the reduction rate of E376Q-MCAD with CnCoA (100 µM) at 4 °C. Anaerobic conditions: 10 mM Glucose / 0.2 µM G.O. in "mixed buffer" containing 250 mM KCl at pH 9.4. The best substrate is C_8CoA (activity measurements for wt-MCAD are giving a slightly similar profile). For higher substrate the dependence is quite linear.

The same type of experiments was done with E376H-MCAD. In this case the mutant has less than 1% of the hwt enzyme activity (Gradinaru et al., 2002). Moreover, maximum of specific activity is shifted to C_{12}CoA (see Figure 2).

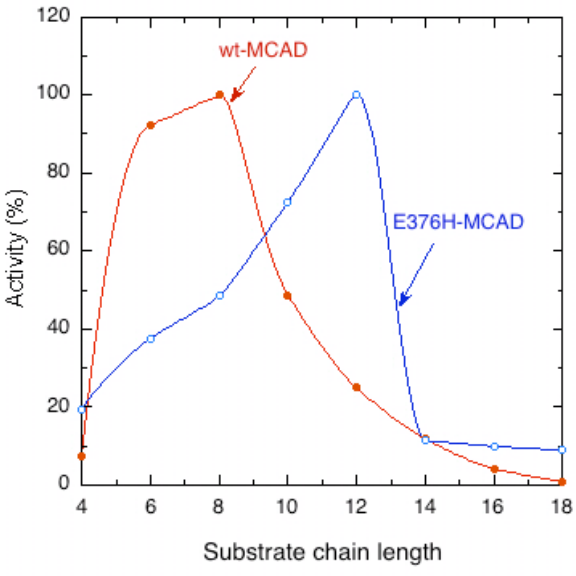

Figure 2. Influence of substrate chain-length on E376H-MCAD activity and comparison with wt-MCAD. All activities were measured with the ferricenium assay in glycine 50 mM containing 250 mM KCl at pH = 9.25 and 25 °C. The final concentration was 150 µM for the substrate, 21.2 nM for wt-MCAD and 2.16 µM for mutant. All assays were performed in at least triplicate.

Similar effects are observed with a MCAD triple mutant (E99G/E376G/T255E-

MCAD) that exhibits a close specificity with VLCAD (Bertrand et al., 1996; Eder et al., 1997).

3.1.2.2. Substrate specificity of Thr136Ala-MCAD

With the ferricenium assay the T136A mutant has approximately 20 % of the specific activity of wt-MCAD (each with C_8CoA). Analysis of substrate specificity revealed that the maximal activity of the mutant is shifted to C_8-C_{10}CoA and is lower with C_6CoA (Figure 3, Panel A). The K_m values of T136A-MCAD with the best substrate are higher than those of wt-MCAD (except C_{12}CoA, Table 1) and show a different dependence of chain length (Figure 3, Panel B). The dependence of the catalytic efficiency, v_{max} / K_m, with substrate chain length indicates that C_{10}CoA is preferred for the mutant (Figure 3, panel C).

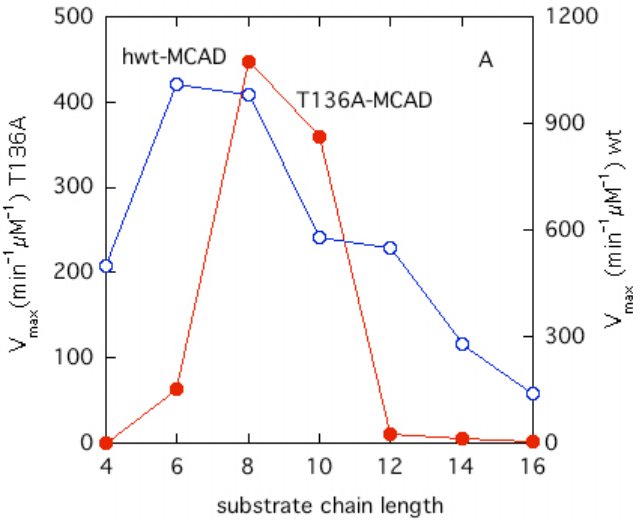

Figure 3. Panel A. Chain-length dependency of activity for T136A-MCAD and comparison with wt-MCAD. Wt-MCAD activities were measured in KPi 0.1 M (pH 7.6) at 25 °C. The mutant (180 nM final concentration) activities were measured in "mixed buffer" containing KCl 250 mM (pH 8). The results for the effect of the chain length on the catalytic efficiency were analyzed using KaleidaGraph program.

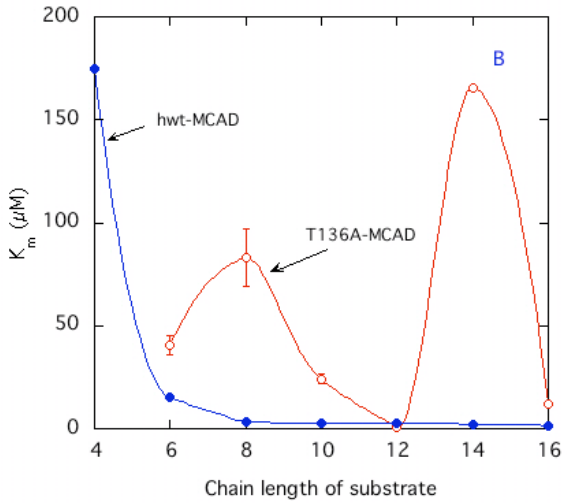

Panel B. Chain-length dependency of K_m values for T136A-MCAD and comparison with wt-MCAD. All activities were measured with the ferricenium assay. The K_m values for T136A-MCAD are larger than those for wt-MCAD. The kinetic parameters of the mutant were calculated by fitting the experimental data to the Michaelis-Menten equation using KaleidaGraph.

Table 1. Substrate chain-length dependence of selected parameters for wt- and T136A-MCAD. Values for wt-MCAD were taken from Nandy et al. (Nandy et al., 1996).

Enzyme	Substrate	V_{max} (min^{-1})	K_m (µM)	V_{max} / K_m ($min^{-1}µM^{-1}$)
wt-MCAD	C_4CoA	500	175	2.9
	C_6CoA	1010	15	67
	C_8CoA	980	3.4	288
	C_{10}CoA	580	2.5	232
	C_{12}CoA	550	2.5	220
	C_{14}CoA	280	2.3	122
	C_{16}CoA	140	1.6	87.5
T136A-MCAD	C_4CoA	0	-	0
	C_6CoA	63	40.7	1.6
	C_8CoA	447	83.2	5.4
	C_{10}CoA	360	24	15
	C_{12}CoA	11.3	1	11.3
	C_{14}CoA	5.5	166	0.033
	C_{16}CoA	1.4	12	0.12

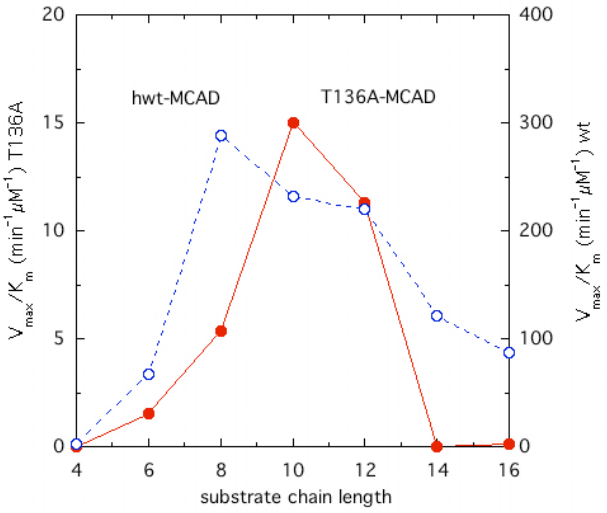

Panel C. Chain-length dependency of catalytic efficiency (v_{max}/K_m) for T136A-MCAD and comparison with wt-MCAD. All activities were measured with the ferricenium assay. The data sets were analyzed by fitting to the Michaelis-Menten equation (see Materials and Methods).

3.1.3. pH dependence of activity for MCAD

3.1.3.1. Role of E376 and E99 in MCAD catalysis

Beinert (Beinert, 1963) and Murfin (Murfin, 1974) have been reported that the activity of MCAD is pH dependent. For study of activity we have used the ferricenium assay described by Lehman (Lehman & Thorpe, 1990). The pH dependence of the activity reflects a pK ≈ 8.2 for wt-MCAD that can be attributed to the ionization of Glu376 (the pK of free Glu-COOH increase from ≈ 4.3 to 8.2 at the active site). The pH dependence of the activities (of wt-MCAD, wt-LCAD and VLCAD with different

substrates) illustrates that the pK's of the enzyme are in the same range with the pH of the mitochondrial matrix (7.8-8.2) (Lemasters et al., 1995).

The second ionizing group at the active center, E99-COOH, also cannot be solely responsible for the dependence (Figure 5) simply because the E99G mutant shows the apparent pK's in the same range as wt-MCAD and has a similar activity. The values of the apparent pK's depend strongly from the substrate chain length (Table 2).

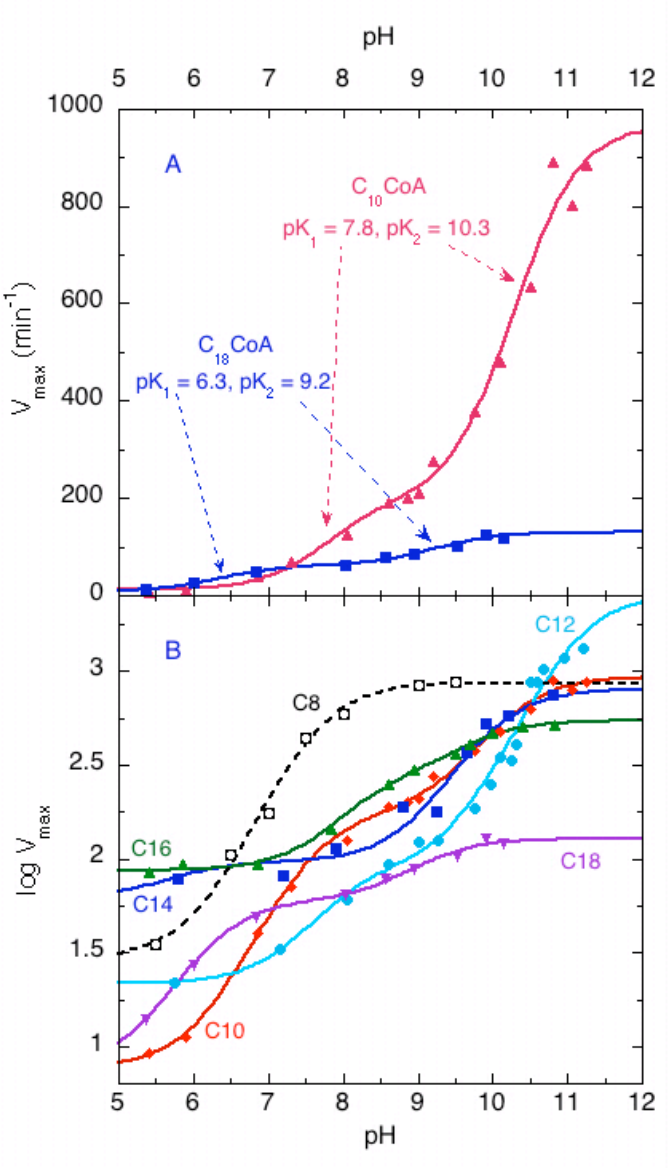

Figure 5. pH dependence of activity (v_{max}) of E99G-MCAD with different substrates.

Panel A. ***Linear representation***
The v_{max} values were obtained using the ferricenium assay (50 mM buffer containing 250 mM KCl at 25 °C). The curves are the best fits obtained using a pH equation (see Dixon equation for two ionizations – Materials and methods) and finite values for v_{max} at lower and high pH.

Panel B. ***Logarithmic representation***
The fits to data points were obtained using a pH equation for two ionizations and finite values for v_{max} at low and high pH. The fit to the data for C_8CoA was obtained using an equation with a single ionization.

Remarkably, while with C_8CoA and C_{14}CoA the activity dependence profile shows a single pK, with another substrates the fits are corresponding to two ionizations (Figure 5, Panel A).

We have investigated the pH dependence of E376H-MCAD activity with C_8CoA. The activity is lower at pH = 6 and increases with pH and the apparent pK is shifted to 9.5 (in wild-type enzyme pK ≈ 8.2; see Fig. 6).

Substrate chain length	pK_1	pK_2	pK_3	pK_4
8	6.1	7.8	-	-
10	6.15	7.5	9.5	10.2
12	7.3	7.9	9.6	11.2
14	5.5	5.7	9	9.9
16	5.4	5.9	8.2	8.9
18	5.3	6.2	8.7	9.1

Table 2. Apparent pK's value obtained from ferricenium assay of E99G-MCAD (15- 30 nM) with C_nCoA (n = 8 ... 18)

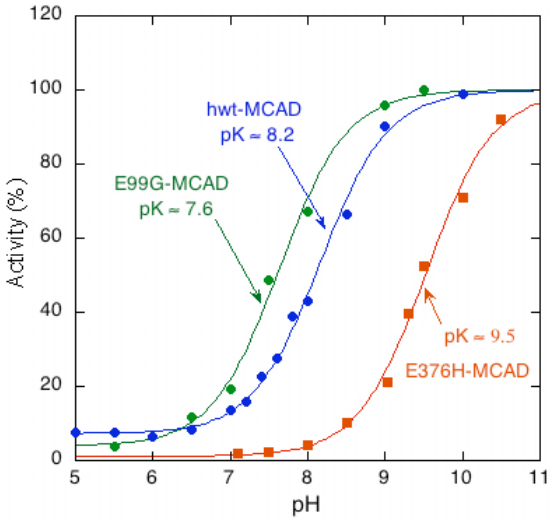

Figure 6. pH dependence of the activity of E376H-MCAD and comparison with wt-MCAD. The velocities are standardized to 100% for comparison. Activity (ferricenium assay) was measured by incubation with 50 µM C_8CoA in 50 mM buffer (see Materials and Methods) containing 250 mM KCl. The maximum/ minimum velocities extrapolated to pH > pK and pH < pK were 13.7/ 2.7 min^{-1} for E376H-MCAD and 885 / 35 min^{-1} for E99G respectively 5800 / 430 min^{-1} for wt-MCAD. The curve for wt-MCAD has been taken from Ghisla et al (Ghisla et al., 1994).

The size of the substrate and the presence of specific functional groups have a profound effect on the active site cavity and some of its prominent properties.

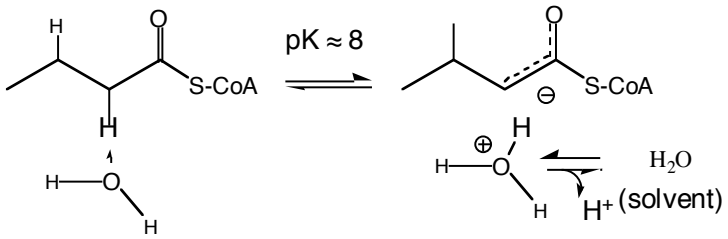

Scheme 1. Self-dissociation of the α C-H in enzyme bound acyl-CoA and transfer of the H^+ to solvent.

In one type of effect the presence of water will be affected, this will modify the dielectric, and this, in turn, will affect ionizations occurring at the active site. In addition it is apparent that the induced changes in protein conformation are also strongly pH dependent, and must reflect ionizations of groups outside the active site cavity.

A remaining possibility is that the observed reactivity is related to the (pH independent) rate of □C-H dissociation that could be mediated by water molecules transferring the abstracted H^+ to solvent (acceptor) as shown in Scheme 1.

3.1.3.2. Contribution of Thr136 and Thr168 in MCAD catalysis

Figure 7 (Panel A) shows the pH-dependence of the activity of T136A-MCAD in comparison with that of wt-MCAD, and documents a shift in the apparent pK of the mutant (0.7 pK units lower). With T136A, ie.e in the absence of the Thr136 H-bond to the flavin N(5) the size of the catalytic cavity is assumed to increase. This could be at the

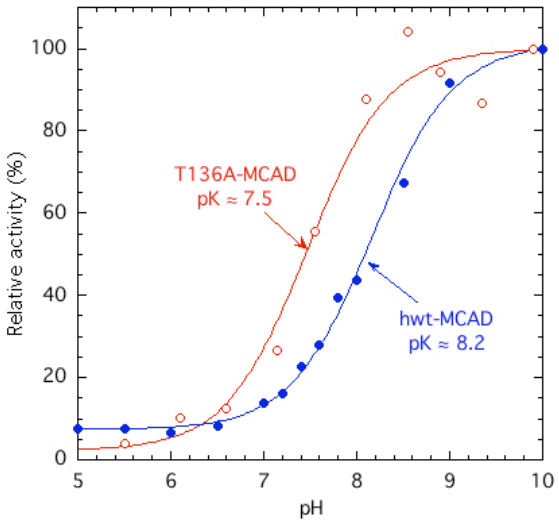

Figure 7. pH dependence of selected parameter of T136A-MCAD and comparison with wt-MCAD. Panel A. pH dependence of activity for T136A-MCAD and comparison with wt-MCAD. The velocities are standardized to 100 % for comparison. Activity of wt-MCAD (ferricenium assay) was measured by incubation with 50 µM C_8CoA in 250 mM KCl / 50 mM buffer (see Material and methods). The activity of the mutant (200 nM) was taken from the maximum velocities resulted from Michaelis-Menten equation. The maximum / minimum velocities extrapolated to pH > pK and pH < pK were 510 / 12 min^{-1} for T136A-MCAD respectively 5800 / 430 min^{-1} for wt-MCAD. The curve for wt-MCAD has been taken from Ghisla et al (Ghisla et al., 1994).

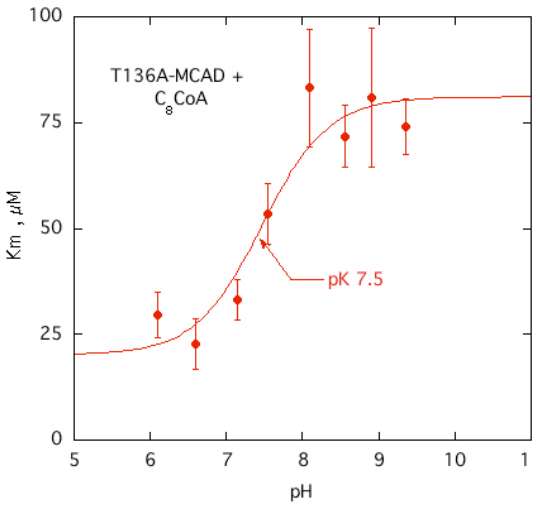

Panel B. pH dependence of K_m for T136A-MCAD. The K_m values were obtained using the *Michelis-Menten* equation. The fits to the data points were obtained using a pH equation (see Dixon equation with one ionization – Materials and methods) and finite values for K_m at lower and high pH.

origin of the lower activity of the mutant (more bound water molecules resulting in decrease of the lypophylicity). The contribution of T136-OH hydrogen bond (with the flavin) is around 1 Kcal·M^{-1}. Interestingly enough, the Km increase in the same fashion with pH (Figure 7 Panel B). The results show that the pK's values derived from the activity/pH and Km/pH profiles are identical.

As reported earlier the activity of T168A-MCAD was less than 20 % the activity of wt-MCAD in the neutral pH range. This activity is markedly pH dependent as is that of wt-MCAD (Küchler et al., 1999). However, when His-Tag enzymes (T168V, T168S and wt-MCAD) were used a similar activity/pH profile resulted. The profile of T168S mutant (wherein the H-bond is retained) is closer to that of wt-MCAD. In the absence of this H-bond (T168V-MCAD mutant) the pK was lowered (0.4 pK units or 0.6 Kcal·M^{-1}).

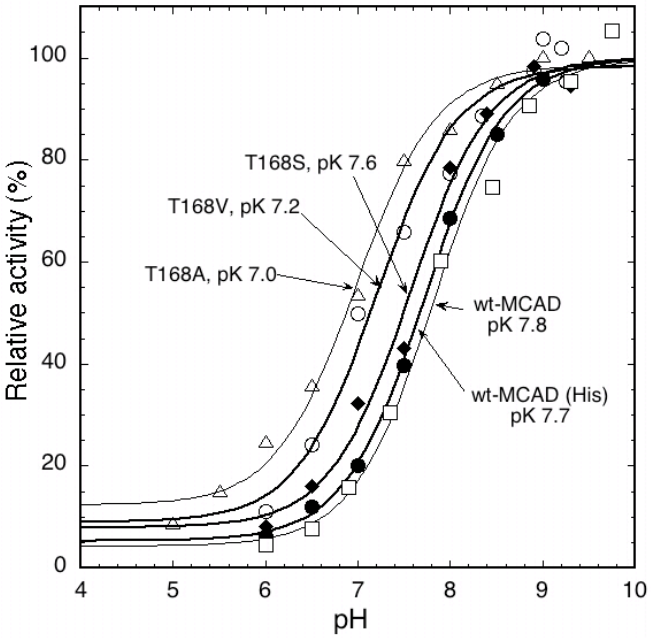

Figure 8. pH dependence of the activity for wt-, T168S- and T168V-MCAD (His-Tag enzymes) and comparison with wt- and T168A-MCAD. The activity was measured using C_8CoA as substrate and in „mixed buffer" containing 250 mM KCl at 25 °C. For wild type-MCAD (60 nM) the data points are the result of a Michaelis Menten analysis. For T168S- (100 nM) and T168V-MCAD (150-250 nM depending on pH) the value were obtained using 200 μM C_8CoA, a concentration that ensures saturation. The curve for T168A-MCAD is shown for comparison and was taken from Küchler et al. (Küchler et al., 1999) The activity values have been normalized to 100 % for the purpose of comparison. The same figure was used to describe the pH dependence of activity in chapter 3.1.3.

In the context of the interpretation of the role of H-bridges Showen et al. write: *"The most common mechanistic description of the nature of the proton-bridging interaction is one in which the binding changes for the primary reaction are physically coupled to the net transfer of a proton across the catalytic bridge"* and *"the formation of a bridge with a proton acceptor can lead to a reduction in the free energy of the activated complex that exceeds the reduction experienced from hydrogen bridging at the same site*

in the preceding reactant state. The result is net transition state stabilization" (Schowen et al., 2000).

3.1.4. Thermal effects and Arrhenius energy of activation

An important decrease in stability of wt-MCAD and mutants with temperature could be observed with the time. For inactivation studies the residual activities of purified human wt- and E376H-MCAD were obtained after incubation of the enzyme at a given temperature without substrate for 15 min (Figure 9). Then activity was measured at 25 °C as described above. The temperature vs. activity profile of both wt- and E376H-MCAD suggested that the stability of the mutant is higher at 30-35 °C and t > 40 °C.

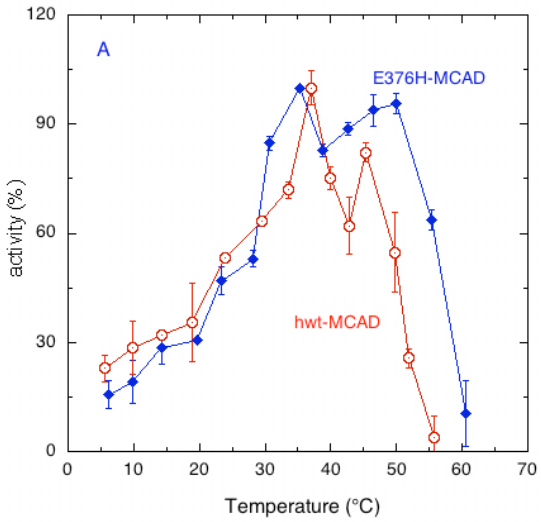

Figure 9. Activity of the wt- and E376H-MCAD are temperature dependent

Panel A. ***Linear representation***
Purified enzymes were incubated in 50 mM Glycine containing 250 mM KCl (pH = 9.5) at temperatures shown for 15 min and activities were then measured using ferricenium assay (160 mM in the final concentration). C_8CoA and C_{12}CoA were the substrates for wt-MCAD respectively E376H-MCAD.

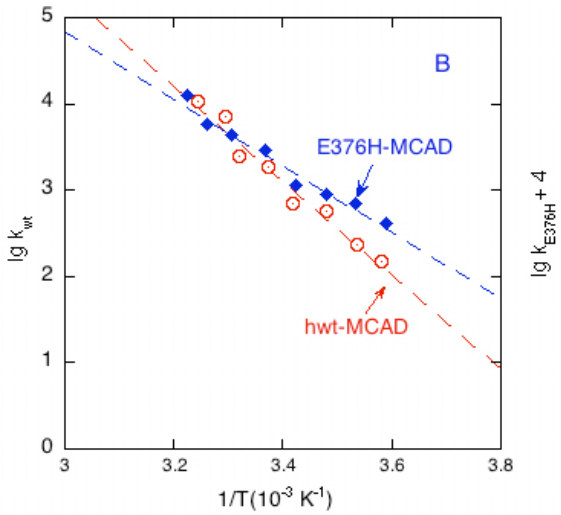

Panel B. ***Logarithmic representation*** Arrhenius activation energies were estimated from the slop of the line as 7.6 Kcal·M^{-1} for wt-MCAD and 10.9 Kcal·M^{-1} for E376H-MCAD (the mutant was more stable at temperature higher than 47 °C and between 30 and 36 °C). The value above 37 °C have been omitted since they correspond to (partial) enzyme denaturation.

The wt-MCAD displays an unusual region of increased stability at 45-50 °C where the activity returns to the level observed at lower temperatures (≈ 30-35 °C). Arrhenius activation energies were estimated as 7.6 Kcal·M^{-1} for MCAD and 10.9 Kcal·M^{-1} for E376H-MCAD. The difference of 3.2 Kcal·M^{-1} may correspond to the stabilization energy provided by □C-H···HOOC-Glu376 H-bond during proton abstraction step.

The time dependence activity of T136A-MCAD with C_8CoA was followed at different temperatures (see Figure 10). The enzyme is quite stable at 25 °C and half-decay inactivation time was shortened for higher temperatures.

Surprisingly, His-Tag MCAD was more stable at 42 °C than the enzyme without His-Tag. With the latter inactivation is approx. 2 times faster (Figure 11). Stability studies with the T168V-MCAD (His-Tag) suggest that the enzyme (mutant and wt-MCAD) still retain almost 74 % of the activity at 42 °C after 4 h at 25 °C (KPi 100 mM, pH 8).

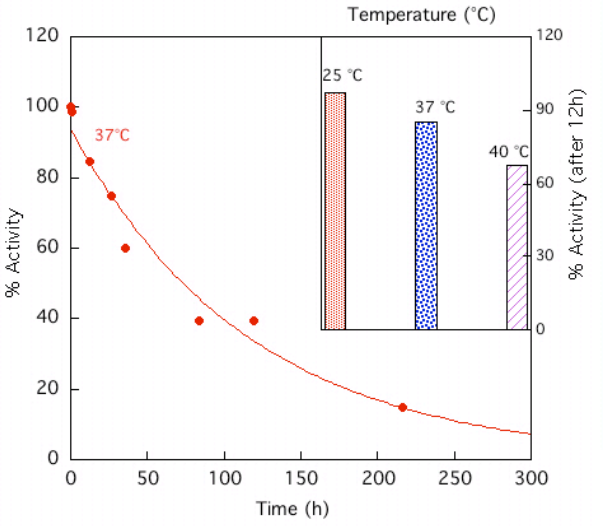

Figure 10. The time dependence of T136A-MCAD activity. The enzyme (13.7 µM) was incubated in "mixed buffer" containing 250 mM KCl at pH 7 and three different temperatures. All the activities were measured with the ferricenium assay at the same pH and 25 °C. The inset compares the remaining activity after 12 h incubation at different temperatures. The mutant is less stable than wt-MCAD.

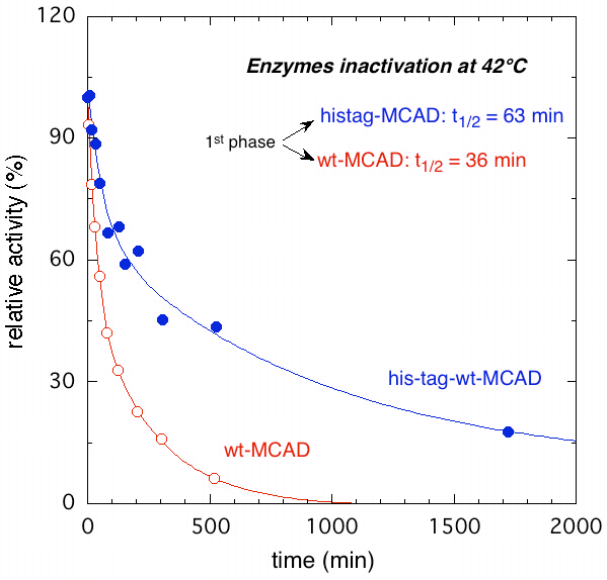

Figure 11. Time dependence of MCAD (with and without His-Tag) activities. The enzymes (2.7 µM) were incubated at 42 °C in the same buffer (Figure 10). All the activities were measured at 25 °C with the ferricenium assay (200 µM dye – final conc.) at pH 7.

3.1.5. DISCUSSION

Glutamate 376 is one of the most important residues in the active site of the MCAD. Site directed mutagenesis studies indicate that in the absence of the base in the active site the enzyme activity is abolished. E376H-MCAD has a lower catalytic efficiency (< 1 % of catalytic efficiency of wt-MCAD). Substrate chain length selectivity of the mutant is shifted to a „higher" substrate (C_{12}CoA).

The distance from the flavin plane to the substrate has a definitory role in H^- abstraction. There are several threonine residues in the vicinity of the cofactor. These residues are anchoring the flavin via H-bond interaction and could affect the orbitals overlapping of the cofactor with the substrate. One similar case was reported for DAAO (T317A mutants shows a decreased affinity for FAD) (Setoyama et al., 2002). Saijo et al. indicate that T136 hydroxyl plays a major FAD-binding of MCAD (Saijo et al., 1998). The absence of this group decreases the catalytic efficiency of the mutant to 5% that of wt-MCAD and affects the chain length specificity.

The pH dependence of the E99G-MCAD activities with different substrates reveals some unexpected profiles. Two pK values are observed for almost all the substrates (except C_8CoA and C_{14}CoA). The $pK_a \approx 9.5$ for E376H-MCAD could be mainly attributed to the imidazol group of His376. The $pK_a \approx 7.6$ for E99G-MCAD is 0.6 pK units lower compared to that found in wt-MCAD corresponding to a difference of ≈ 0.8 Kcal·M^{-1}, thus the contribution of the E99 base is smaller but can't be neglected. A similar difference was observed for T136A-MCAD (0.7 pK units $\approx$ 1 Kcal·M^{-1}) supporting the role of the H-bonds at the active site.

The activation energies derived from Arrhenius plots are higher for E376H-MCAD the mutant being much stable than wt-MCAD at higher temperatures. T136A-MCAD is quite stable relative to wt-MCAD (after 1 weak the activity was practically not changed).

Purification of His-Tag MCAD from *E.coli* extracts was much faster and the presence of 6His-Tag to the C-terminus has a small influence on catalytic properties of the enzyme. Moreover, His-Tag MCAD is slightly more stable than "normal" recombinant MCAD.

3.2. Studies with the active site E376Q-MCAD mutant

3.2.1. On the role of the active site base in MCAD catalysis

MCAD is selective for substrates of medium chain length, preferring octanoyl- and decanoyl-CoA, and catalysis their dehydrogenation to yield trans enoyl-CoAs. This reaction has been intensively studied in the past 20 years (Ghisla et al., 1984; Ikeda et al., 1985; Pohl et al., 1986; Schopfer et al., 1988; Engel, 1992; Hazekawa et al., 1995; Vock et al.,1998; Engst et al., 1999; Ghisla & Thorpe, 2004; Kim & Miura, 2004), and is initiated by attack of the active center Glu376-COO^- onto the substrate αC-H (Scheme 1, A). The pKa of this function is lowered by some 10 pK units upon binding to MCAD, mainly as a result of formation of two tight H-bonds of the thioester carbonyl at the active center (Engst et al., 1999).

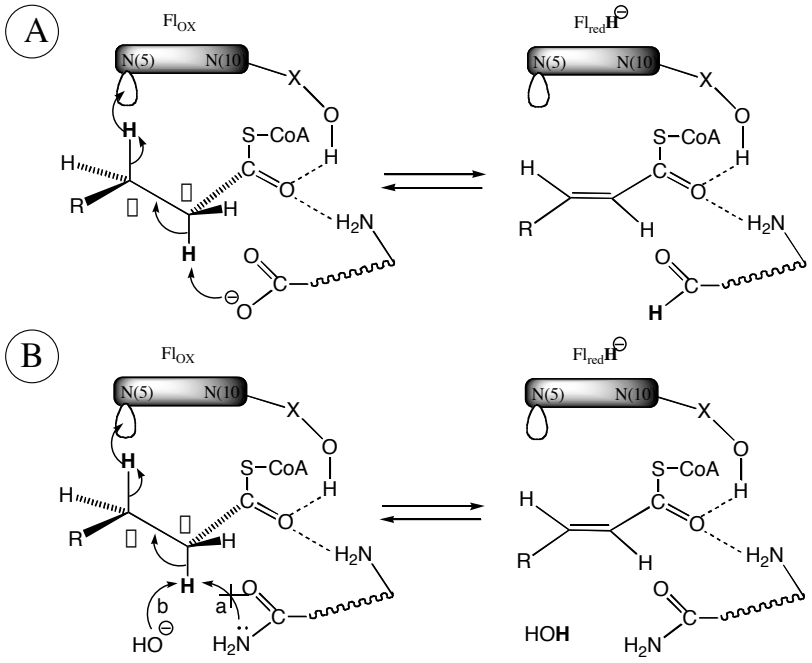

Scheme 1. Chemical mechanism of α,β-dehydrogenation exemplified by MCAD
Panel A. Glu376-carboxylate is one of the main components of the driving force of the reaction.
Panel B. In the E376Q-MCAD proton abstraction by the water (HO^-) could be the driving force of the reaction.

In addition electronic ground state interactions with the oxidized flavin contribute to this activation (Nishina et al., 2003; Gradinaru et al., 2005). Glu376 was identified as the base initiating catalysis (Powell & Thorpe, 1988; Bross et al., 1990) based on the effects induced by the Glu376Gln substitution (Bross et al., 1990).

Interestingly within the ACAD family the function of Glu376 can be assumed by a different Glu residues that is placed topologically at the same position, but lye on different segments of the protein chain (Nandy et al., 1996) (the Glu residue placed in position 261 for long chain- and 254 for isovaleryl-CoA dehydrogenase (Djordjevic, et al., 1994; Mohsen & Vockley, 1995)). A surprising finding emerging from the study of the Glu376-MCAD mutatants (Engst et al., 1990) was that the Glu376Gln mutant has an activity in the dehydrogenation reaction (Scheme 1) that is some five orders of magnitude lower than that of wt-MCAD but has finite values (Bross et al., 1990). This activity has been confirmed by independent studies (Gopalan & Strivastava, 2002). Since it is unlikely that the amide group of glutamine functions as a base abstracting a H^+ in the type of reaction depicted in Scheme 1, this activity has remained a puzzle. Its solution constitutes a mechanistic challenge that is expected to be of basic importance for the understanding of □,□ -dehydrogenation. It should be noted that activity also remains in the case of replacement of Glu376 with other residues such as Gly, His, Cys and Asp (Engst et al., 1990; Ankele et al., 1991; Gradinaru et al., 2002). This residual activity is thus probably not due specifically to the Gln376 group but is brought about by effects of (side chains) in the MCAD active center.

In this context it should also be noted that the active site of MCAD is characterized by several unusual properties: it has a pronounced hydrophobic character, this being a factor contributing to the considerably high pKa ≈ 6-8 of Glu376-COOH (this value depending on the presence of ligands) (Rudik et al., 1998; Vock et al., 1998; Engst et al., 1999). The cofactor flavin is effectively shielded from solvent as reflected by the extremely low rate of oxygen reactivity of its reduced form in the presence of product (DuPlessis et al., 1998). In the present chapter I have attempted to uncover the features that bring about the unusual reactivity of Glu376-MCAD mutants and to shine some light into its mechanisms. During the study we have come across some unexpected and unusual properties of MCAD that pertain to the access and exchange of solvent borne H^+ / HO^- at the active center and that we consider to be of general mechanistic interest.

3.2.2. Interaction of Glu376Gln with substrate

The absorption spectrum of the mutant enzyme (Figure 1) is essentially identical to that of wt-MCAD (Crane et al., 1956; Hall & Kamin 1975; Thorpe et al., 1979) under similar conditions suggesting a minimal differences in polarity at the active center.

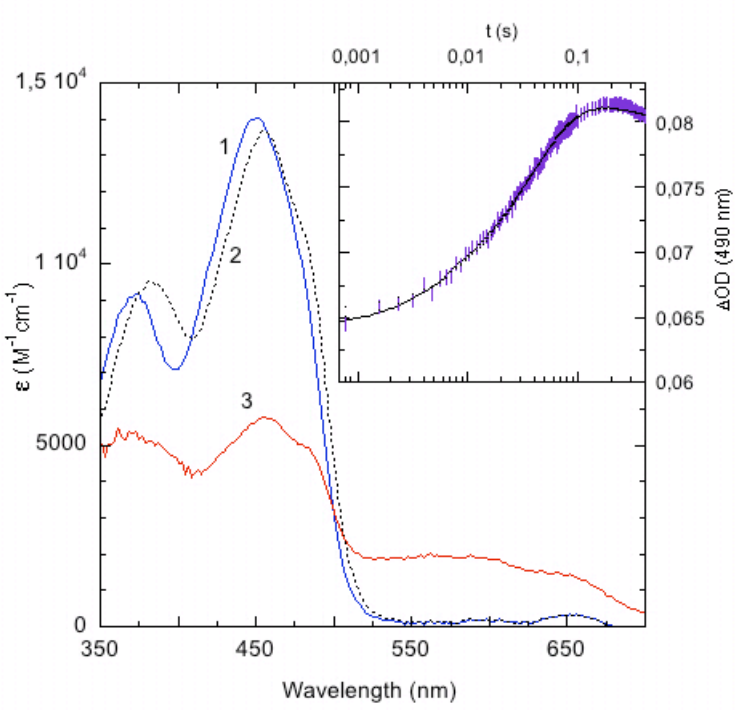

Figure 1: Rapid spectral changes accompanying binding of C_8CoA to Glu376Gln-MCAD. The spectra were recorded with the stopped-flow spectrophotometer. The enzyme, 12 µM was prepared in "mixed buffer" containing 250 mM KCl (pH 9.3). E376Q-MCAD was reacted with 8 equivalents C_8CoA (96 µM final) in the same buffer at 25 ºC. Curve 1 is the spectrum of the enzyme *before* mixing. Curve (2) was obtained at ≈ 0.8 ms upon the end of flow. Curve (3) was recorded after 150 s. The insert shows the differences between the aforementioned curves. Note that curve (1-2) does not reflect formation of the long wavelength band and flavin reduction. In contrast this is the case for curve (2-3).

With wt-MCAD substrate binding cannot be studied since its rate is of the same magnitude as that of the following dehydrogenation reaction. With the E376Q mutant however, the rate of the latter is slower by at least 4-5 orders of magnitude; this mutant is ideally suited to investigate the processes involved in substrate binding. An assessment of the binding kinetics is also required for a proper study of the following steps with E376Q mutant. Thus, binding of octanoyl-CoA was studied with the stopped-flow instrument (Figure 2). Figure 1 shows that the interaction with substrate perturbs the spectrum of the oxidized flavin in a manner that is similar, but not identical, to that observed upon binding of a variety of "neutral" ligands to wt-MCAD (Pohl et al., 1986) (ligands that

carry a negative charge and give rise to CT-transitions induce different perturbations (Thorpe & Massey, 1983; Lau et al., 1988; Wang & Thorpe, 1991; Vock et al., 1998)).

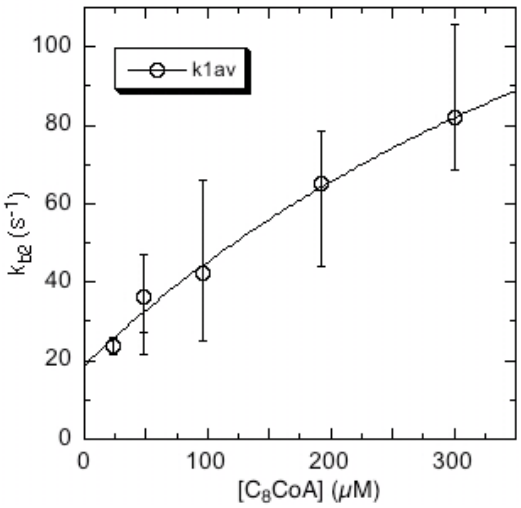

Figure 2. Effect of the substrate concentration (C_8CoA) on the reduction rate of the flavin. The reaction was performed in the same conditions as in Figure 1 (legend). The data points (o) are the average of 4-8 single measurements that were analyzed with the program Specfit that carries out a global wavelength analysis. The bars indicate the scatter of the single data points and the line is the fit obtained using an algorithm based on Michaelis-Menten equation.

It is noteworthy that the perturbations of the flavin spectrum signal a transition to a more hydrophobic environment as evidenced by the batochromic shift of the main absorbtion band, and its higher resolution (Muller et al., 1973).

Binding can thus be followed based on the difference spectra depicted in the insert of Figure 3. The rates of the spectral perturbations are dependent on the concentration of substrate and follow the same kinetic pattern at all wavelength. The insert of Figure 1 shows a representative trace recorded at 490 nm, one of the maxima of the difference spectra (Figure 3). They consist of an absorbance increase up to ≈ 0.1 s, followed by the beginning of the reduction phase.

The increase is not strictly monophasic. Under the specific conditions of Figure 3, i.e. at a [C_8CoA] = 100 μM at its onset 5-10 % of the changes occur at a rate that is approx. one order of magnitude faster than that of the main phase of absorbance increase. At higher [C_8CoA] this minor phase cannot be observed and was thus neglected for primary analysis. Secondary analysis (Figure 4) was done by the method of Strickland et al. (Strickland et al., 1975) that assumes a two step process (Scheme 2).

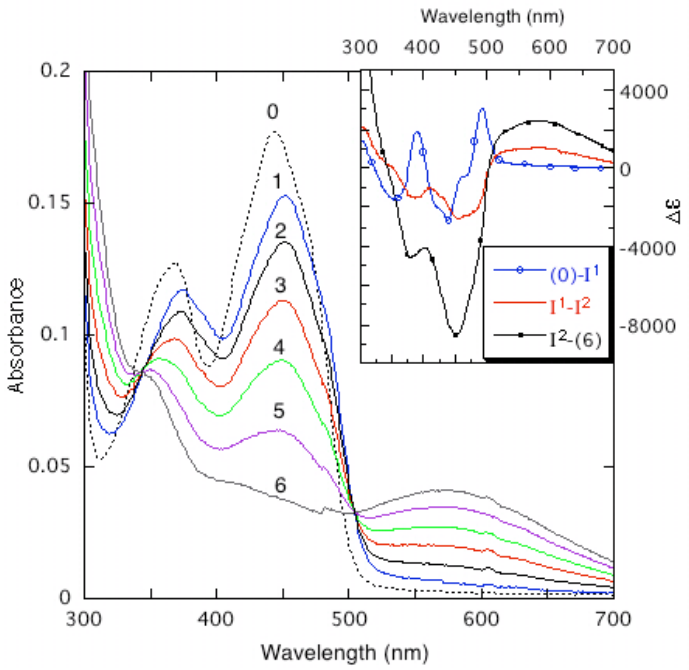

Figure 3. Course of the enzyme flavin reduction by C_8CoA. Glu376Gln-MCAD, 11.7 µM was in „mixed buffer" containing 250 mM KCl (pH 9.25). The enzyme was reacted in anaerobic conditions with 96 µM C_8CoA and the course of the reaction was followed at 4 ºC by repetitive scanning in a conventional spectrophotometer. Curve (0) is the enzyme before addition of substrate. Curves 1, 2, 3, 4, 5 and 6 are representative curves obtained after 12, 76, 236, 540, 1104 and 3588 s. The set of the original curves was analyzed using the program Specfit that performs a kinetic multi wavelength analysis and estimates the spectral components. In this case spectra (0) and (6) were selected as starting and end points and the program identifies the spectra of two intermediates for a 3-phasic process. The first intermediate (I^1) corresponds to curve (2) in Fig. 1, the second (I^2) is intermediate between curves (1) and (6) (not shown). The inset shows the difference spectra between the starting species and I^1 that corresponds to that of Fig. 1 insert. Note that the spectral changes occurring during phases 1 and 2 of the reduction process are very similar but not identical (insert).

The behavior reflects formation of a first, equilibrium complex E_{ox}~~S via K_{b1} (680 ±170 µM). In a second equilibrium E_{ox}~~S is converted to E_{ox}~S. The value at the saturation in Figure 2 is k_{b2} (207 ± 35 s^{-1}; the forward step), and the ordinate intercept is the reverse rate constant k_{-b2} (19 ±1 s^{-1}). This yields an overall binding constant $K_{d,b}$ ≈ 60 µM under the conditions of Figure 4.

The following steps $k_{r1,2}$ (Scheme 2) are much slower and do not interfere with this analysis. These are followed in a conventional spectrophotometer and their spectral course under anaerobic conditions is depicted in Figure 3. This consists in a slow decrease of the absorbance of oxidized flavin that corresponds to its reduction and leads isosbestically to a species with spectrum corresponding to that of the reduced enzyme-C_8enoyl-CoA complex described for wt-MCAD (Kumar & Srivastava, 1994).

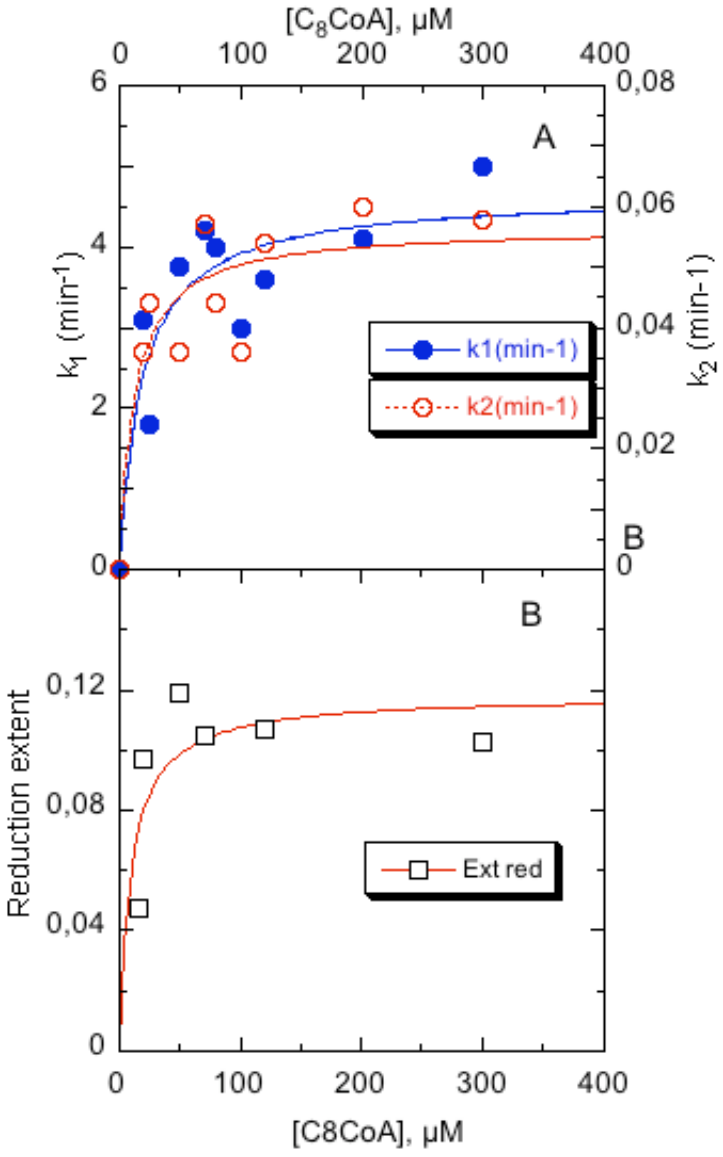

Figure 4. Dependence of the observed rate of enzyme flavin reduction on the substrate (C_8CoA) concentration. The mutant (E376Q-MCAD), 11 µM was in 50 mM KPi containing 0.3 mM EDTA, 10% glycerol at pH 7.6 and 25 ºC. The enzyme was reacted anaerobically (glucose 10 mM / glucose oxidase 0.2 µM) with C_8CoA. The course of the reaction was followed photometrically.
Pane A. Both of the rates are increasing in the same fashion with substrate concentration
Pane B. Reduction extent (450 nm) has maximum values at higher concentration of the substrate

As detailed below, the course of the reduction reaction consists of two phases of similar extent with rates (k_{r1} and k_{r2}) that differ by a factor 3-10 depending on the conditions. The rates of the two phases show saturation behavior (Figure 4) reflecting an apparent $K_d \approx$ 20-30 µM. This value is in reasonable agreement with the equilibrium constant $K_{d,b}$ described above. The extent of reduction encompassing both phases also is dependent on the concentration of C_8CoA. Thus with [E376Q-MCAD] ≈ [C_8CoA] ≈ 10^{-5} M approx 50 % "reduction" is observed and the [C_8CoA] dependence of the

reduction rates $k_{r1,2}$ reflects an interaction constant ≈ 15 μM that is again in reasonable agreement with the estimates of $K_{d,b}$ described above. This also demonstrates that the steps K_{r1} and K_{r2} of the Scheme 2 must be reversible, albeit at very slow rate. When experiments are carried out with a > 5 fold molar excess of substrate, the extent of formation of the reduced enzyme-product complex, as reflected by its CT-absorbtion in the 550-600 nm region, is smaller. This is attributed to exchange of product with excess substrate in the reduced enzyme-substrate complex as is also observed with wt-MCAD (Schopfer et al., 1988). Based on these findings and on the observation that at [C_8-CoA] > [E376Q-MCAD] also a decrease of reaction rates occur, most kinetic studies presented in this work were carried out with a [C_8-CoA] = 8•[E376Q-MCAD] ≈ 80 μM. The spectral perturbations occurring upon substrate binding at 25 °C (Figure 1) and 4 °C (Figure 3) are similar but not identical. This pertains in particular to the ratios of the difference peaks and the extinction coefficients. The overall spectral course of the ensuing flavin reduction reaction is similar to that observed with wt-MCAD (Kieweg et al., 1997). However, with the important difference that the rates are some 5 orders of magnitude slower. A further difference, compared to wt-MCAD is the effect of oxygen on the apparent rates of reduction. Specifically, the second phase, k'_{r2} that is 2-3-fold slower under anaerobic conditions and depending on the pH. This is attributed simply to the competition with oxygen reoxidation that become important when the rate of the second phase is very slow ($t_{1/2}$ > 10 min at pH 9.3) (Wang & Thorpe, 1991).

3.2.3. Analysis of primary data and estimation of rate constants

As discussed above, and in accordance with studies by others carried out with substrate analogs (Schopfer et al., 1988; Johnson et al., 1992; Qin & Srivastava, 1998; Peterson et al., 2000), the interaction of substrate with MCAD is a multistep process (Scheme 2). The separation in kinetic terms of rates involving binding (suffix “b”) from those that involve substrate dehydrogenation and concomitant flavin reduction (suffix “r”) is of about one order of magnitude and thus much better in the present case compared to wt-MCAD. However, and since the rates of these steps vary depending on substrate concentration, separation is not always sufficient to allow a clear-cut distinction. With wt-MCAD flavin

reduction in general consists of two phases (Reinsch et al., 1980; Pohl et al., 1986; Schopfer et al., 1988). The problems and difficulties inherent to the evaluation of this situation have been pointed out previously and have also been discussed recently in their basic aspects by Maniscalco et al (Maniscalco et al., 2004). Data such as those depicted in Figure 3 (experiments conducted at 4 ºC and absorbance changes at 450 nm) can be fitted using an equation with 3 exponential terms (equation 5a; Materials & Methods). This procedure yields rate constants that are referred to as k'_{b2}, k'_{r1}, and k'_{r2} and are listed in Table 1.

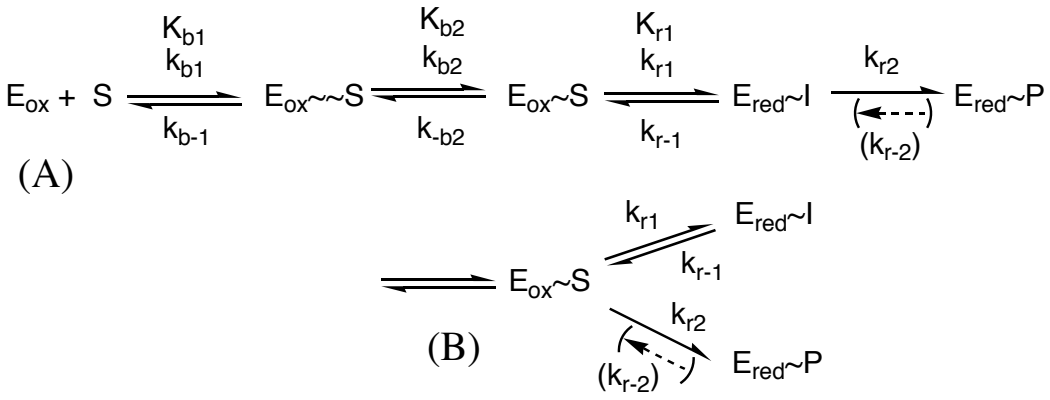

Scheme 2. Minimal kinetic scheme describing the steps involved in the reaction of E376Q-MCAD with the substrate C_8CoA. Processes describing substrate binding carry the suffix "b" and those involving reduction of the flavin cofactor the suffix "r". E_{ox}~~S and E_{ox}~S are substrate complexes of oxidized enzyme. E_{red}~I and E_{red}~P are the first and the second species observed during flavin reduction where E_{red}~P is the complex of reduced enzyme with octenoyl-CoA. (A) and (B) refer to alternative kinetic sequences occurring sequentially or in parallel.

For traces obtained at 25 ºC two exponential terms are sufficient and yield k'_{r1} and k'_{r2}, the first rapid phase (binding, k'_b) being too fast to be assessed. For the reaction at 4 ºC the tree phases are assigned as follows: k'_b reflects the "tail" of the absorbance changes occurring during substrate binding (see rapid kinetic experiments described above and Figure 1). k'_{r1}, and k'_{r2} reflect the two phases of enzyme flavin reduction. The values of k'_{r1} and k'_{r2} are separated by factors of 3-10, the exact ratio depending on the conditions and specifically on the KIEs associated with k'_{r1} and k'_{r2}. In particular when the separation tends towards the lower value clearly a borderline situation occurs.

In addition, steps K_b and K_{r1} constitute equilibria for kinetic purposes (see dependence of [E_{red}~P] from [C_8-CoA] described above and Figure 2). As pointed out elsewhere, the consequence of this is an uncertainty in the interpretation of an exponential apparent ‘‘k’’ and in the attribution to specific mechanistic events.

In view of this we have carried out a comprehensive simulation analogous to that reported previously for the reaction of wt-MCAD with the substrate butyryl-CoA (Schopfer et al., 1988; Maniscalco et al., 2004). It should be stressed that the term “simulation” refers to the procedure implemented in the global analysis program Specfit®. In our case this procedure consists in a gradual approach in which some of the 15 variable parameters listed in Scheme 2A are optimized in successive steps, while the others are held “fixed”. The detailed criteria and procedure on which this is based are outlined in the methods section. Briefly the rates of the binding steps were taken from the rapid reaction studies (Figure 2), those of steps involving enzyme reduction (Figures 1 and 3) were subjected to simulation while k_{r2} was treated as irreversible.

The values obtained from the Specfit based simulations of spectra (300-700 nm) *vs* time profiles were used to simulate traces obtained at single wavelengths (450 nm), in particular those for the study of proton inventories (see below). Examples of the simulations are shown in Figure 5 exemplarily for 0, 45 and 96% D_2O, and the corresponding data are collected in Table 1. Simple visual inspection of Figure 5 evidences a conspicuous SKIE, the magnitude of which varies somewhat with time, but is of the order of 6-8. The panel representing the residuals shows that the deviation of experimental data and simulation trace is < 2 % and demonstrates the absence of substantial systematic errors. Similar results were obtained throughout the 0-100 % D_2O range (n fraction D, Figures 3, 6). As a control a fit (3-exponents) of the simulation data was done; the obtained trace is practically superimposable to the fit of the experimental data points (not shown, see data in Table 1). This is a further and clear demonstration of the possible ambiguity of analysis based on “simple” multiexponential terms.

The traces for 0, 45 and 96 % D_2O (Figure 5) and at the other “n” values were simulated satisfactorily based on Scheme 2A using the same overall K_d (i.e. K_{b1} x K_{b2}) and the same rates for the single binding steps. This suggests that an IE on binding, if present, is < 1.1. Comparison of the standard deviation and sum of squares parameters

listed in Table 1 for the simulations without and with a finite k_{r-1} shows consistently better values for the latter.

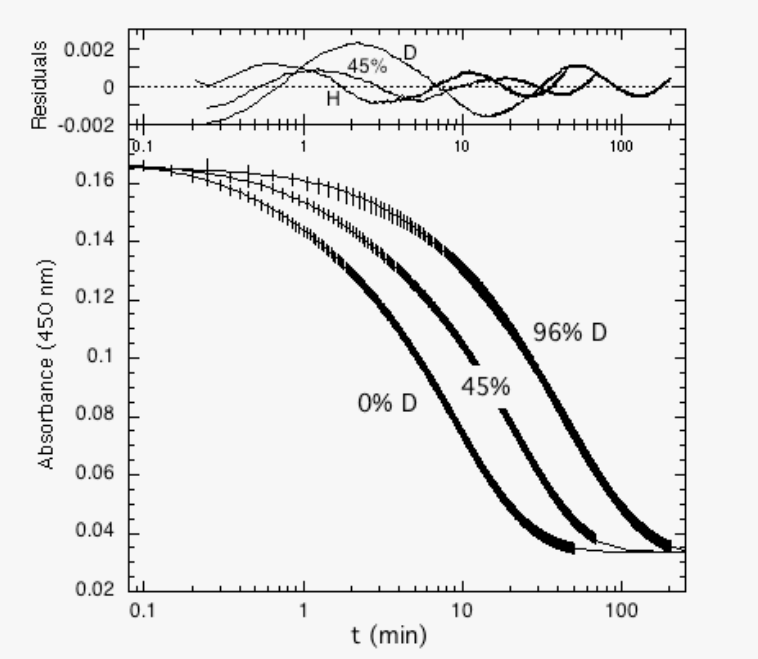

Figure 5. Analysis of absorbance changes vs. time for the reduction of the enzyme flavin in Glu376Gln-MCAD. Glu376Gln-MCAD, 11.7 μM was in "mixed buffer"containing 250 mM KCl at pH 9.25. The enzyme was reacted anaerobically with 96 μM C_8CoA and the course of the reaction was followed at 4 ºC; the absorbance changes were recorded at a single wavelength (450 nm). (l) represents the single data points. The curves ( ) are the results of simulation carried out using SpecFit., and based on Scheme 2 (see text for details). The data and trace for 45 % D_2O were expanded by 6 % and normalized to the same starting point as the other traces for better comparison. The top of the figure shows the residuals. The parameters obtained from this analysis are listed in Table 1.

The occurrence of a true equilibrium for the steps K_r is also required by the dependence of the extent of final reduction from the concentration of substrate (see above). In contrast to this k_{r2} can be treated as being irreversible for practical purposes ($k_{r2} >> k_{r-2}$). This follows from the observation that enzyme reduction goes to completion in the presence of a small (≈ 8-fold) excess C_8CoA, i.e. that in the final spectra E_{ox} is practically absent (Figure 3). The rates k_{r1} and k_{r2} obtained from simulations are significantly larger compared to those obtained from 3-exponential fits. This is due to the fact that reverse steps are ignored in the latter procedure. The simulation can be performed also based on a kinetic scheme in which k_{r2} and k_{r1} occur in parallel and branch at the locus of E_{ox}~S (Scheme 2B). This case, however, requires $k_{r-1} > k_{r1}$, it is less accurate with respect to the extinction coefficient of E_{red}~I and yields overall simulations of inferior quality.

Tabel 1. Parameters obtained from the evaluation of data & traces of Figure 5

Parameter	H_2O			96 % D_2O		
	Value	Error (±)	%	Value	Error (±)	%
Ph.1 ΔOD	0.025	0.0002	0.8	0.011	6.8e-05	0.6
k_1 (min^{-1})	1.08	0.02	1.8	0.80	0.008	1.0
Ph.2 ΔOD	0.075	0.003	4.0	0.092	0.0005	0.5
k_2 (min^{-1})	0.117	0.003	2.5	0.03	9.4e-05	0.3
Ph.3 ΔOD	0.039	0.002	5.1	0.038	0.0004	1.0
k_3 (min^{-1})	0.030	0.004	13.3	0.0086	0.00015	1.7
End point	0.026	0.0014	5.4	0.026	0.0001	0.4
Chisq	4.7e-05			4.3e-06		
R^2	0.99993			1		
1/2	9			27		
2/3	4			3.5		

This suggests that the sequential model depicted in Scheme 2A is qualitatively better, as was similarly concluded earlier for the reaction of wt-MCAD with butyryl-CoA (Schopfer et al., 1988).

The picture emerging from analysis of the data obtained at 25 °C is quite different with respect of the reversibility of k_{r1}. In this case both fitting with a two-exponent equation and simulation with irreversible k_{r1} and k_{r2} yields much superior results compared to the case with k_{r-1} being $\geq k_{r2}$. The two sets of data (simulation vs. fitting - not shown) yield comparable results both in terms of the absolute values of rates and dependency from *n*. However, those from simulation have better error parameters, show a smaller degree of scatter and reflect a larger KIE.

An important conclusion to be drawn from comparison of the two types of analysis of primary data (exponential fitting vs simulation) is that in the first case an accurate attribution of rates of specific magnitudes to individual steps is not feasible. This is so in particular when reversible steps occur in the system (Scheme 2) and the separation of the rates of individual steps is insufficient (< 5-fold). On the other hand it appears that KIEs will be reflected in k'_r rates with sufficient accuracy to permit their

qualitative use in specific mechanistic studies and in particular for comparative purposes (see below).

3.2.4. pH dependence of Glu376Gln-MCAD reduction with substrate

Since substrate dehydrogenation does require H^+-dissociation from the substrate □C-H in absence of a specific base (see Introduction), it was anticipated that this would require involvement of solvent or HO^-. The rates of enzyme reduction were thus studied in the accessible pH range 6.5-10. Figure 6 depicts the course of reactions conducted either in the H_2O or D_2O.

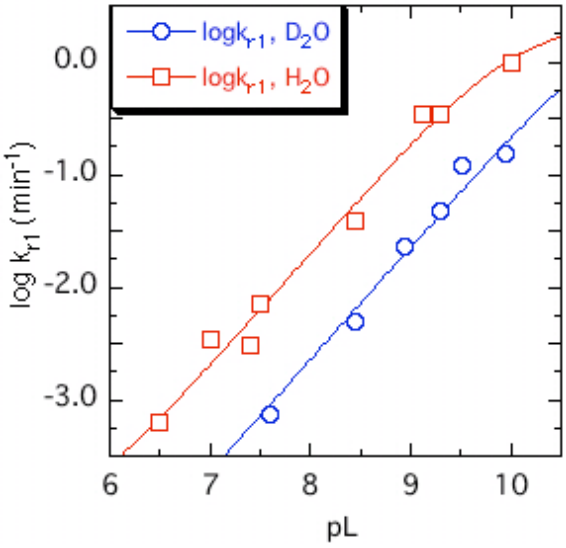

Figure 6. Logarithm of the flavin reduction rates (of Glu376Gln-MCAD in H_2O or D_2O) as a function of pH. The reactions were conducted as described in the legend to Figure 3 either in H_2O or in 96% D_2O buffers; the latter were obtained by diluting a concentrated enzyme solution into D_2O. pL for D_2O solution is pH_{obs}+0.4. The lines are the fits obtained using Dixon equation (Dixon & Webb, 1979).

It is demonstrates that the rate of the first reduction phase k'_{r1} (Scheme 2) increases linearly with HO^- up to ≈ pH 10, where a "break" (decrease in slope) is probable. While the specific data shown in Figure 3 are ambiguous with respect to a "break", such a behavior was observed at 25 ºC, and also for k'_{r2} (not shown), thus giving support to this interpretation.

Comparable "breaks" are observed clearly with the mutants described in the next section. Whether this "break" would reflect protein inactivation, a specific microscopic pK or a change in rate-determining step cannot be deduced and its elucidation is beyond the purpose of the present study.

The pH dependence of k'_{r2}, is similar (not shown) in that it shows the same slope. However, at pH < 8 k'_{r2} is too slow to be assessed reliably ($t_{1/2}$ > 3 h). The analogous pH dependence of k'_{r2} was also studied in D_2O. The slopes for H_2O and D_2O are parallel and

reflect a SKIE ≈ 8.5 over the whole accessible pH range. The same behavior was also observed at 25 ºC for H_2O and D_2O where the isotope effect is ≈ 3-4.

3.2.5. pH dependence of the reduction of Glu376Gly- and Glu376Gln+Glu99Gly-MCAD with C_8CoA

This study was carried out to: a) assess the possible role in α-C-H proton abstraction of Glu99, a group with potential base functionality that is also present at the "bottom" of the active center (Kim et al., 1993); b) to gain information on whether the activity observed with the Glu376Gln mutant is specific to the 376Gln amide group itself. The pH dependence of the enzyme flavin reduction rates for these mutants was measured as described above for Glu376Gln-MCAD under anaerobic conditions. The dependence of k'_{r1} from pH is depicted in Figure 6. With the Glu376Gln+Glu99Gly-double mutant there are significant differences compared to Glu376Gln-MCAD. First the rate of the first phase is approx two-fold faster and it shows a much clearer indication to attain a constant, pH independent level above pH 9 with a corresponding „break" (Figure 7). Further, while the rate of the Glu376Gln mutant decreases by approx. 4 orders of magnitude from pH 10 to 6, with the double mutant the decrease is only ≈ 50-fold in the same range, and at low pH there is clear indication of a "second break" that leads to a pH independent rate at pH < 7. The two breaks reflect apparent pK's ≈ 7.4 and ≈ 9.0. Over the whole pH range, the rate of the double mutant is substantially higher compared to that of Glu376Gln-MCAD.

Most unexpectedly the Glu376Gly-MCAD mutant shows an activity *vs* pH profile that has a substantially different couse compared to that of Glu376Gln-MCAD and Glu376Gln+Glu99Gly-MCAD. First, its "activity" in the dehydrogenation reaction is approx. 2 orders of magnitude higher at pH 6-7 compared to Glu376Gln-MCAD. Second, this activity then decreases above pH ≈ 7.5 reflecting an apparent pK ≈ 8.6 (Figure 7). The data points at pH > 10 are compatible with a second "break" with a pK around pH 9.5, the fit based on two apparent pK's (Figure 7, curve b) being much superior to that with a single one (c). At high pH the activity of this mutant is approx. 1/10 of that of Glu376Gln-MCAD.

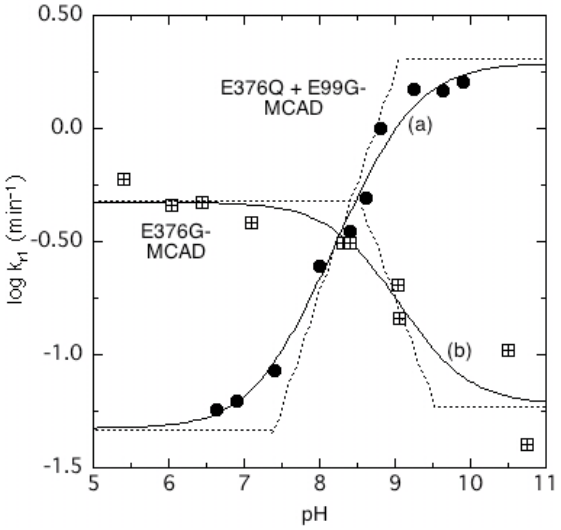

Figure 7. pH dependence of the flavin reduction rates for Glu376Gln+Glu99Gly-MCAD and Glu376Gly-MCAD.
The reactions were conducted in "mixed buffer" containing 250 mM KCl at 25 °C. Reduction of E376Q /E99G-MCAD (10 µM) with 10 equivalents of C_8CoA was performed in aerobic conditions and E376G-MCAD (6.5 µM) was reacted with 50 µM substrate in the presence of 0.2 µM glucose oxidase and 10 mM glucose (anaerobic conditions). The (—) lines are the fits based on Dixon equation (Dixon & Webb, 1979). The dashed lines represent segments with slope = 1 or 0.

3.2.6. Proton inventory of Glu376Gln-MCAD reduction with the substrate octanoyl-CoA

Based on the hypothesis, that dehydrogenation with the Glu376 mutants reflects the rate of "spontaneous" or H_2O/HO^- assisted dissociation of the substrate □C–H we have attempted to gather information of the mode of transfer of the resulting H^+ to solvent (or solvent borne acceptors). Proton inventories can yield useful informations on such processes (O'Leary et al., 1981; Schowen & Schowen, 1982; Pollard-Knight & Cornish-Bowden, 1984; Cho et al., 1994; Karpefors et al., 2000; Schowen et al., 2000; Maniscalco et al., 2004) and are obtained by measuring the dependence of kinetic rates from the fraction n = $[H_2O]/[D_2O]$, the atom fraction of deuterium in the solvent. The data obtained by this procedure were then used to obtain the proton inventories depicted in Figs 8 and 9, where the dependence of k_{r1}, k_{r-1} and k_{r2} from "*n*" are depicted. It should be pointed out that during the course of measurements no exchange of H at the positions □C-H or ßC-H occurs. This was verified by incubating C_8CoA (40 mM) in an NMR tube in the presence of Gln376Glu-MCAD (0.5 μM) or in its absence at pD 7.6 and 25 °C. These conditions are similar to those employed earlier to study the rates of hydrogen exchange at these same positions by ^{1}H-NMR in the presence of wt-MCAD (Ghisla et al., 1984).

The data points obtained at 4 °C and 25 °C (Fis 8 and 9) are fitted using equations 27, 19, 17b respectively 18 (see Materials & Methods) (Venkatasubban & Schowen, 1984). The various parameters obtained from the fitting are listed in the Table 2.

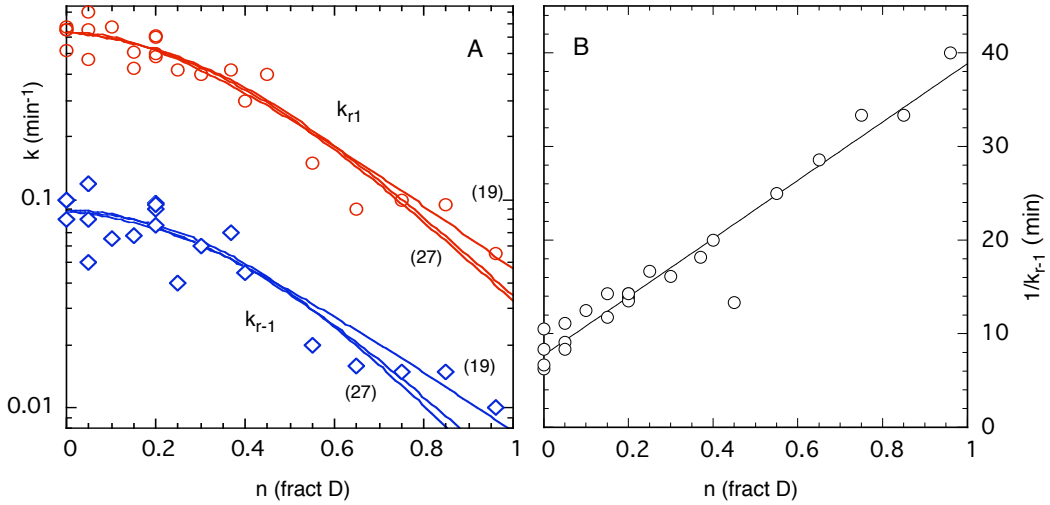

Figure 8. Proton inventories for the rates of the phases observed for spectral changes accompanying the interaction of Glu376Gln-MCAD with C_8CoA. The experiments were carried out at 4 ºC and pH 9.25, and analysis of the primary data was done as shown in Fig. 7. **Panel A** Plot of k_{r1}, and its reversal k_{r-1}. The curves through the data points are fits obtained based on equation 19 and 27 (Materials and Methods). **Panel B.** Plot of k_{r2} and fit based on equation 17b (Materials and Methods). Observed KIE ≈ 5.

Figure 9. Proton inventories for the rates of the two phases of flavin reduction 25 ºC. The experiments were conducted at pL 8.8 and 25 ºC. k_{r1} and k_{r2} are the data obtained from simulation of primary traces based on Scheme 3. k'_{r1} and k'_{r2} data were obtained from fits of primary data based on triexponential equation. The lines through the data points are fits obtained based on equation 18 (Materials and Methods). Observed KIE ≈ 4.5 (k_r) and ≈ 3 (k'_r).

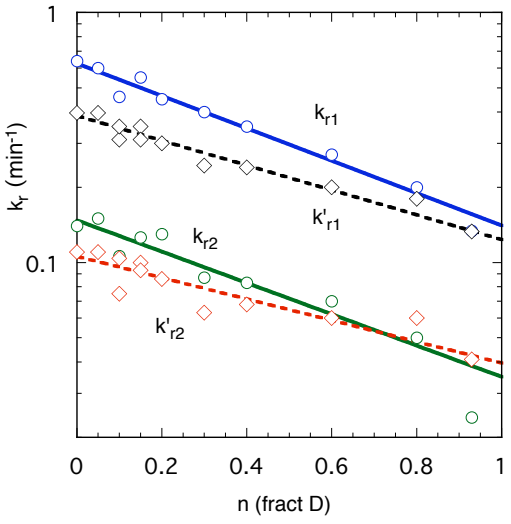

As depicted in Figure 7 when the interact is followed spectroscopically at 450 nm the three phases discussed above can be distinguished. The first corresponds to the spectral perturbations accompanying substrate binding and the ensuing ones to enzyme flavin reduction/substrate dehydrogenation.

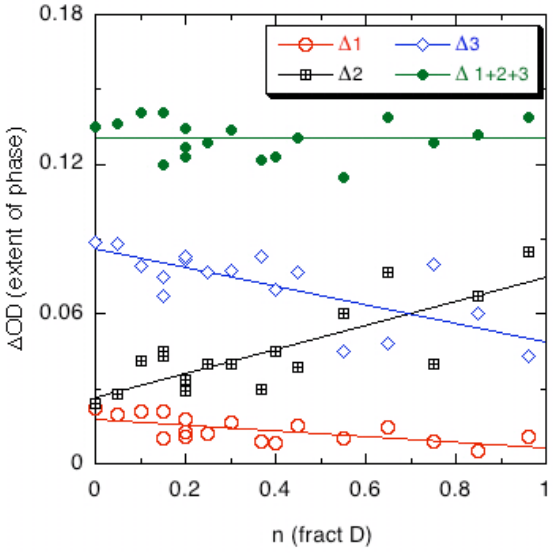

Figure 10. The extents of reduction of FAD depend on the deuterium fraction for interaction of Glu376Gln-MCAD with C_8CoA. The data are from analyses such as described in Figure 8. The lines through the data points are linear fits.

Table 2. Parameters obtained from proton inventories such as shown in Fig. 5. See legend of the Figure 8 and text for details.

Parameter		k_b	k_{r1}	k_{r2}
□	4°C /	*(a)*	4.6 ±0.7	2.5 ±1.1
	25°C		*(b)*	*(b)*
□	4°C /	0.6 ±0.036	0.04 ±0.01	0.07 ±0.04
	25°C	-	*0.32 ±0.035*	*0.37 ±0.06*
k_o	4°C /	1.34 ±0.026	0.14 ±0.004	0.06 ±0.002
	25°C	-	*0.38 ±0.01*	*0.11 ±0.005*
Chisq		0.14	0.0017	0.0005
			0.0048	*0.0011*
R^2		0.79	0.95	0.91
			0.94	*0.81*
(observed) 4°C /		1.6	5.6	5.4
KSIE	*25°C*	-	*3.2*	*2.6*

The total extent of absorbance changes (□OD in Figure 10), i.e. the sum of those occurring in the three phases, is fairly constant. The "extent" of each phase was obtained from corresponding fits as outlined above, and is depicted as a function of "n" in Figure 10. There appears to an apparent, approximately linear correlation wherein the extent of the "binding phase" decreases approx. 3-fold from 0 to 10% D_2O. The relative

extent of the subsequent phases shown opposite behavior, phase 2 decreases approx. 2-fold, while phase 3 increases by a similar amount.

3.2.7. DISCUSSION

Mechanism of substrate binding and of dehydrogenation

Binding of C_8CoA, the best substrate of MCAD, is compatible with the minimal two-step process depicted in Scheme 2. However, the experiments of Figure 1 suggest that further steps that do not manifest marked spectral effects also should be included. It should be kept in mind that binding of the large CoA substrates will encounter major steric constraints. The active site cavity, in which the fatty acid tail is bound, is a narrow "tube" containing, in the uncomplexed state, 8 H_2O molecules in a linear arrangement held together by H-bonds. Upon binding of C_8CoA 7 of these H_2O are expelled (Kim et al., 1993). Binding is thus likely to require extensive movements/re-arrangements of protein domains around the active center a process most likely to be affected by the presence of of several H-bonds within the protein scaffold. Their rupture could be concerted, and this would be at the origin of the observed, substantial KIEs. In agreement with a multistep binding is the relative slowness of the process. Prereaction complex is impared in the presence of amide group near to αC-H of substrate.

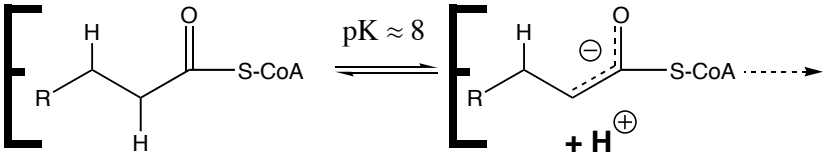

Scheme 3. Ionisation of the αC-H element of acyl-CoA substrates at the active center of MCAD. In the case of the best substrate, C_8CoA, the pK value is ≈ 8.

The interpretation of the the steps following binding, i.e. of substrate dehydrogenation is even more complex and for its discussion a few mechanistic key point should be recalled: The active center of MCAD has the capacity to lower the microscopic pKa of a bound ligand αC-H by some 10-13 units compared to the free state (Rudik et al., 1998; Vock et al., 1998). In the case of C_8CoA this pK would be around 8 (Scheme 3). With wt-MCAD the abstracted H^+ will be ligated by the active center base Glu376-COO^- this occurring concertedly with transfer of the αC-H to the flavin as a hydride (Ghisla &

Thorpe, 2004). With the Glu376Gln mutant, however, the putative H^+ generated as shown in Scheme 4 also requires binding to a "base". An inspection of the 3D-structure around the active site shows the presence of Glu99 at its "bottom". While this would be a logical candidate, its role as a base is excluded since the Glu376Gln+Glu99Gly-MCAD (double mutant) exhibits an activity profile similar to that of Glu376Gln-MCAD (Figure 4). The changes in slope shown in Figures 6 and 7 are not to be attributed to specific groups at the active center for the simple reason that there are none that can account for them. Specifically, the apparent pK $\geq$ 10 (Figure 6) cannot be attributed to Glu99 since a similar "bend" is present also when Glu99 is replaced with Gly (Figure 7). It is thus likely that these apparent pK's correspond to changes in mechanisms, or that they reflect pK's of groups outside the active site that govern specific movements of protein domains, or affect access of solvent / transport of H^+.

The profile of Figure 6 shows a linear increase of the reaction rate with $[HO^-]$. This leads to the conclusion that in the case of Glu376Gln-MCAD abstraction of H^+ from the αC-H is either directly promoted by solvent borne HO^-, or by H_2O linked to HO^-. The corresponding rate equation wold be:

$$k_{obs} \approx k \bullet [E_{ox}{\sim}S] \bullet [HO^-] \qquad \text{eq. (I)}$$

The sister pH profile for Glu376Gly-MCAD (Figure 7) is an apparent puzzle since, by intuition, one would expect a similar mechanism and consequently a similar $[HO^-]$ dependence. However, it should be noted that the two profiles are crude mirror images (on the ordinate), and a simple interpretation would be that shifts of the underlaying apparent pKs lead to their "cross-over". Indeed, this would agree with the Dixon's rules, that demand that the "bends" reflected by the two types of profiles (upward vs downward) reflect the same type of ionisation (complexed vs free species) (Kim et al., 1993); the apparent pKs would thus have the same origin. Attribution of these apparent pK's to specific microscopic ionisations or to changes in mechanism is not possible based on the present data. Intriguing is also the observation is that at pH 6-7 the activity of the Glu376Gly mutant is 1-2 orders of magnitude higher compared to that of Glu376Gln-MCAD. A possible clue arises from inspection of the active site of MCAD: The space occupancy of the Gln side chain can be assumed to correspond to that of 3-4 H_2O molecules. With the Glu376Gly mutant the space around the substrate αC-H position

would thus be more hydrophilic, lessen the forces that keep the active site tight, and thus promote proton abstraction/neutralisation and/or access of solvent borne species.

Interpretation of solvent KIE and of proton inventory studies

Of the dependences $k_{r1n}(n)$ of rate constant k_{r1} and of its reversal, k_{r-1}, on atom fraction of deuterium (n) in the aqueous solvent, the most dramatic is that for the rate constant $k_{r1n}(n)$ shown in Figure 8. For this case, the rate constants at low n remain fairly constant to around n = 0.2, and then drop sufficiently for an overall solvent isotope effect for k_{10}/k_{11} of 12-18 to be produced. A limited number of qualitatively different models can be expected to reproduce this kind of curve. We have been able to produce quantitative or semi-quantitative agreement with the experimental data for two kinds of models (see Materials and Methods). First model has been used to fit the data considering that ϕ = 6 and Z = 80 (Figure 8A, Table 2). The overall result is a normal isotope effect of 80-90, arising from a very large number of hydrogenic sites. Second, a single site becomes more tightly bound as the reactant state is converted to the transition state, such that its isotopic fractionation factor ϕ changes from ϕ = 1.0 in the reactant state to ϕ = 6 in the transtion state. The multisite isotope effect of 80 has considerable precedent from studies of solvent isotope effects on k_{cat}/K_M in the action of serine hydrolases (reviewed in (Schowen, 2004: in press)) and seems a reasonable mechanistic hypothesis. The single-site transition-state fractionation factor of ≈ 6, however, is much more difficult to accept. While fractionation at individual protein sites has been found in some NMR studies to generate values larger than unity (LiWang & Bax, 1996; Bowers & Klevitt, 2000; Veglia et al., 2002; Fenoll et al., 2004), reliable values this large would require so stiff a potential around the isotopic center as to seem *prima facie* unphysical. For the second model a value of w_a = 0.8 produces a line (equation 28, Materials and Methods) that is close to indistinguishable from that for the one-step model. This model would correspond to a situation in which two steps in succession (we cannot deduce the order of the steps in series) occur and their steady-state combination then generates k_1. The step with k_a as rate constant is around 80% rate-limiting in H_2O and corresponds to a mechanism in which the reactant state has an enzyme-bound hydroxide ion (ϕ = 0.5) which then becomes bound to a proton being abstracted from substrate in the transition state so that ϕ = 1. The

step with k_b as rate constant is around 20% rate-limiting in H_2O and generates a multi-site isotope effect of 90, probably arising from very small changes in binding at very many backbone NH(D) sites, most simply in a protein conformational change.

In principle, the results can be described equally well on the one-step model and on the two-step model. However, the one-step model requires the assignment to the transition state of an unprecedented fractionation factor around 6, suggesting the presence of an exchangeable hydrogen in a very steep potential well. The two-step model, in contrast, requires in one step an enzyme-bound hydroxide ion with the normally observed fractionation factor, an idea that is supported by the pH dependence (Figure 6), and in a second step a conformation change or similar event that produces a large normal isotope effect presumably arising from many small isotope effects at backbone hydrogenic sites, as has been observed in other enzymatic reactions. Thus on the grounds of plausibility, the two-step model appears preferable.

Mechanistic conclusions

As also pointed out elsewhere (Ghisla & Thorpe, 2004), MCAD appears to seal itself off from the environment during catalysis, the reasons for this being the necessities of the chemistry of the enzyme both for the dehydrogenation step and the prevention of reaction with dioxygen (Ghisla & Thorpe, 2004; Kim & Miura, 2004). This shielding of the active site appears to be extremely effective, and access of solvent borne molecules such as HO^- appears to require the concomitant rupture of a series of H-bonds such as in a rearrangement of a protein domain. This would result in the observed large medium SKIEs. In the general sense, the observation of such a large SKIE is in accordance with the presence of a very rigid frame around the active site. The cavity close to the flavin and inside contains 8 H_2O molecules in the absence of ligands, while a single one of these is found in the reduced enzyme-product complex (Kim et al., 1993). The number of H_2O present molecules is likely to vary depending on the size of the substrate (MCAD accepts C_4-C_{16}CoA substrates (Ghisla & Thorpe, 2004)). It is thus conceivable that some of the bound water molecules become fixed among the active site upon substrate binding (compare to step (**3**) -> (**4**), Scheme 3). As the result, the enzyme~substrate complex ((**4**) in Scheme 4, E_{ox}~S in Scheme 3) might be heterologous with respect to its H_2O content. Thus there would be more than one structure that tends to be trapped in fractions of the

total. This could lead to different forms of reactants (E_{ox}~S•nH_2O) where water-networks may modulate the reactivity of the complex and in particular affect medium effects in proton inventories.

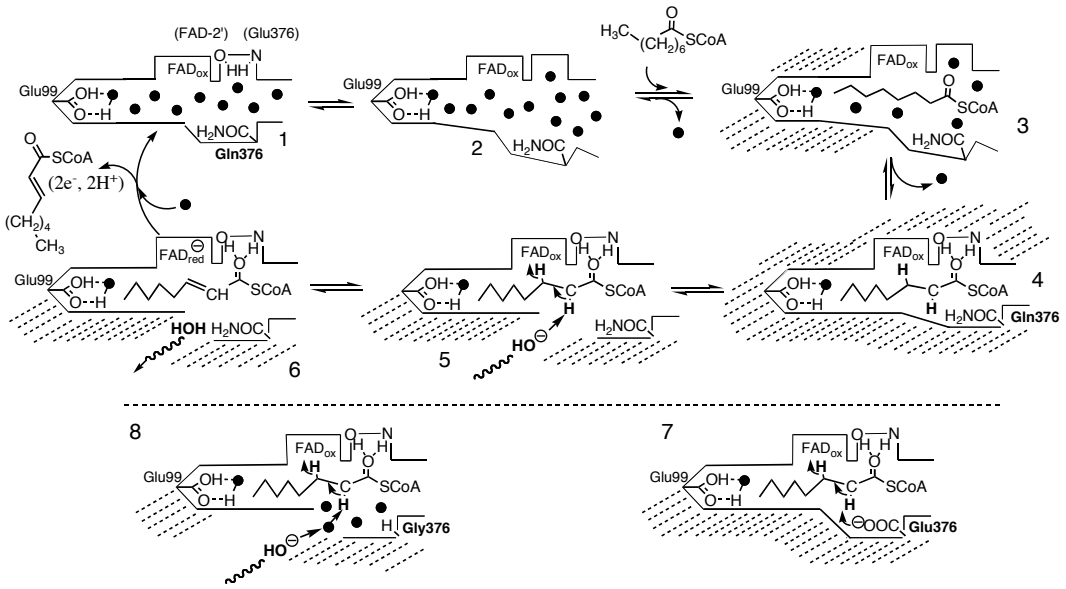

Scheme 4. Representation of the processes envisaged to occur at the active center of MCAD mutants during substrate dehydrogenation. Dots (•) represent H_2O molecules, shaded areas indicate regions of restricted access (shown only in selected diagrams for clarity). (**1**) Represents the active site of "empty" MCAD adapted from the 3D-structure of uncomplexed enzyme (Kim et al., 1993) in which Glu376 has been substituted for Gln376. It contains 8 H_2O molecules linked by H-bonds. (**2**) is an "open form" into which substrate enters to form (**3**) a primary encounter complex E_{ox}~~S (compare to eq. (2)). In a subsequent step the substrate thioester carbonyl docks into the "oxycarbanion" hole" and this triggers the expulsion of all but the one H_2O molecule linked to Glu99 at the bottom of the cavity. This process is reflected by the transition to a more hydrophobic environment (see Fig. 1) and forms species (**4**), (equivalent to E_{ox}~S in Scheme 2). (4)-(6) are characterized by their being shielded from solvent and having a restricted accessibility to oxygen. For access of solvent borne HO^- and its reaction with the substrate C-H (**5**), the active site, or some of its domains, must "open up", this requiring the rupture of several H-bonds. Flavin reduction (**5** -> **6**) leads to formation of the product complex (**6)** that that might stabilize by expulsion of water**. (7)** represent the E_{ox}~S complex with wt-MCAD, which relaxes by transfer of the Glu-COO^- negative charge onto the flavin. In the case of the Gly376Gly mutant (**8**) the space occupied by Glu376 in wt-MCAD is likely to be taken up by 3-4 H_2O molecules. These might facilitate attack of solvent borne HO^- or the transfer of H^+ to bulk solvent.

This could generate several exponential terms, each with its characteristic rate constant that would correspond to the different phases of enzyme reduction (corresponding to k'_{r1} and k'_{r2} in Scheme 2). In agreement with this is the observation that with some substrates (Wenz et al., 1985) and in particular with C_{14}-CoA, a substrate with „large tail" dehydrogenation by MCAD is monophasic (Gradinaru, R. & Ghisla, S. unpublished observation) indicating that factors related to the substrate moiety can affect the rates and ratio of the phases. The deviant behavior of the Glu376Gly-MCAD mutant (Figure 7) can be rationalized analogously: The presence of some „additional" H_2O molecules that

replace the Glu-side chain modiefies the fine tuning of the dehydrogenation reaction in an unexpected way to produce effects depicted in Figure 7.

Since for Glu376Gln- and Glu376Gly-MCAD mutants proton-transfers that accompany dehydrogenation *must* be occurring along water-chains then the large solvent isotope effects and complicated proton-inventories become easier to understand (solvent isotope effects obtained from stopped-flow experiments for wt-MCAD are considerable lower; at pH 7.6 SKIE was 1.2-1.4).

Thus solvent isotope effects could originate in:

(a) overall conformational changes;

(b) formation and adjustment of fixed water networks;

(c) transfer of protons along these networks;

(d) uptake of hydroxide ion or equivalent release of a proton before reaction,

(e) all of the above, or many in combination.

The present data have clearly demonstrated that in the mutant the networks of water molecules are more important.

3.3. Studies on the T168A-MCAD mutant

3.3.1. Introduction

A peculiarity of the chemical mechanism of acyl-CoA dehydrogenases is that the α,β-dehydrogenation involves the rupture of two kinetically stable C-H bonds. While a H^+ is abstracted from the αC-H by an active site carboxylate (Glu376 in MCAD (Bross et al., 1990)), a hydride is transferred from the βC-H directly to the flavin cofactor position N(5) (Ghisla et al., 1984). The replacement of normal oxidized flavin with the isoelectronic 5-deaza-flavin analogon (Scheme 1) reduces the rate of cofactor reduction by substrate (C_8CoA) by a factor > 10^6.

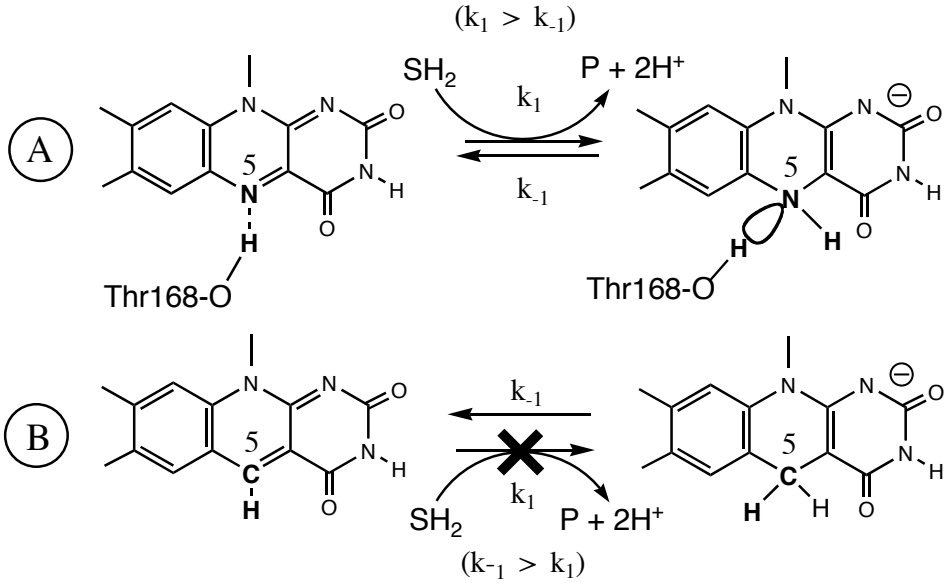

Scheme 1: α,β-dehydrogenation reaction catalyzed by ACADs (A). The Thr168-OH function forms a tight (2.93 Å) H-bond to the flavin N(5) position. This interaction is not possible with enzyme that has been reconstituted with isoelectronic 5-deaza-FAD (B). Similarly the Thr168A mutant lacks this H-bond.

This difference alone (corresponding to > 8 Kcal•M^{-1}) cannot be accounted for solely by the difference in redox potential between normal and deaza-flavin (≈ 120 mV corresponding to ≈ 2.8 Kcal•M^{-1} (Hemmerich & Massey, 1977)). In fact, while the

reactivity of deaza-flavin in general reflects this difference in potential (Hemmerich & Massey, 1977). Thus the rate of the reverse reaction (k_{-1} in Scheme 1) for the 5deaza-FAD-MCAD is faster than that of normal MCAD (Ghisla et al., 1984). Further, differences in electronic properties of the flavin cofactor used to reconstitute MCAD appear to follow linear free energy correlations (Satoh et al., 2003). This opens the possibility that this H-bond plays a hitherto unrecognized role in substrate activation and FAD fixation by ACADs.

In the present chapter I want to discuss the role of the Thr168-flavin H-bond in substrate activation and catalysis. Thr168Ala mutant had received attention earlier since it is the only human genetic mutant of MCAD in which a group at the active center is affected (Kuchler et al., 1999) (Scheme 2). In this context we have expressed previously T168A-MCAD and studied some of its properties, in particular its stability and substrate specificity that are relevant for an assessment of the effects of such genetic mutations on fatty acid metabolism (Bernert & Sprecher, 1977; Kuchler et al., 1999).

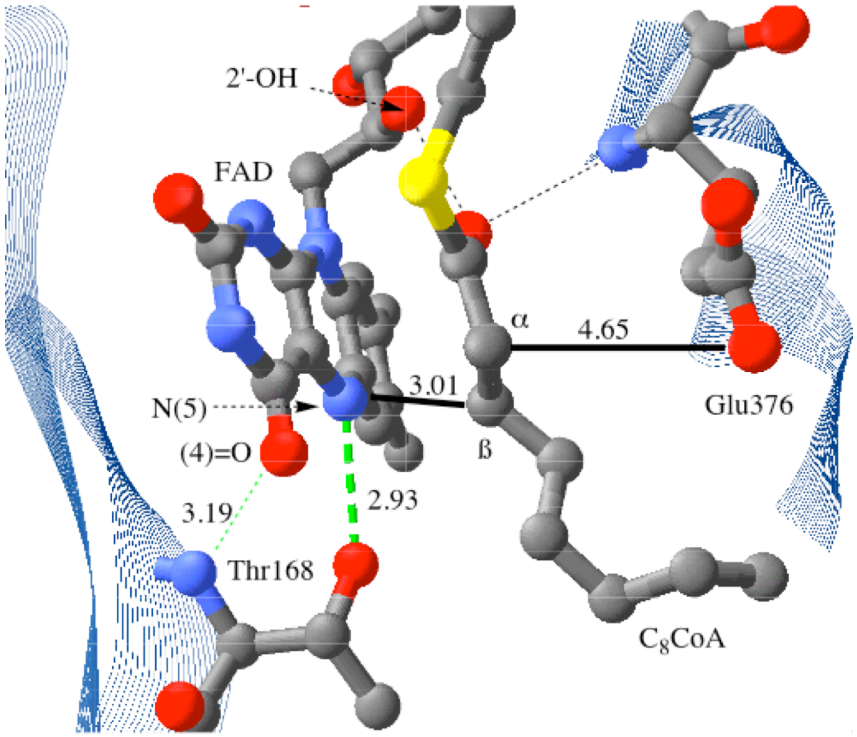

Scheme 2. Arrangement of relevant functional groups, flavin and substrate at the active centre of MCAD. Three important H-bonds between Glu 376NH, FAD-2'OH and the substrate thioester respectively N(5) of the cofactor (blue) and Thr168 are representated bydashed lines.

3.3.2. Reaction of T168A-MCAD with the substrate C_8CoA

The turn-over properties of T168A-MCAD with substrates of various chain length have been reported earlier (Kuchler et al., 1999) and show that V_{max} is ≈ 20% that of wt-MCAD with C_8CoA and at pH 7.6. In addition the mutant V_{max} shows dependence from the nature of the electron acceptor suggesting an effect on the rate of electron transfer. The Thr168-OH H-bond to the flavin N(5) could affect the properties (stability) of the flavin neutral radical and obligate intermediate in the transfer of electrons to the acceptor ETF. In order to assess the role of the H-bond in question in a more direct fashion, and to circumvent the effects due to the oxidative half-reaction, we have investigated the dehydrogenation step of T168A-MCAD with the stopped-flow instrument and with C_8CoA as substrate (Figure 1, Panel A and B).

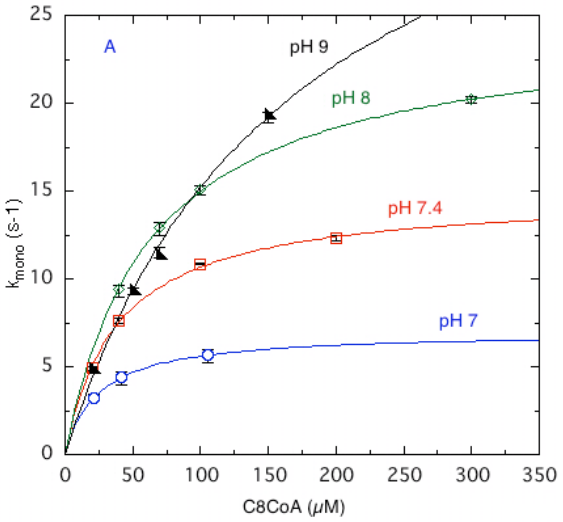

Figure 1. Panel A. Kinetics of the reaction of T168A-MCAD with the substrate C_8CoA. The bars (|) represent data points, and the curve (—) is the fit obtained using a monoexponential decay equation. The main panel depicts the concentration dependence of the observed (monophasic) rates of flavin reduction from the substrate concentration at pH values indicated. The curves (—) through the data points are the fits obtained using the Michaelis Menten equation and the vertical bars indicate the scatter of single measurements.

Panel B. pH dependence of the parameters (Kd and k_{red}) obtained from the representations in Figure 1 (Panel A). The fit through the data points was obtained using an adapted pH equation (Dixon & Webb, 1979).

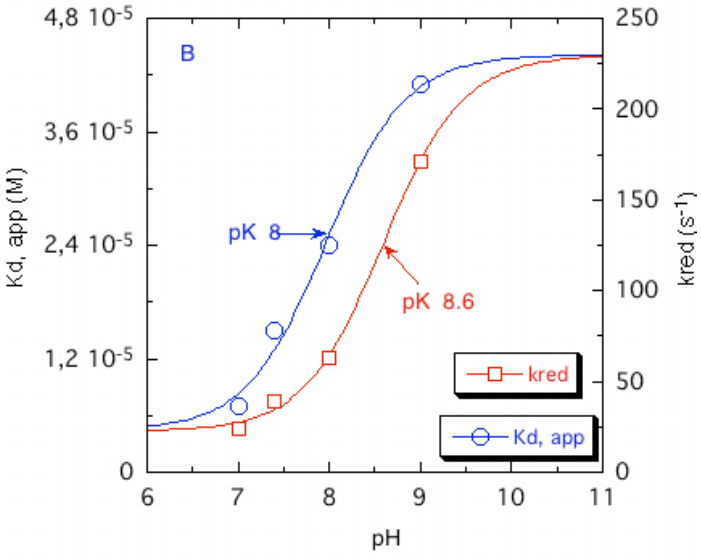

Substrate dehydrogenation of wt-MCAD occurs in two phases of approx. similar extent that are separated by roughly one order of magnitude (Pohl et al., 1986; Schopfer et al., 1988). In sharp contrast to this, with T168A-MCAD the course of the reaction is monophasic under all conditions and shows saturation dependence (Figure 1, Panel A). We should mention that at pH < 7 and pH > 9 the enzyme instability is increased. The reaction rate and the apparent Kd are markedly dependent on pH as shown in Figure 1 (Panel B). The apparent pK's that can be estimated from this dependence (pK ≈ 8 and ≈ 8.6 for K_d and k_{red} respectively) are probably related to the intrinsic pK of the 376Glu active center base.

3.3.3. Determination of redox potential of T168A-MCAD

The modulation of the electron-transfer properties of human MCAD has been studied using wt-MCAD and several active site mutants (E376Q, E376H and E99G-MCAD). The 2-e^- redox potential E_m of uncomplexed mutants is 30-40 mV higher than of wt-MCAD and indicate that specific charges could affect the electron-transfer properties of the enzyme (Mancini-Samuelson et al., 1998). It is known that the redox potential is affected by the type of ligand (Johnson et al., 1995). It was thus expected that the Thr168-OH H-bridge to the flavin N(5) influences this parameter. For its determination (Minnaert, 1965; Massey, 1991) the redox dye indigo monosulfonate (redox potential E_{m7} = -157 mV (Sullivan et al., 1923)) had to be used and was synthetized for the purpose. Other dyes either not possess appropriate redox potentials or were interacting /binding with/to MCAD. A total incubation time > 3 hrs was necessary for the redox potential determination (Figure 2A). The obtained E_m = -180 mV at pH 8 is ≈ 40 mV lower than the value determined in parallel with wt-MCAD.

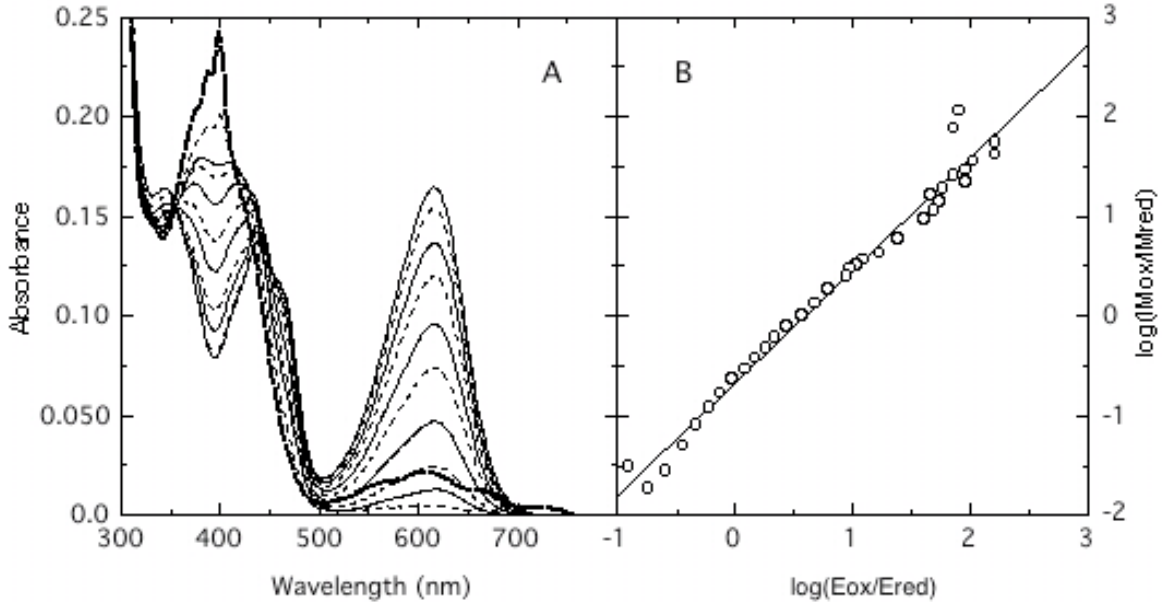

Figure 2. Determination of the redox potential of T168A-MCAD
Panel A. Selected spectra obtained during the course of the anaerobic reduction of T136A-MCAD (10 µM) in 50 mM KPi, pH 8 contain 10 % glycerol, 200 µM xanthine, and 5 µM benzyl viologen and 10 µM indigo monosulfonate as redox standard ($E_{m,7}$ = -157 mV (Sullivan et al., 1923)). The traces shown are representative selection and were recorded at 0, 53, 68, 87, 97, 107, 117, 131, 141, 161, 194 min after addition of xanthine oxidase (18 nM final concentration).
Panel B. Nernst plot as described by Minnaert (Minnaert, 1965); n = 1

3.3.4. Interaction with acyl-CoA substrate analogs that form anionic species

The transition state for the dehydrogenation reaction has an appreciable enolate character (the negative charge migrates from carboxylate base through the thioester to flavin prosthetic group). Hydride abstraction does not occur in the case of substrate analogues (substitution of the C-3 methylene group with oxa, thia, keto and others groups) but enzyme-bound enolate forms a charge transfer complex with the adjacent oxidized flavin. Some of these species show intense long-wavelength absorbance (colored species with high extinction coefficients) making them useful spectral probes of the acyl-CoA dehydrogenase (Thorpe & Massey, 1983).

3.3.4.1. Interaction of 3-keto-octanoyl-CoA with Medium Chain Acyl-CoA Dehydrogenase

Figure 3 depicts the spectral effects observed upon binding of 3-keto-octanoyl-CoA to T168A-MCAD. As with wt-MCAD (Engel & Massey, 1971; Powell et al., 1987),

a pronounced long wavelength absorption appears that is attributed to the CT interaction between the oxidized flavin and the anionic form of the ligand. The maximum of this band is shifted by ≈ 50 nm to the blue compared to that of the wt-MCAD complex (Figure 3, insert). In the pH range 6-9 the CT-absorption remains unaltered; this is compatible with the □C-H pK of the ligand being lowered by > 4 pK units as is the case of wt-MCAD (pK of free acetoacetyl-CoA ≈ 8.8 (Stern 1956)). Thus the similarity of the perturbations of the oxidized flavin absorption bands observed with the 168A mutant compared to wt-MCAD and the similar binding constant (Table 2) suggests that the T168A mutation does not affect the basic mode of interaction of this ligand with the flavin.

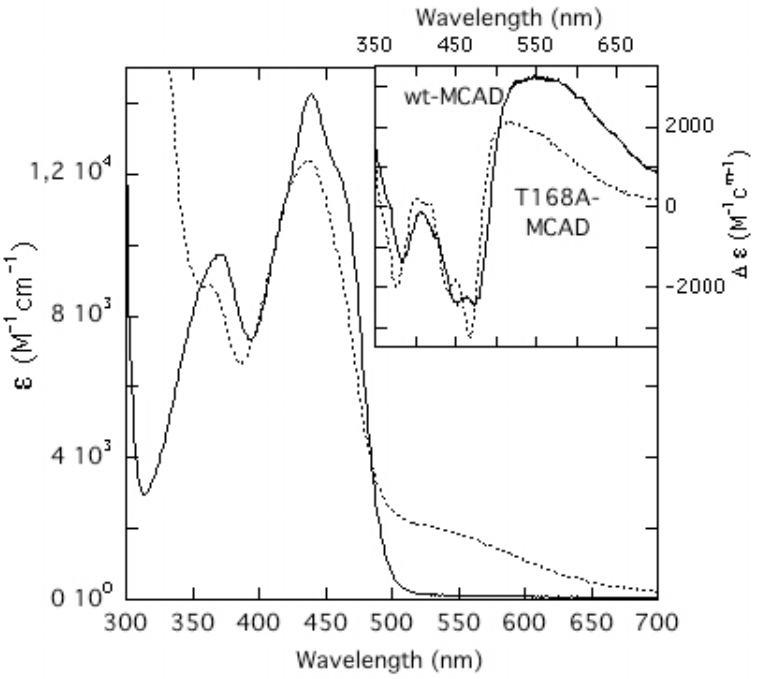

Figure 3. Interaction of T168A and wt-MCAD with 3-keto-octanoyl-CoA The oxidized enzyme (T168A), 13.6 µM in "mixed buffer" containing 250 mM KCl at pH = 7.8 and 25 °C, was titrated with 36 equivalents of 3-keto-C_8CoA. The inset shows the difference spectra between free and ligand complexed enzymes. Difference spectra are resulted after binding of the ligand (2.2 respectively 36 equivalents) to wt- (6.75 µM) and T168A-MCAD (13.6 µM) in aerobic conditions (pH 7.75 and 25 °C).

3.3.4.2. Interaction of 4-NPA-CoA with Medium Chain Acyl-CoA Dehydrogenase

Binding of this analog to wt-MCAD induces the appearance of two new absorptions (Vock et al., 1998). One, around 500 nm is due to the anionic form of the ligand itself, the

second, maximal in the 700-800 nm region, is due to the CT interaction of anionic ligand with the oxidized flavin. Upon binding to wt-MCAD the □C-H pK of 4NPA-CoA is lowered some 9 units compared to that of the free species (Vock et al., 1998). With T168A-MCAD and at pH up to 8 the interaction with 4NPA-CoA causes no similar effects (not shown); the observed spectral perturbations correspond to what is induced by binding of ligands that do not undergo ionization or are not undergoing polarization.

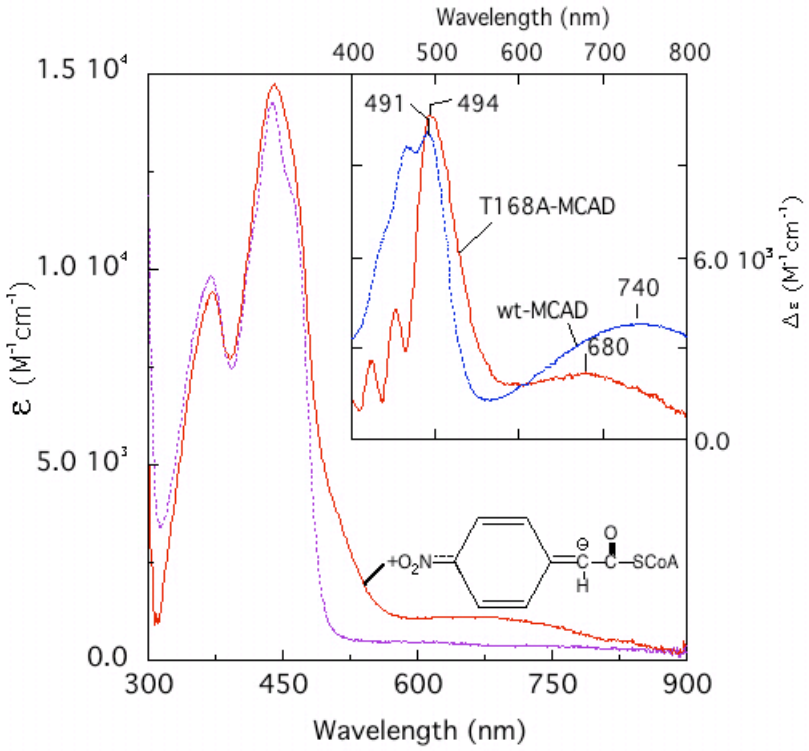

Figure 4. Interaction of T168A-MCAD with 4-Nitrophenyl-acetyl-CoA. The main panel depicts the absorption spectrum of uncomplexed enzyme (blue) ≈ 10 µM at pH 9.0 (conditions as detailed in the legend to Fig. 3). Addition of increments of the ligand lead to the appearance of a longwavelength absorbance extending up to 900 nm, and curve (red) is that obtained in presence of the ligand (the same quantity of ligand was added to the reference cuvette, final concetration was 784 µM, and the spectrum is corrected for dilution). The insert shows the difference spectrum between complexed and uncomplexed T168A-MCAD. It is estimated that at pH 9.0 only ≈ 30 % of the bound ligand is ionized and gives rise to the absorbance changes in the 490-495 nm area. For the sake of comparison this absorbance (curve red) is normalized to the value of that observed with wt-MCAD.

This is different at pH ≥ 9.0 where binding of 4NPA-CoA leads to the appearance of the two absorptions band that reflect ligand anion formation and resemble what is observed with wt-MCAD at low pH (Figure 4 and insert). The spectral changes associated with binding reflect a Kd ≈ 30 ± 5 µM at pH 9 that compares to a Kd ≈ 70 µM for wt-MCAD

(Table 1). A study of the interaction with T168A-MCAD at pH > 9 was not possible due to instability of the protein. Nevertheless, it is possible to estimate the pKa for deprotonation of bound 4NPA-CoA using the assumption that $\Delta\varepsilon_{490\text{-}500}$ of the anionic form is similar (≈ 10, 000 $M^{-1}cm^{-1}$) for binding to wt- and T168A-MCAD. Thus the observed $\Delta\varepsilon_{494}$ ≈ 3300 $M^{-1}cm^{-1}$ at pH 9 yields a pK for bound 4NPA-CoA ≈9.3. While this is a rather crude approximation and since there are no similar absorptions at 494 and 680 nm at pH 8.5 (not shown) the pK can be safely estimated to be between 9 and 10.

3.3.4.3. Interaction of 3-thia-octanoyl-CoA with Medium Chain Acyl-CoA Dehydrogenase

This type of analog ($3SC_8CoA$) was introduced by Thorpe's group (Lau et al., 1988) and has become widely used to assess the nature of CT-complexes of ACADs, and the acidity of the acyl-CoA thioesters αC-H at their active centers (Vock et al., 1998; Engst et al., 1999; Dmitrenko et al., 2003; Nishina et al., 2003; Satoh et al., 2003) More specifically, in the reaction between 3-thia-acyl-CoA and MCAD, the complex "freezes" at the stage after α-proton abstraction in the form of a charge-transfer state. $3S\text{-}C_8CoA$ binds to T168A-MCAD and, at high pH, induces spectral effects similar to those reported for wt-MCAD (Figure 5). However, the extinction of the CT band observed in the mutant case is only ≈ 30% that of wt-MCAD (Figure 5, insert, Table 1). More significant is the pH dependence of the effects depicted in Figure 6 (Panel A and Panel B) where these are compared to what was reported for wt-MCAD (Vock et al., 1998; Engst et al., 1999). From the pH dependence of such absorptions the microscopic pK for deprotonation of the chromophoric ligand can be estimated, and by comparison of this pK with that of the free species the extent of "activation" (or pK lowering) can be inferred (Vock et al., 1998). Panel A shows that the microscopic pK of the analog in the complex is ≈ 6.6, i.e. it is increased by ≈ 1.4 units compared to the same in wt-MCAD. Figure 6B represents the analysis of the pH dependence of the binding constant K_d according to the Dixon rules. From this comparison both differences and analogies emerge.

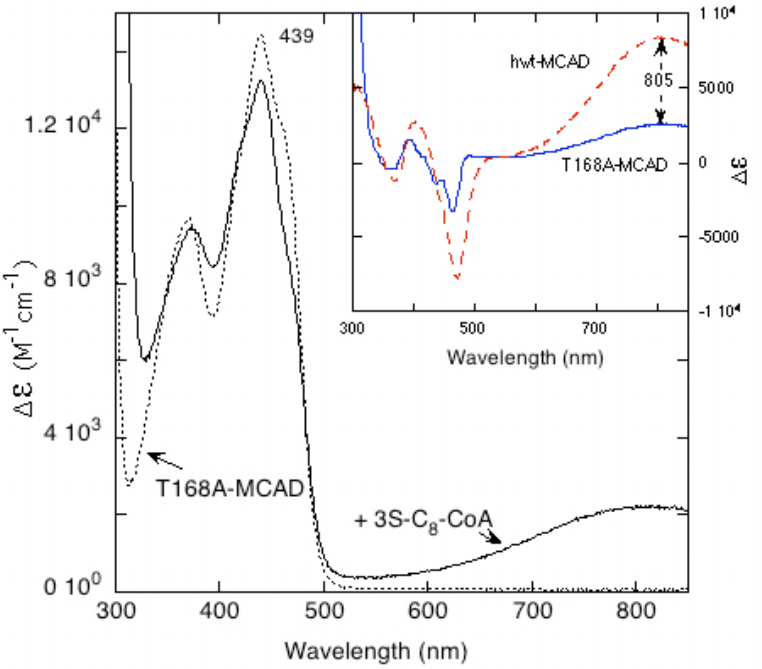

Figure 5. Interaction of T168A-MCAD with 3S-C_8CoA. Curve (---): spectrum of the uncomplexed enzyme (10.1 µM). Conditions were depicted in the legend of Figure 3 (pH 7.8 and 25 °C). Curve (—): Upon addition of a total of 1.3 mM 3S-C_8CoA (intermediate additions are not shown for clarity). Insert: difference spectrum between complexed and uncomplexed species, and, for comparison, the difference spectrum between free wt-MCAD and its complex with 3S-C_8CoA (adapted from (Vock 1998)). The interaction constants (apparent Kd's) were estimated from such experiments carried out at various pH values.

A main difference consists in the "orientation" of the two profiles: with wt-MCAD an overall decrease of the apparent binding constant occurs with increasing pH; with the T168A-MCAD the contrary is the case: Furthermore, according to Dixon (Dixon & Webb, 1979), with wt-MCAD two plateaus with constant pK values are apparent at low and high pH (dashed lines) that are connected by a segment with a positive slope = 1, the intercepts of the (dashed) lines corresponding to the pKs of an involved group in the complex EL ($pK_{EL} \approx 5.2$, upward curvature) and free species E (or L) ($pK_E \approx 6.3$, "downward curvature") (Vock et al., 1998). With the T168A mutant at pH < 6 and > 9 the apparent K_d appears to increase linearly with pH and to approach lines with a slope = -1. It should be pointed out, however, that at lower pH, the progress of the curve is uncertain since data points at pH < 6 could not be obtained due to instability of the enzyme. Thus the (probable) occurrence of further ionizations that would manifest as "bends" cannot be identified in this range. The main similarity between the wt- and the T168A-MCAD

pH profiles is that the curvatures of the traces exhibit the same type of 'bend' with the same type of curvature (i.e. first "upward" then "downward") on going from low to high pH. This is compatible with the same groups being at the origin of the corresponding apparent pKs. The intersections depicted in Fig. 6B reflect a pK ≈ 6.3 within the complex EL, respectively one of free enzyme (pK_E ≈ 8.6). The first pK value corresponds (within the precision of the determination) to the pK reflected by the pH dependence of the CT-band (pK ≈ 6.6, Figure 6, Panel A). The second is attributed to the microscopic pK of the active center Glu376 of T168A-MCAD, as was done with wt-MCAD were a pKa ≈ 6.3 was found (Vock et al., 1998).

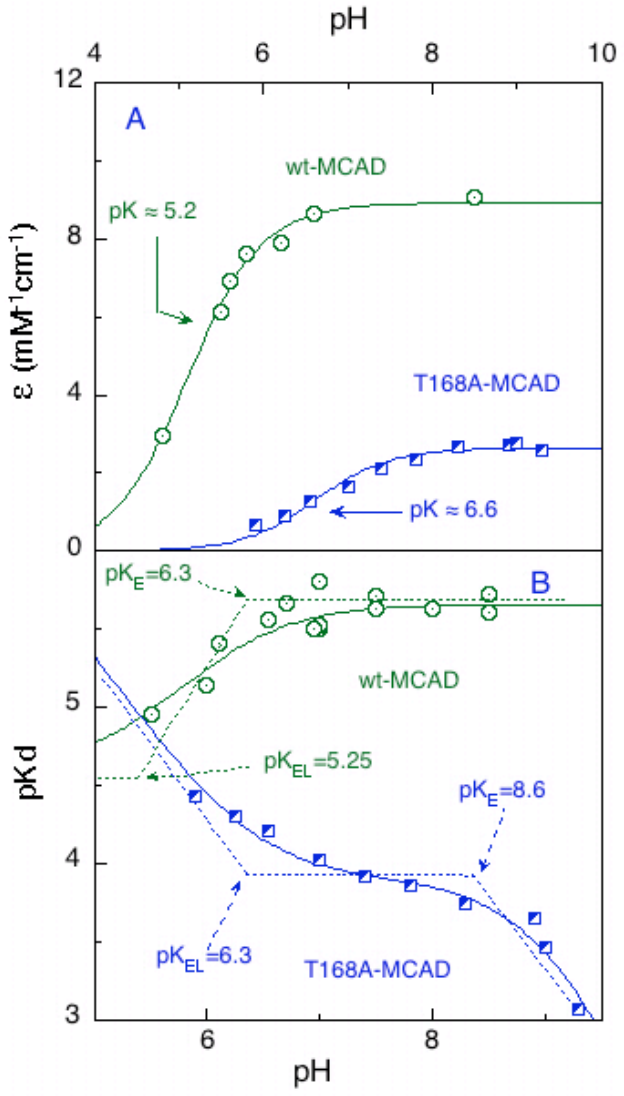

Figure 6. ***Panel A.*** **pH dependence of interactions accompanying binding of 3S-C_8CoA to T168A-MCAD**
Panel A: Dependence of the CT-band (805 nm, ●-●) from pH. The pH profile for the same set of reactions with wt-MCAD is also shown for comparison (O-O). The data points are the extinction coefficients estimated for full complex formation from experiments such as those of Figure 5. ***Panel B***. pH dependence of the pK_d values estimated from the same experiments plotted according to Dixon (Dixon & Webb, 1979). The segments (….) have slopes = 1 or 0. Note that their intersections occur at the pK values of enzyme-ligand (EL) or of free enzyme (E). T168A-MCAD: (●-●), and wt-MCAD: (shown for comparison, and data taken from (Vock et al, 1998),○-○. Titrations could not be carried out at pH < 5.8 due to the instability of the protein.

The appearance of the CT-band and the spectral perturbations accompanying the 3-thia-octanoyl-CoA interaction with T168A-MCAD were studied at pH 7.0 using the stopped-flow instrument. The observed spectral changes were complete within the mixing time of the instrument and thus very fast (> 500 s^{-1}). As a comparison the same

reaction with wt-MCAD has a k >> 600 s^{-1} at 1 °C, and only a minor part of the reaction can be monitored (Engst, 1993).

Table 1. Selected properties of T168A-MCAD species and comparison with wt-MCAD.

Substrate / ligand Structure	Parameter	T168A-MCAD	wt-*MCAD*
Octanoyl-CoA / C_8CoA 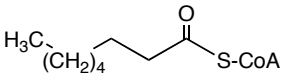	k_{fast} (s^{-1})	40	>500[a]
	CT λ_{max} (nm)	545	572
	ε($mM^{-1}cm^{-1}$) of reduced enzyme	3.3	3.5
(3)S-C_8CoA 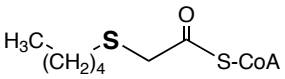	k_{obs} (s^{-1})[b]	>500	> 600[d]
	$K_{d,app}$ (µM)	140[b]	0.8± 0.08[c]
	CT λ_{max} (nm)	800-810	800-810
	ε($mM^{-1}cm^{-1}$) of CT band	2.6	7.6
	pK	≈6.6	5.2
3-keto-octanoyl-CoA 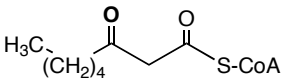	$K_{d,app}$ (µM)	5.5	3
	CT λ_{max} (nm)	525	580
	ε($mM^{-1}cm^{-1}$) of CT band	2.6	3.7
4-NO_2-phenylacetyl-CoA 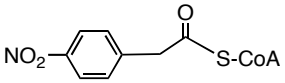	$K_{d,app}$ (µM)	30±5 (pH 9.0)	≈70 (pH 9.0)
	CT λ_{max} (nm)	≈680	740
	ε($mM^{-1}cm^{-1}$) of CT band	≈0.8	3.8

a) rate of first phase of enzyme reduction at pH 7.8, 1 °C in KPi 50 mM (Kieweg, V. & Ghisla, S. unpublished).
b) „mixed buffer“ containing 250 mM KCl, pH 7.8 / 25 °C
c) Tris 50 mM / pH 8.1; 25 °C
d) Kieweg, V., dissertation.

3.3.5. Computational studies on the THR168 H-bond effect (by Olga Dmitrenko and Robert Bach)

The aim of the present calculations was to assess the effect of the Thr168 H-bond on the energy profile of the reaction and to attempt a correlation with the experimentally obtained parameters. Initial coordinates were derived from the X-ray structure of MCAD (Kim et al., 1994). First we consider the model system, which consists of two reactants, the (preformed) thioenolate anion and Fl_{ox}. The 2'-OH group of the ribityl moiety is

mimicked by a $–CH_2CH_2OH$ group that forms the hydrogen bond to the substrate carbonyl oxygen (Figure 7). As discussed in one prior study (Dmitrenko et al., 2003), the pre-reaction complex is stabilized by charge-transfer and H-bonding (OH…O=C<) interactions. The energy of complexation relative to isolated reactants is 22.2 Kcal•M^{-1}. The overall reaction (see equation below) involving transfer of the thioenolate α-hydride to the flavin N(5) is exothermic (ΔE = -9.3 Kcal•M^{-1}) with a relatively small barrier for hydride transfer, $\Delta E^{\ddagger}$ = 7.8 Kcal•M^{-1} (Figure 7). The transition structure in this system (TS-1) has almost equal H-C and H-N distances, 1.326 Å and 1.312 Å. It should be noted that inclusion of the (protonated) Glu376-COOH function in the model decrease the exothermicity and increases the barrier of the reaction (Table 2).

As the next step, and in order to understand the effect of Thr168, the fragment ($HOCH_2CH_2NH(C=O)H$) was included in the model as shown in Figure 8. This mimicks a hydrogen bond from Thr168-OH to the flavin N(5) and an amide N-H hydrogen bond to C(4)=O. In the transition state, the H-C distance (1.312 Å) is now markedly shorter than that to N(5) (1.340 Å). This indicates that formation of the N-H bond precedes rupture of the C-H bond.

Table 2. Energetic parameters calculated for the MCAD hydride transfer reaction and effect of the Thr168 H-bond. Reaction barriers and energetics ($\Delta E^{\neq}$ and ΔE, Kcal•M^{-1}) are listed for the model systems that have oxidized flavin and the anionic form of the thioester model as reactants, with and without the Thr168 H-bond. We used calculations at the B3LYP/6-31G(d) + ZPVE and B3LYP/6-31+G (d,p) + ZPVE levels of theory.

Model system	$\Delta E^{\neq}$	$\Delta E_{reaction}$	$\Delta E^{\neq}$	$\Delta E_{reaction}$
	B3LYP/6-31G(d)		B3LYP/6-31+G (d,p)	
$CH_3CH_2CH(C=O)SCH_3^{\ominus}/Fl_{ox}$ (**1**)	9.2	-4.7	7.8	-9.3
$CH_3CH_2CH(C=O)SCH_3^{\ominus}/Fl_{ox}$ +THR168 (**2**)	7.9	-2.9	6.7	-
HOOC-CCH_3 +$CH_3CH_2CH(C=O)SCH_3^{\ominus}/Fl_{ox}$ (**3**)	11.7	0.2	-	-
H(C=O)-N**H**-$(CH_2)_3$COO**H** +$CH_3CH_2CH(C=O)SCH_3^{\ominus}/Fl_{ox}$ (**4**)	13.9	3.3	11.8	-1.6

The Thr168 H-bonding to Fl_{ox} (to N(5) and C(4)=O) reduces the barrier for hydride transfer by ≈ 1.1 Kcal·M^{-1}, while the overall hydride transfer reaction is less exothermic by 1.8 Kcal·M^{-1} (B3LYP/6-31G(d), See Table 2). It should be noted that addition of the Glu376 model (base) makes the reaction more endothermic with a higher barrier.

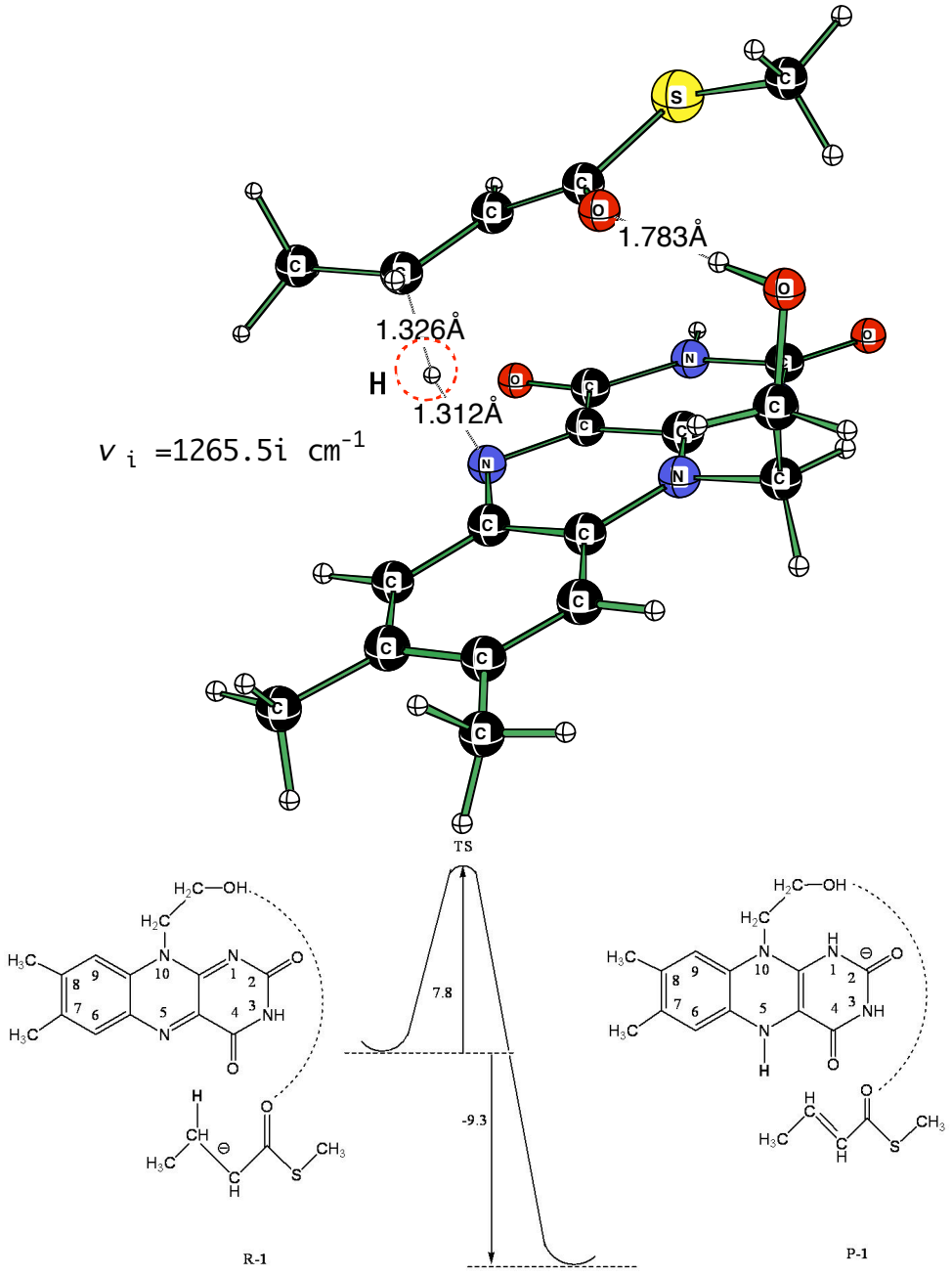

Figure 7. Transition structure optimized for hydride transfer. The geometry optimization was at the B3LYP/6-31+G (d,p) level for the $CH_3CH_2CH(C=O)SCH_3^{\ominus}/Fl_{ox}$ system and the transferring hydride is shown in bold. The reaction barrier and reaction energy (Kcal•M^{-1}) are at the B3LYP/6-31+G (d,p)+(ZPVE) level of theory. Imaginary frequency (ν_i) and zero-point vibrational energy (ZPVE) are at the B3LYP/6-31G(d) level.

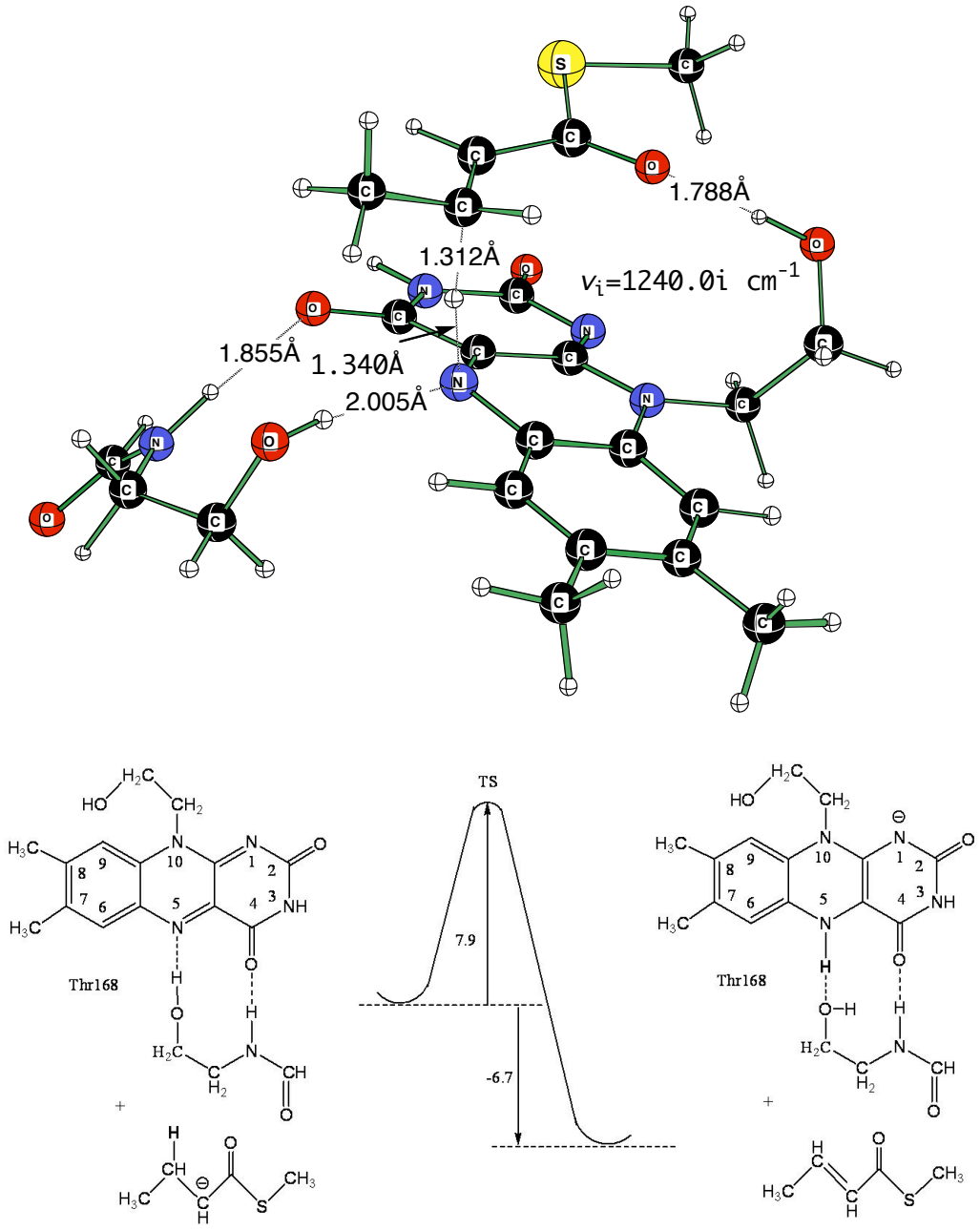

Figure 8. Transition structure optimized for hydride transfer and including the flavin N(5)-Thr168 H-bond. The system includes $CH_3CH_2CH(C{=}O)SCH_3^{\ominus}$/$Fl_{ox}$ and THR168 models at the B3LYP/6-31+G (d,p) level. The hydride is shown in bold in the lower structure diagrams and is highlighted by a red ring in the 3D-graph. Imaginary frequency (ν_i) and zero-point energy (ZPVE) are calculated at the B3LYP/6-31G(d) level.

In order to estimate the extent of charge transfer and the agreement with the experimental data, we extended previous TD DFT (B3LYP) calculations on the model of the charge-transfer model complex of MCAD with anionic ligand 3S-C_8CoA (Figure 10). This model consist of Fl_{ox} with the N(10)-CH_2-CH_2-OH bridge mimicking the hydrogen interaction to the thioester carbonyl and the relevant elements of ligand 3S-C_8CoA, i.e. $CH_3SCH(C{=}O)SCH_3^{\ominus}$ (anionic form, Figure 10). In the previous study [8] a calculated Franck-Condon (FC) transition = 957 nm [TD B3LYP/6-31G(d)//B3LYP/6-31+G (d,p)] was obtained that was assigned to the charge-transfer transition. Its value is in reasonable agreement with the experimental one (805 nm, Figure 5).

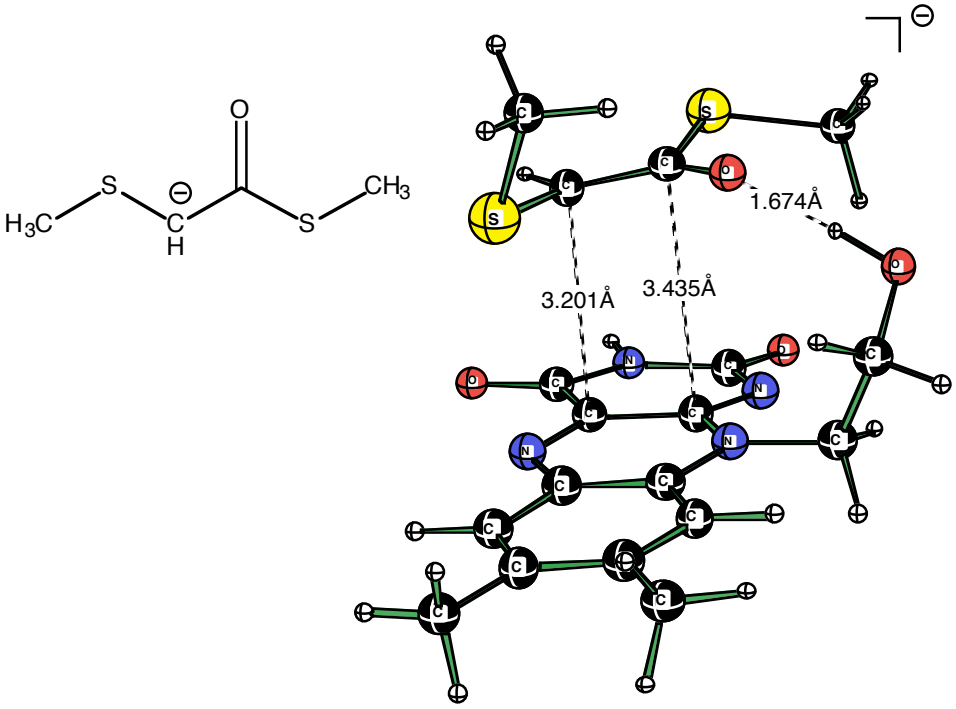

Figure 10. **Transition structure optimized for hydride transfer and including the flavin N (5)-Thr168 H-bond.** The complex, $CH_3SCH(C{=}O)SCH_3^{\ominus}/Fl_{ox}$, was optimized at the B3LYP/6-31+G (d,p) level of theory (Becke 1993). The total energy of complexation (including OH…O=C< bonding) is 15.6 Kcal•M^{-1}.

The predicted CT band position is highly dependent upon the level of theory at which the complex has been optimized. A complex optimized with a smaller basis set [6-31G(d)] is tighter than the B3LYP/6-31+G (d,p)-complex, and it has a shorter wavelength of the CT transition (859 nm). Thus, the dependence of the results on the basis set is dictated by a high sensitivity of the CT band to the contact distance between enolate and flavin, which in turn, depends upon the flexibility of the basis set used in the optimization. Since the

model does not include all the functional residues of active site in studies of the acyl-CoA dehydrogenase with the redox-inactive thioester analog 3-thia-octanoyl-CoA, one should not necessarily expect excellent agreement with experiment. External steric and electrostatic interactions that are not taken into account in the present models may affect the contact distance. Interestingly, when the thienolate is replaced by the 3-thia-butanoyl-CoA model enolate ($CH_3SCH(C=O)SCH_3^{\ominus}$, Figure 10), the complexation energy is reduced significantly (15.6 vs. 22.2 Kcal•M^{-1}) and the distance between substrate and flavin is markedly increased (C1C10a=3.44 Å C□C4a=3.20 Å).

3.3.6. DISCUSSION

The flavin cofactor at the active site of ACADs interacts with the protein via H-bonds to the positions N(1)-C(2)=O, N(3)-H, C(9)=O and, of particular relevance in the present context, N(5) (Kim & Miura, 2004).

Table 3: Sequence alignment of amino acid residues around the group (Thr or Ser) that forms a H-bond with the flavin N(5) position. In the case of MCAD Thr is the last residue of strand 3 (position 168) close to the loop that interconnects strand 3 and next structural motif (strand 4 or helix) on the Si-side of the flavin. The sequences and alignments were obtained from a BLAST search and from (Kim et al., 1993; Djordjevic et al., 1995; Tiffany et al., 1997; Battaile et al., 2004; Fu et al., 2004)

Acyl-CoA dehydrogenase	Abbreviation	Sequences
Medium chain-	MCAD hum	IINGQKMWI**T**NGGKAN
Iso(3)valeryl-	i3VD	ILNGNKFWI**T**NGPDAD
Very long chain-	vLCAD2 (ACAD-9)	ILNGSKVWI**T**NGGLAN
Short chain-	SCAD	VLNGTKAWI**T**NSWEAS
Butyryl (bacterial)	BCAD(M.e.)	TLNGSKIFI**T**NGGAAD
Glutaryl-	GD	TLNGTKTWI**T**NSPMAD
Iso(2)valeryl-	i2-VD (SBCAD)	VLNGSKMWI**S**SAEHAG
Long chain, branched	LCAD	ILNGSKVFI**S**NGSLSD
Isobutyryl-	iBD (ACAD-8)	ILNGSKAFI**S**GAGGSD
Very long chain-	vLCAD1	TLNGSKLWI**S**NGGLAD
Consensus or		LNG K WI**T**
conservative exchange		I F **S**

The latter is unusual within the flavoprotein family. However, an amino acid functional group that forms such a H-bond is strictly conserved in the ACAD family as shown in Table 3 (either a threonine or a serine that is part of a rather well conserved loop). This contrasts to the case of Acyl-CoA oxidases where such an interaction is absent (Nakajima et al., 2002). Since, compared to MCAD, the active site of the oxidases is more flexible and open to solvent in order to allow access/reactivity with oxygen, it is likely that the N(5)-H-bond contributes to the rigidity of the active site in the dehydrogenase subfamily (Ghisla & Thorpe, 2004; Kim & Miura, 2004).

The effect of this interaction manifests in the absorption spectra of the oxidized chromophore. Comparison of uncomplexed Thr168Ala-MCAD and wt-MCAD (Thorpe et al., 1979) evidences that spectrum of the former has a more resolved shape of the two main bands. This indicates a more hydrophobic environment (Biemann et al., 1983) and suggests that the role of the Thr-OH function is not taken over by H_2O. Similarly, at low pH with 3S-C_8-CoA and 4NPA-CoA as neutral ligands an enhancement of the spectral resolution is observed (not shown). With the same ligands at higher pH and also with 3-keto-octanoyl-CoA, an additional transition is observed (Figure 3) that is attributed to the CT-complex between bound, anionic ligand and the oxidized flavin. From the absence of effects of pH on the spectra is concluded that with 3-keto-octanoyl-CoA the microscopic pK_a for ligand αC-H deprotonation lies below pH 5. This correspond to a pK shift > 5 pK units. With 3S-C_8CoA a $pK_a \approx 6.6$ is found (Figure 6, Pane A) that compares to a $pK_a \approx 5.2$ for wt-MCAD (the pK_a for the uncomplexed species is ≈ 16.5 (Lau et al., 1988) corresponding to a pK shift of ≈ 10 pK units). The differences between wt- and T168A-MCAD is corresponding to a minor „activation“ for the latter (≈ 1.4 pK units $\hat{=}$ 2 Kcal·M^{-1}; Figure 6A). With 4NPA-CoA and T168A-MCAD the analogous pK shift is from ≈ 13.6 (free species (Vock et al., 1998)) to 9-10, i.e. the pK is lowered by ≈ 5 pK units (≥ 5.5 Kcal•M^{-1}). As a comparison with wt-MCAD the extent of pH decrease is by ≥ 9 pK units (from 13.6 to 5.2 (Vock et al., 1998)). The difference in “activation” of ≥ 4 pK units (≥ 5.5 Kcal·M^{-1}) between wt- and Thr168Ala-MCAD is thus substantial and can hardly be attributed solely to the N(5)···Thr168-OH interaction.

The binding constants K_d for binding of 3S-C_8CoA and 4NPA-CoA do not differ substantially for T168- and wt-MCAD (Table 1, Figure 4) suggesting that the T168A

mutation does not alter the mode of binding. However, the higher K_d value for 4NPA-CoA (Table 1) indicates major steric constrains and possibly also electronic effects. The pNO_2 group of this analog can interact with Glu99 at the "bottom" of the active site (Kim et al., 1993) and upon anionization the negative charge will be delocalized into the pNO_2-phenyl ring. With 3S-C_8CoA the corresponding negative charge will be localized very much as the substrate during deprotonation of the αC-H. The rate of this process with 3S-C_8CoA αC-H appears to be similar with the T168A mutant and wt-MCAD. This suggest that there are no major differences in the orientation of Glu376, the H^+-abstracting base (Ghisla & Thorpe, 2004), ligand and flavin. In contrast to this, with 4NPA-CoA steric constraints and the interaction with Glu99 at the "bottom of the active site" discussed earlier (Vock et al., 1998) probably mask the effects of the N(5) H-bond in question.

We assumed that the difference in the extent of "activation" (difference in αC-H pKs corresponding to $\approx$ 2 Kcal·M^{-1} for 3S-C_8-CoA within the complex) is an effect attributable to the T168-N(5) H-bond. This effect would be reasonable for a H-bond with a 2.93 Å length. However, this also implies that the effect is "transmitted" effectively via the interaction of the orbitals of the flavin to the ligand.

A similar effect of the H-bond is also seen in the difference between the $2e^-$ redox potentials of Thr168Ala- and wt-MCAD $\approx$ 40 mV corresponding to $\approx$ 1.8 Kcal·M^{-1}. Such effects are fully consistent with recent results from Miura's group (Nishina et al., 2003), which evidentiate a linear correlation between the redox potential of MCAD reconstituted with modified flavin cofactors with the αC-H pK_a of bound 3S-C_8CoA.

As demonstrated by the data reported in Figure 1 and Table 1, T168A-MCAD is reduced rapidly by octanoyl-CoA. There are two main differences compared to the behavior of wt-MCAD: With the latter flavin reduction occurs in general in two phases the rates which differ by approx. one order of magnitude (Schopfer et al., 1988). The ratio of the velocities and relative extent of the phases depend also on the substrate chain length and pH. Remarkably, with the T168A mutant flavin reduction is essentially monophasic! This argues against heterogeneity within the tetramer (Reinsch et al., 1980), although it cannot rigorously exclude it. The second difference regards the rates of the observed coenzyme reduction (k_{red}) by the substrate C_8CoA that is approx. two orders of

magnitude lower in the pH range 7-9 compared to wt-MCAD (a direct comparison is not possible due to the different pH profiles, Figure 1B). This corresponds to a $\Delta\Delta G$ = 1.2-2.4 Kcal·M^{-1}and again it appears reasonable to attribute the effect primarily to the Thr168-OH-bond. However, it should be stated that this is merely a rather crude estimation since a direct comparison of kinetic parameters is difficult: The reason is that the profile of activity versus substrate chain length is different for the mutant and wt-MCAD, and the pH dependence of the rates have different profiles reflecting different apparent pK's.

The above estimates appear to be in good agreement with the theoretical calculations. The latter indicate that the H-bonding in the model that simulates the Thr168-OH bond to the oxidized flavin N(5) reduces the hydride transfer barrier by 1.1 Kcal·M^{-1} that would translate into an approx 6-fold increase of the rate of the forward reaction. On the other hand the calculations (Table 2) indicate a decrease of the reaction exothermicity by 1.8 Kcal·M^{-1} that correspond to a 20-fold rate increase in the reverse process.

In general the DFT calculations suggest that the Thr168-OH hydrogen bond has a moderate, but noticeable effect on the overall dehydrogenation reaction.

In conclusion it appears that the T168-OH bond to the flavin N(5) plays an hitherto unrecognized, but important role in catalysis/substrate activation by MCAD. It also affects MCAD stability as reported earlier in the context of studies on the effects of genetic diseases on ß-oxidation in humans (Küchler et al., 1999). With respect to the absence of reactivity of 5d-FAD-MCAD mentioned in the introduction it should be recalled that the ratio of steps k_1/k_{-1} (Scheme 1, (A)) that represent dehydrogenation is not substantially different from unity with MCAD and many substrates. This equilibrium is shifted substantially "to the right" (Scheme 1) only with the "best" substrates such as C_8CoA. The effects of the T168 H-bond (≈ 1-2 Kcal·M^{-1}) and of the difference in redox potential (≈ 5.6 Kcal·M^{-1}) due to N->C substitution at pos. 5 of the flavin will be cumulative and this is likely to induce a decrease in the rate of k_{red}, the dehydrogenation step (k_1 in Scheme 1) by 3-4 orders of magnitude thus shifting the equilibrium of Scheme 1, (B) far to the left and provide a rationale for the absence of activity of 5d-FAD-MCAD.

Since, compared to MCAD, the active site of the oxidases is more flexible and open to solvent in order to allow access/reactivity with oxygen, it is likely that the N(5)-H-bond contributes to the rigidity of the active site in the dehydrogenase subfamily (Ghisla & Thorpe, 2004; Kim & Miura, 2004).

3.4. Studies on the T136A-MCAD mutant

3.4.1. Introduction

Hydrogen bond interactions or networks thereof are widely found in biological systems. They play a critical role in static frameworks as well as in dynamic processes, including enzymatic catalysis, when the reversibility of the processes is dictated by weak interactions. Many enzyme employ transition-state proton bridges as an element in their strategy to accelerate the reaction (Richard, 1998; Schowen et al., 2000; Cleland, 2003; Maniscalco et al., 2004).

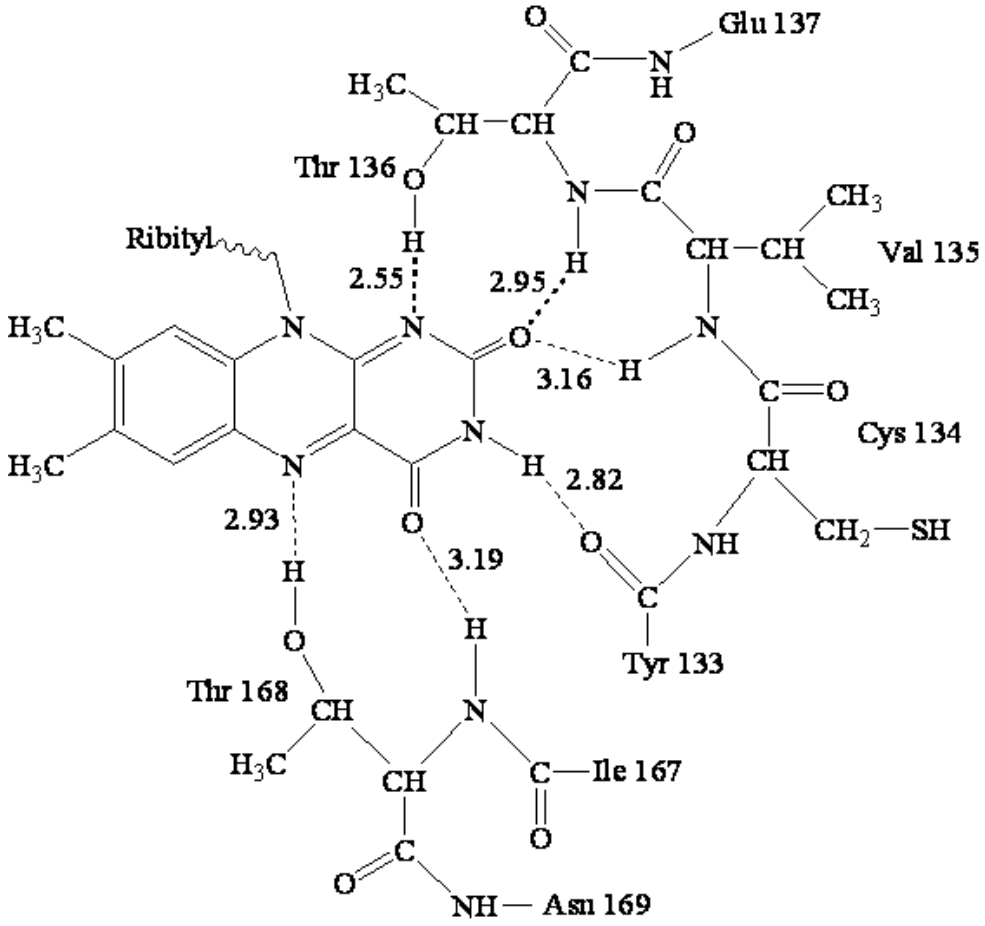

Scheme 1: H-bonds surrounding isoallozaxine ring at the active center of MCAD. Thr136-OH forms a tight (2.55 Å) H-bond to the flavin N(1) while C(2)=O is involved in an interaction with N H from an amide group (2.95 Å). The scheme also shows other H-bonds between hydrophilic part of the FAD ring and other aminoacids.

In flavoenzyme-catalyzed reaction, hydrogen bonds associated with the cofactor and with the substrate are important for their activation and for the mutual alignment required for catalysis. In MCAD the FAD is bound in an extended conformation, with the isoalloxazine ring buried at the interface between two helix domains and one β-sheet domain (Kim et al., 1993). Within the H-bond network that fixes the FAD at the active site, Thr136-OH is thought to form a particularly important H-bond with N(1) of the FAD isoalloxazine ring (Scheme 1). Among the 6 H-bonds formed by the isoalloxazine ring with aminoacids at the active site of MCAD one is of the donor and five of the acceptor variety.

In an earlier study Saijo et. al have adressed the role of Thr136 residue in the biogenesis and expression of MCAD by studying several Thr136X mutants (Saijo et al., 1998). It was found that only T136S-MCAD was folded into a tetramer at yields similar to those found with wt-enzyme. Expression and folding of other mature mutants (T136D- and T136L-MCAD) was seriously impaired. Good results in the expression and purification of T136S-MCAD were obtained also in *E.coli.* In contrast, good expression of T136D-MCAD was achieved only in the presence of FAD, while hydrophobic substitution such as in T136L-MCAD strongly reduced the folding/assembly of the tetramer and the presence of FAD had no influence on the process.

In the present chapter we have investigated the role of Thr136-OH by substituting it with Ala. Various properties of the mutant such as the redox potential have been studied and the results were correlated with theoretical calculation.

3.4.2. Physical properties

The visible absorbtion spectrum of T136A-MCAD (Figure 1) differs slightly from that of wt-MCAD; the first flavin band at 454 nm is red-shifted, while the second band at 373 nm is identical for both of the enzyme.

The effect of pH on the absorbtion spectra was examined in UV-Vis range. At neutral pH, the spectrum of the mutant shows λ_{max} at 456nm. When the pH was increased a blue shift for λ_{max} and a marked decrease in absorbance occur (Figure 2).

The pH dependent changes (Figure 3 insert) reflect an apparent pK ≈ 9.6. These spectral changes do not correspond to those that go along with deprotonation of free flavin at the N(3)-H position in which a strong increase and shift of the band at ≈ 380 nm

is observed (Molla et al., 2000). On the other hand the decrease in extinction of the 450 nm band corresponds approximately to the difference in extinction coefficient between free FAD ($\varepsilon \approx 10800\ M^{-1}cm^{-1}$) and the flavin in MCAD ($\varepsilon \approx 14800\ M^{-1}cm^{-1}$) (Kieweg et al., 1997).

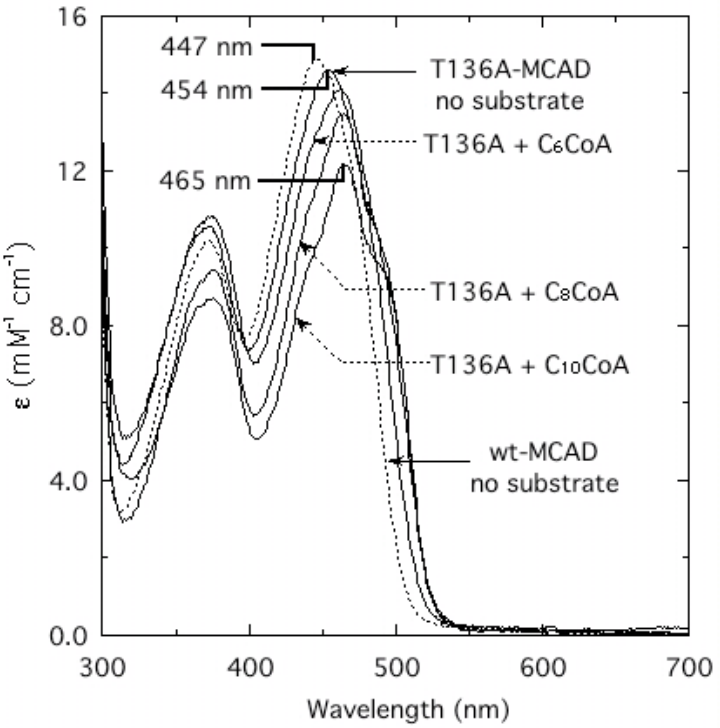

Figure 1. Spectral changes observed upon incubation of T136A-MCAD with substrates of varying chain length. The mutant was 6.5-10 µM in 50 mM "mixed buffer" containing 250 mM KCl, at pH 7 and 25 °C. The acyl-CoA substrates with the indicated chain length were added (12-15 equivalents) to the oxidized enzyme under aerobic (C_6CoA) or anaerobic condition (glucose 10 mM / glucose oxidase 0.2 µM). Spectra were recorded after approx. 5 min at which time spectral changes had ceased. The spectrum of wt-MCAD in the absence of substrate(s) is shown for comparison.

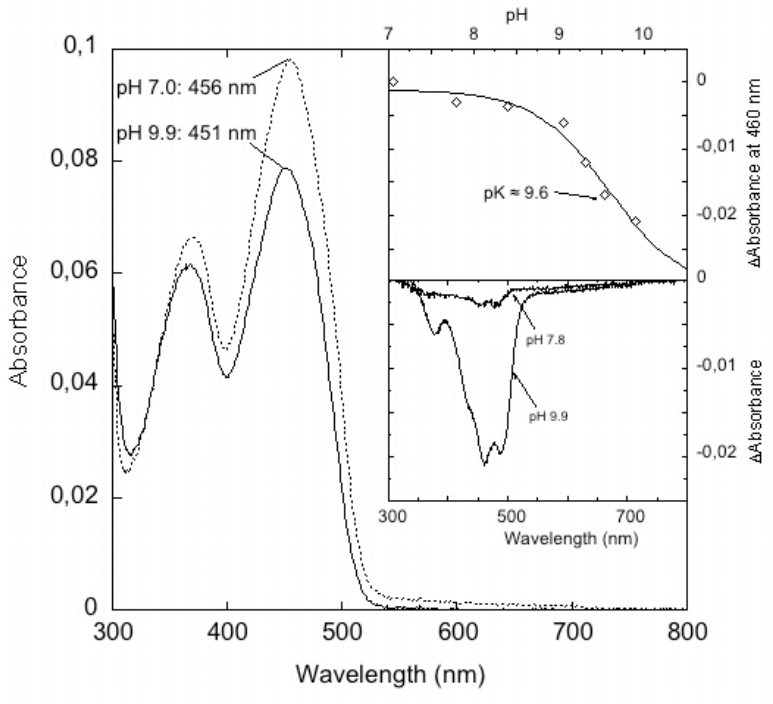

Figure 2. Effect of pH on the isoalloxazine UV-Vis spectrum. Conditions: T136A-MCAD (---), 5.5 μM, in KPi 100 μM, pH 7, 25 °C. The pH was adjusted using Na_2CO_3 (pH < 9) or NaOH (pH > 9). The inserts show spectral changes at 460 nm at different pH values respectively the difference spectra at pH 7.8 and 9.9.

It is thus likely that the observed ionisation disrupts the interactions between the flavin and the protein frame at the

active site, while FAD remains bound. This is compatible with the difference spectra that go along with the change in pH (Fig. 2, insert).

3.4.3. Reaction with substrates

First, we have examined the reaction of the mutant using substrates of varying chain length under anaerobic or aerobic conditions (Figure 1). The enzyme is partially reduced (≈ 20 %) by substrate (C_{10}CoA) under anaerobic or aerobic conditions. in the second case, after 4-5 min a slow reoxidation ensues. This is in contrast with the T168A-MCAD mutant that is reduced completly and faster even under aerobic conditions (see previous chapter). However, the extent of reduction is inversely proportional to the substrate chain length (Figure 1). Figure 3 shows the titration of T136A-MCAD with C_8CoA. The spectrum of the complex is characterized by a broad absorbtion band in the long wavelength region typical of the charge transfer interaction of the flavin with the electron deficient product C_8-octenoyl-CoA (Figure 3). The maximal absorbtion is at 555-585 nm (wt-MCAD charge transfer complex with the same substrate shows a similar similar band (Engel, 1992)).

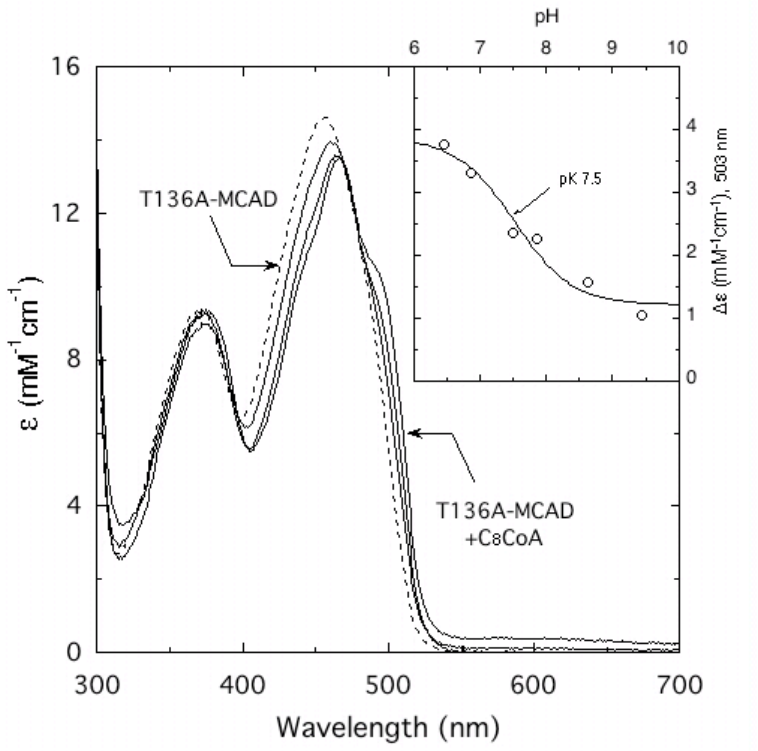

Figure 3. Reaction of T136A-MCAD (---) with C_8CoA or C_{10}CoA: Spectrum of T136A-MCAD, 6.85 µM, in 50 mM "mixed buffer" containing 250 mM KCl, pH 7, and at 25 °C. The traces shown in the main panel are those of the species obtained upon addition of 0, 1.16, 3.46 and 37.6 equivalents of C_8CoA (descending order at 450 nm). The inset shows the dependence the extent at 503 nm with pH of the mutant (10 µM) after reaction with 15 equivalents of C_{10}CoA in anaerobic conditions (see Figure 1)

Further, we investigated spectral changes of the flavin after substrate binding depending on pH. The pK value estimated at 7.5 (Figure 3 insert) coincide with pK resulted from pH dependence of K_m with C_8CoA (Chapter 3.1.3.2).

Second, we have investigated the dehydrogenation step of T136A-MCAD with the stopped-flow instrument and using the best substrate, C_{10}CoA (Figure 4). The first observed phase is fast (700 s^{-1}) and is followed by a second, which is one order magnitude slower. The reaction was investigated as a function of substrate concentrations. It appears that the first rapid phase that corresponds to an increase of absorbance at 460 nm and the first phase of reduction show saturation behavior. Similarly the extent of reduction is increasing with substrate concentration and also shows saturation (Figure 4, inset).

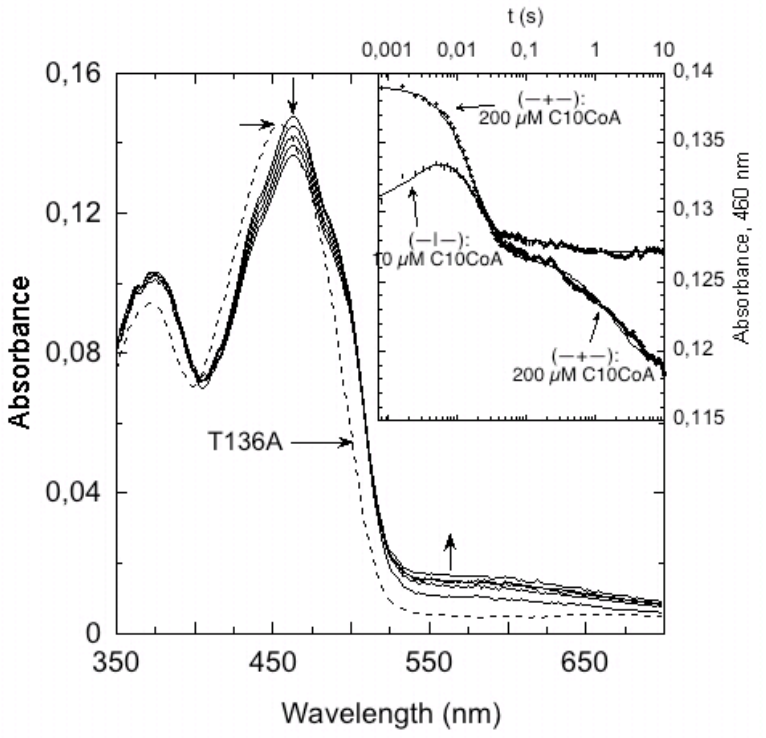

Figure 4. Rapid reaction Thr136A-MCAD with C_{10}CoA. T136A-MCAD (---), 10 μM final concentration, in "mixed buffer" containing 250 mM KCl, pH 8, 25 °C was mixed with the 100 μM of the substrate in the stopped flow instrument at 25 °C. Selected spectra were recorded at 0.8, 8.8, 16.8, 26.4 and 100 ms. The insert shows the course of reaction at 460 nm at two different concentrations of the substrate.

3.4.4. Catalytic properties and substrate specificity

The catalytic parameters of T136A-MCAD with substrates of various chain lengths using ferricenium assay are illustrated in Table 1 (Chapter 3.1.2). The V_{max} value of the mutant with C_8CoA is ≈ 20% that of wt-MCAD at pH 7.6 ($T.O._{max}$ = 260 min^{-1}). In general, the mutant shows a weaker affinity for substrates and a preference for C_{10}CoA.

The mutant is stabile in buffers containing high concentrations of salts (the activity is essentially unaltered after one week at 25 °C).

3.4.5. Determination of oxidation/reduction potentials

The oxidation/reduction potentials for the two one electron steps were determinated spectroscopically for wt- and T136A-MCAD using the method described by Massey (Massey, 1991), and with indigo monosulfonate as reference dye in the presence of the xanthine/xanthine oxidase as electron donating system (Figure 5) (Minnaert, 1965; Dutton, 1978; Wilson, 1978; Massey, 1991; Pollegioni et al., 2000). For wt-MCAD indigo disulfonate was used.

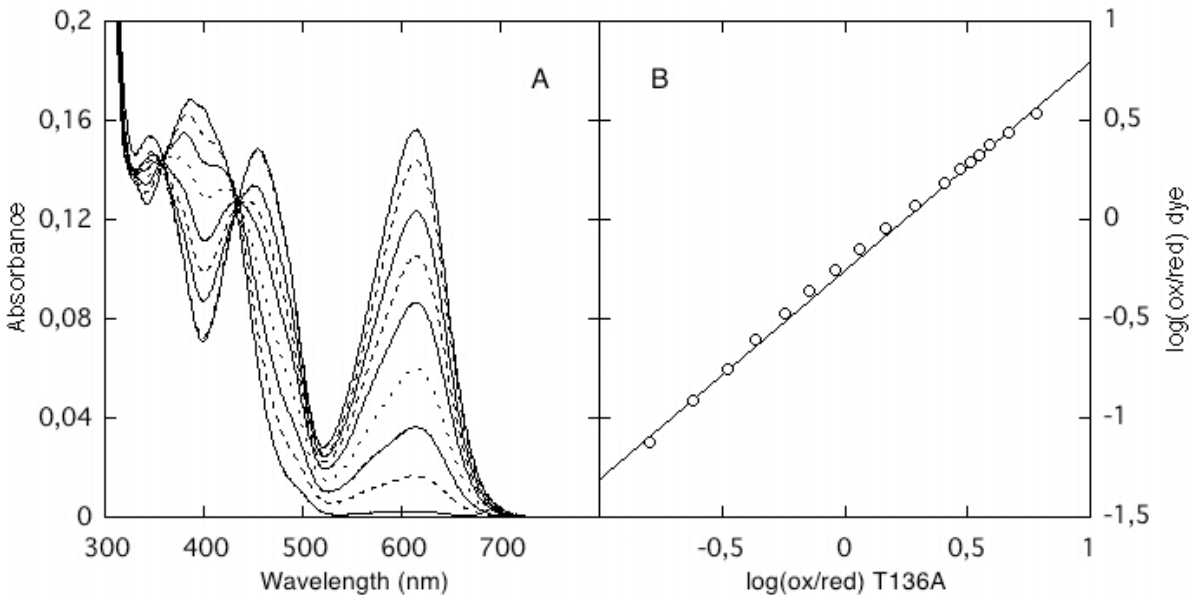

Figure 5. Determination of the redox potential of T136A-MCAD
Panel A. Selected spectra obtained during the course of the anaerobic reduction of T136A-MCAD (9 µM) in 50 mM KPi, pH 8 containing 10 % glycerol, 200 µM xanthine, and 5 µM benzyl viologen and 10 µM indigo monosulfonate (redox standard, $E_{m,7}$ = -157 mV). The traces shown are a representative selection and were recorded at 0, 21, 41, 51, 61, 71, 81 and 91 min after addition of xanthine oxidase (18 nM final concentration).
Panel B. Nernst plot according to Minnaert; n = 1 (Minnaert, 1965).

We found that cresyl violet acetate, a dye with a slightly lower redox potential that of indigo disulfonate, binds to MCAD (the complex has a maxima at 625 nm). Other option was Nile blue hydrogensulfat. This dye had a redox potential in the same range

with the previous one but two disadvantages: lower solubility, it is bind to DNA at pH 8 (Adkins & Burmeister, 1996). Our best alternative for redox titration of T136A-MCAD was indigo 5-monosulfonate (Figure 5, Panel A). The line of the Nernst plot in Figure 5 (Panel B) has a slope of 1, which is in agreement with the theoretical expected value for a two-electron/two electron couple. This is in agreement with equilibrium being established between the redox components during the reduction experiments. At pH 8, the potential of the T136A is lower than wt-MCAD (-212 mV for the mutant and –182 mV for wt-MCAD) (Mancini-Samuelson et al., 1998). From this it can be deduced that one of the main functions of this H-bond is the adjustement of the redox potential.

3.4.6. Interaction of T136A-MCAD with ligands

3.4.6.1. Interaction of 4-NPA-CoA with MCAD

Binding of 4-NPA-CoA to wt-MCAD induces the appearance of two absorbtions. At higher pH binding of the ligand is reflected by ligand anion formation (two supplementary absorbtions band) (Vock et al., 1998).

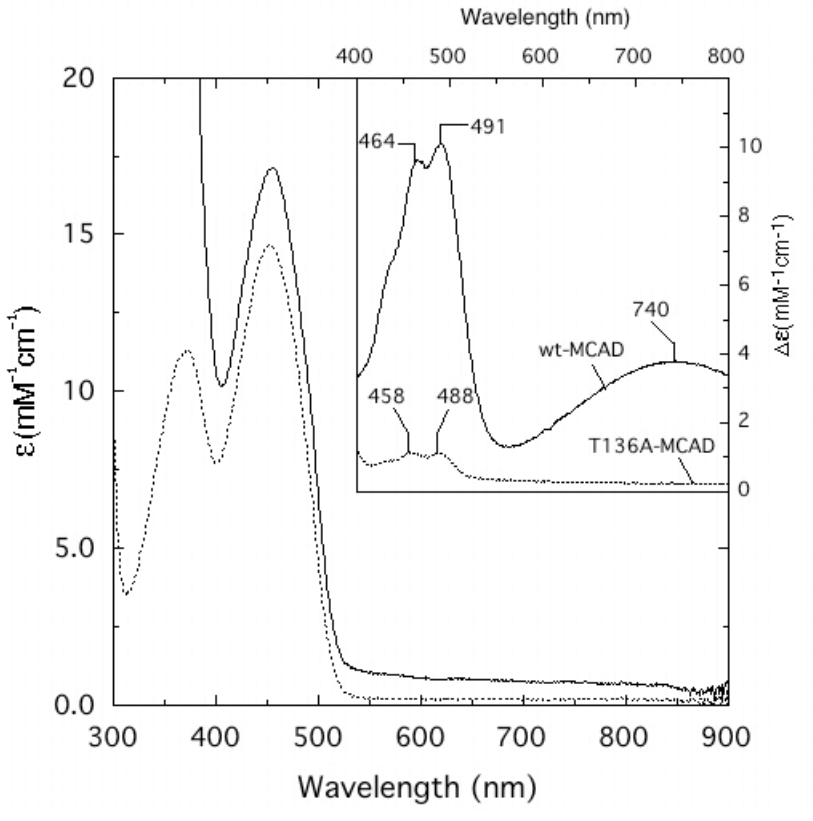

Figure 6. Interaction of T136A-MCAD with 4NPACoA. Curve (---): spectrum of uncomplexed enzyme (7.5 µM) in "mixed buffer" containing 250 mM KCl at pH 9 and at 25 °C. Curve (□): spectrum of the species obtained upon addition of a total of 70 µM 4NPA-C_8CoA (intermediar additions are not shown for clarity). Insert: difference between absorbtion spectra of complexed and uncomplexed species of either wt- (Vock et al., 1998) or T136A-MCAD.

In addition a band at ≈ 740 nm is formed that is attributed to charge transfer interaction between the anionic ligand as donor and the oxidized flavin as acceptor (Vock et al., 1998). The extinction of charge transfer complex of the mutant is weaker than that observed with wt enzyme. The position of the absorption of the anionic form of the ligand is similar for both the enzymes while the extinction coefficient at 490-500 nm is only one order of magnitude lower for the mutant (Figure 6 insert). The spectral changes associated with binding reflect a $K_d \approx 20\ \mu M$ at pH 9 (at pH 8 the value of the K_d was double) that compares to a $K_d \approx 70\ \mu M$ for wt-MCAD.

3.4.6.2. Interaction of $3SC_8CoA$ with MCAD

The complex of the wt-MCAD with $3SC_8CoA$ simulates a metastable intermediate during

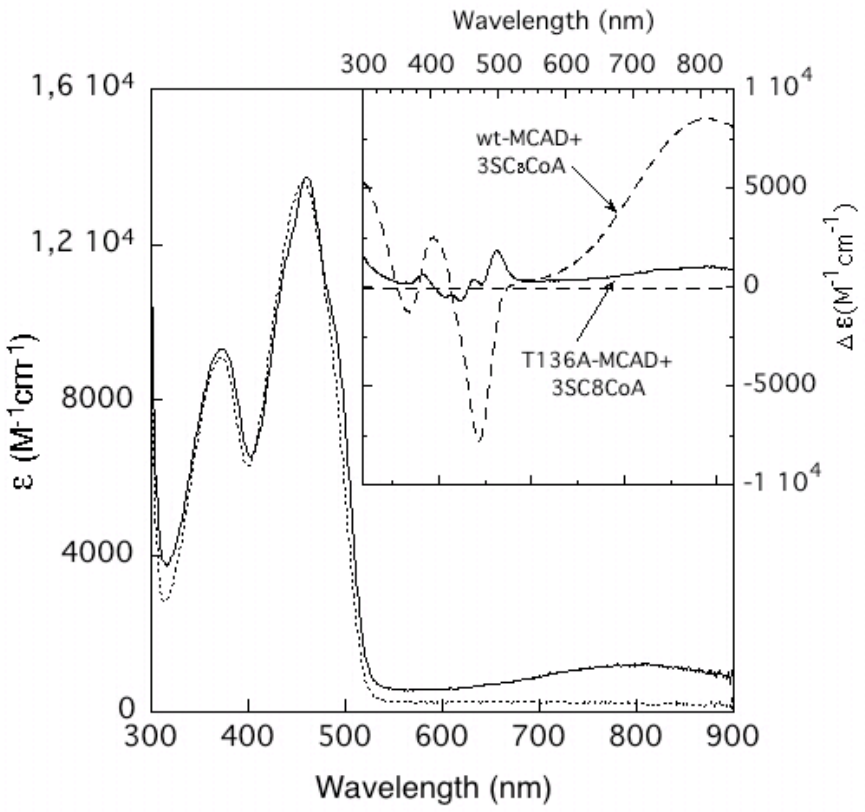

Figure 7. Interaction of T136A-MCAD with 3SC8CoA. Curve (---): spectrum of the uncomplexed enzyme in "mixed buffer" containing 250 mM KCl, pH 8. Curve ( ): spectrum of the charge transfer complex after addition of a total of 1.8 mM $3S\text{-}C_8CoA$ (intermediary additions are not shown for clarity). Insert: difference spectrum between complexed and uncomplexed species

□-proton abstraction and □-hydride transfer in the catalysis of MCAD with a natural substrate (Lau et al., 1988; Satoh et al., 2003). 3SC_8CoA binds to T136A and induces spectral effects that are quite different compared to those reported for wt-MCAD (Figure 7). The dependence of extinction coefficient of the complex with the pH is depicted in Figure 8. The microscopic pK of the analog in the complex with T136A-MCAD is ≈ 6.8, i.e. it is increased by ≈ 1.6 units compared to the same in wt-MCAD (this correspond to 2.2 Kcal·M^{-1}). The binding constant (K_d) was higher for the T136A-MCAD (30-40 µM at pH = 7-9) compared to 0.8 µM for wt-MCAD and the extinction coefficient of the mutant at the maximum of the CT absorbance is only ≈ 10 % that of wt-MCAD.

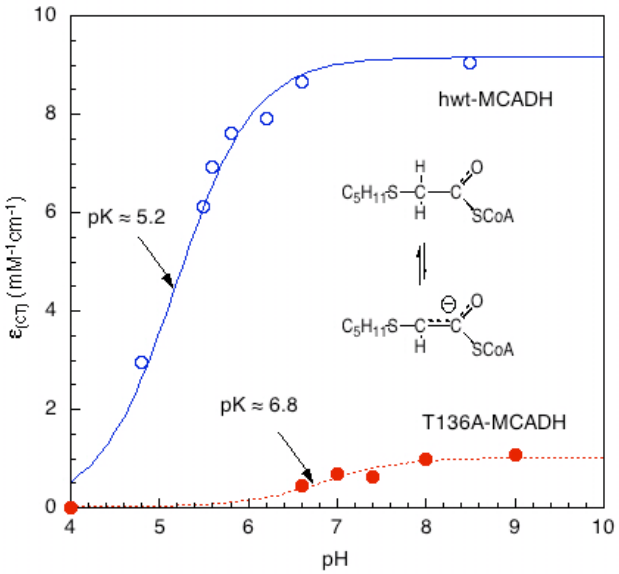

Figure 8. Effect of the pH on the charge transfer complex extinction coefficient of 3S-C_8CoA with T136A-MCAD. pH dependence of the CT-band (800 nm ●—●). The pH profile of wt-MCAD is shown for comparison (❍—❍). The data points are the extinction coefficients estimated for full complex formation from titration of the mutant with the ligand (Vock et al., 1998).

3.4.6.3. Computational studies on the THR136 H-bond effect (by Olga Dmitrenko and Robert Bach)

These studies were undertaken to complement the experiments described above and in order to obtain a semiquantitative assessment of the effects of the H-bond in question.

The Thr136-OH H-bond to the flavin N(1)-C(2)=O moiety should have an influence on the hydride transfer in that it might affect both the transition and the product states (Scheme 2). First they have optimized the pre-reaction complex, transition structure and product complex in the system which consist only of two components,

thioenolate and Fl_{ox} with the 2'-OH group of the ribityl moiety represented by a $-CH_2CH_2OH$ group that forms the hydrogen bond to the substrate carbonyl oxygen.

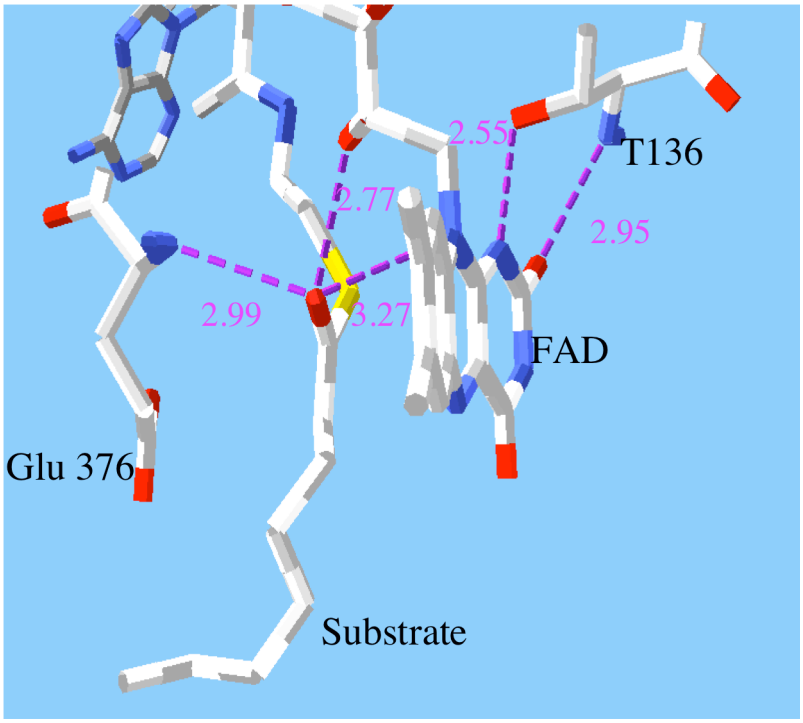

Scheme 2. Arrangement of the relevant functional group (T136A), flavin and the substrate at the active site of MCAD. The image was generated using SwissPDBViewer

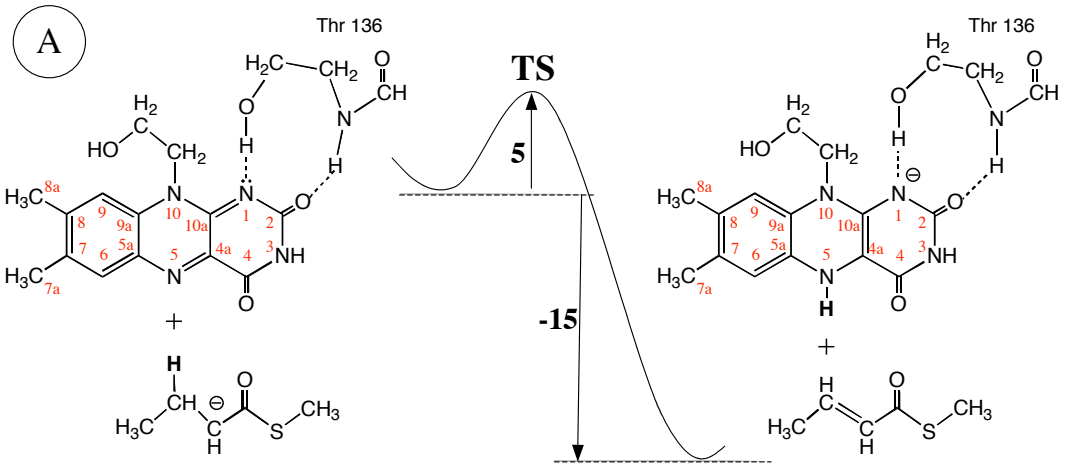

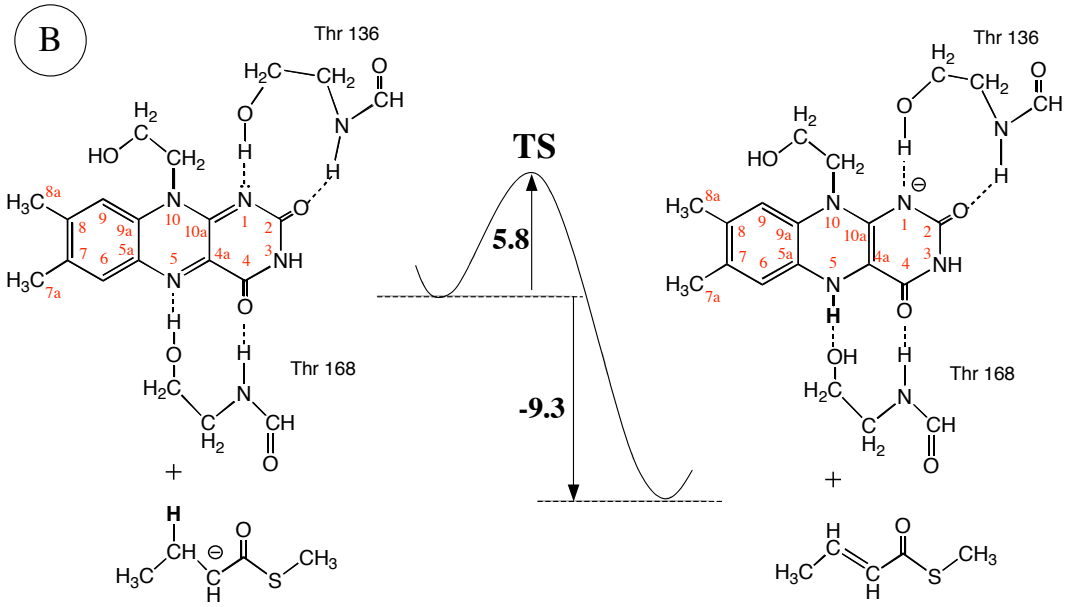

Figure 9. Transition structure optimized for hydride transfer and including flavin N(1)-Thr136 H-bond The system A includes $CH_3CH_2CH(C=O)SCH_3^{\ominus}/Fl_{ox}$ and THR136 models at the B3LYP/6-31+G (d,p) level. The system B includes $CH_3CH_2CH(C=O)SCH_3^{\ominus}/Fl_{ox}$ and THR136 + THR168 models at the B3LYP/6-31+G (d) level. The hydride is shown in bold in the lower structure diagrams.

As it has been discussed in a recent study the pre-reaction complex is stabilized by charge-transfer and H-bonding (OH…O=C<) interaction (Bach et al., 2002; Dmitrenko et al., 2003). The energy of complexation relative to isolated reactants is 22.2 Kcal·M^{-1}. The reaction is exothermic (ΔE = -9.3 Kcal·M^{-1}) with the barrier $\Delta E^{\neq}$ = 7.8 Kcal·M^{-1}. In the model ($HOCH_2CH_2NH(C=O)H$ molecule was chose to represent T136. For this system resulted reaction barrier was 2.7 Kcal·M^{-1} lower and the exothermicity increased by 5.6 Kcal·M^{-1} (Figure 9). The product complex formed after H^- transfer is thus more stable. This bears directly on the "extent of reduction" of the flavin and agrees with the experimental data that show a considerably smaller extent of reduction for the Thr136Ala mutant (Figure 2).

3.4.7. DISCUSSION

The flavin cofactor at the active site of MCAD interacts with threonine residues via strong H-bonds (Kim et al., 1993). In the present chapter we studied the effect of the interaction of this bond with the N(1)-C(2)=O moiety of the isoalloxazine ring. It should be pointed out that a group capable to form such a H-bond is conserved within the ACAD family as shown in Table 1.

Table 1: Sequence alignment of amino acid residues around the group (Thr or Ser) that forms a H-bond with the flavin N(1) and C(2)=O position. In the case of MCAD Thr is at position 136 and the second residue of a loop that interconnects sheet 1 and helix 9 on the Si-side of the flavin. The sequences and alignments were obtained from a BLAST search and from (Kim et al., 1993; Djordjevic et al., 1995; Tiffany et al., 1997; Battaile et al., 2004; Fu et al., 2004).

Acyl-CoA dehydrogenase	Abbreviation	Sequences
Medium chain-	MCAD pig	LMCAYCV**T**EPGAGSD
Butyryl (bacterial)	BCAD (M.e.)	TKLGAFGL**T**EPNAGTD
Glutaryl-	GD	ELLGCFGL**T**EPNSGSD
Isobutyryl-	iBD (ACAD-8)	EKFASYCL**T**EPGSGSD
Long chain, branched	LCAD	KCIGAIAM**T**EPGAGSD
Very long chain-	vLCAD (ACAD-9)	EHIAAFCL**T**EPASGSD
Very long chain-	vLCAD (ACADVL)	ETVAAFCL**T**EPSSGSD
Iso(2)valeryl-	i2-VD (SBCAD)	EKVGSFCL**S**EAGAGSD
Iso(3)valeryl-	I3-VD	EYIGALAM**S**EPNAGSD
Consensus or		**T**E GSD
Consevative exchange		**S** T

The absorbtion spectrum of oxidized, uncomplexed T136A-MCAD (Figure 1) has a similar profile with that one of wt-MCAD. In agreement with the lower redox potential the cofactor was only partially reduced by substrate.

Binding of the 4NPA-CoA to T136A-MCAD was slightly stronger in comparison with wt-MCAD, but extinction coefficient value of charge transfer band was diminished (Figure 6). The pKa ≈ 6.8 for 3S-C_8CoA is 1.6 pK units higher compared to that found with wt-MCAD (Figure 8) corresponding to a difference of 2.2-2.3 Kcal·M^{-1}. A similar contribution (2 Kcal·M^{-1}) was observed for T168A-MCAD. The charge transfer complex band has a lower intensity suggesting that orbital overlapping is impared.

QM/MM computational studies yield the following effects: a) the hydrogen bond of Thr136 (in the model molecule) reduces the hydride transfer barrier by 2.7 $Kcal \cdot M^{-1}$ and b) it increases reaction exotermicity by 5.6 $Kcal \cdot M^{-1}$ (Figure 9).

In conclusion, contribution of Thr136-OH···N(1) H-bond was deduced using experimental and theoretical approaches. We find a good agreement (10-20 % differences were observed) between theoretical calculation and experimental measurements.

3.5. Role of Thr168 in Human MCAD: A study based on Directed Mutagenesis

3.5.1. Introduction

In a general sense the expression and purification of proteins carrying a His-Tag at either the N- or the C-terminal end can be a most convenient method compared to traditional approaches (Ghisla 2004). It is quick and can leads to good yields of active proteins. In some cases, however, the incorporation of the His-Tag has adverse consequences that can manifest in a variety of fashions (Halliwell et al., 2001; Mast et al., 2004). Attempts to adapt this approach for the production of MCAD and mutants by inserting a His-Tag at the N-terminal end have not been successful (P. Bross, personal communication). However, the expression and purification of active, recombinant MCAD from rat carrying a His-Tag at the C terminal end has been described recently (Zeng & Li, 2004). While this is good news, there are some important differences between rat and human MCAD (Zeng & Li, 2004). These are relevant in the context of the study of human genetic defects that require comparison of a variety of enzymatic properties. Furthermore, and as a basis for such comparisons, a careful determination of the properties of normal MCAD *vs* His-Tag-protein is important. We have thus set out to express His-Tag, human MCAD, and some of its mutants, and in particular such ones that carry an alteration of Thr168. Indeed Thr168Ala-MCAD has been found as a genetic defect in humans (Andresen et al., 1997).

3.5.2. Characterization of His-Tag-MCAD and Thr168X mutants

Upon IPTG induction (0.1 mM) His-Tag-MCAD was expressed to ≈ 2-3 % of the total protein in cell lysates (as estimated from specific activity measured using the ferricenium assay (Lehman & Thorpe, 1990)). Purification by Ni-NTA chromatography (Bornhorst & Falke, 2000) followed by gel filtration yielded 15-20 mg protein for 8 L incubation medium corresponding to a 30-40% yield, and with a purity of $> 95\%$ (Figure 1). His-Tag-MCAD is much more stable at 42 °C and pH 7 compared to "normal" enzyme, it loses ≈ 80 % of its initial activity within 25 hrs (see Figure 11, chapter 3.1.4).

The absorption spectrum of normal His-Tag-MCAD is very similar to that of normal MCAD in the 300-600 nm range; it shows a small ≈ 2 nm blue shift of the band in the visible and also minor alterations in the difference spectra (Figure 2 insert). It has, however a higher $A_{270}/_{445}$ ratio = 5.6 that is attributed to the increased absorbance in the far UV due to the His-Tag. Some eloquent differences between the absorbtion spectra of the oxidized form of T168A- respectively His-Tag-T168V-MCAD and the wt-enzyme were observed.

Figure 1. SDS-PAGE electrophoresis of His-Tag-MCAD. M: marker; line 1: protein after Ni-NTA column, line 2: main fraction after gel filtration. line 3: "normal" wt-MCAD (no His-Tag)

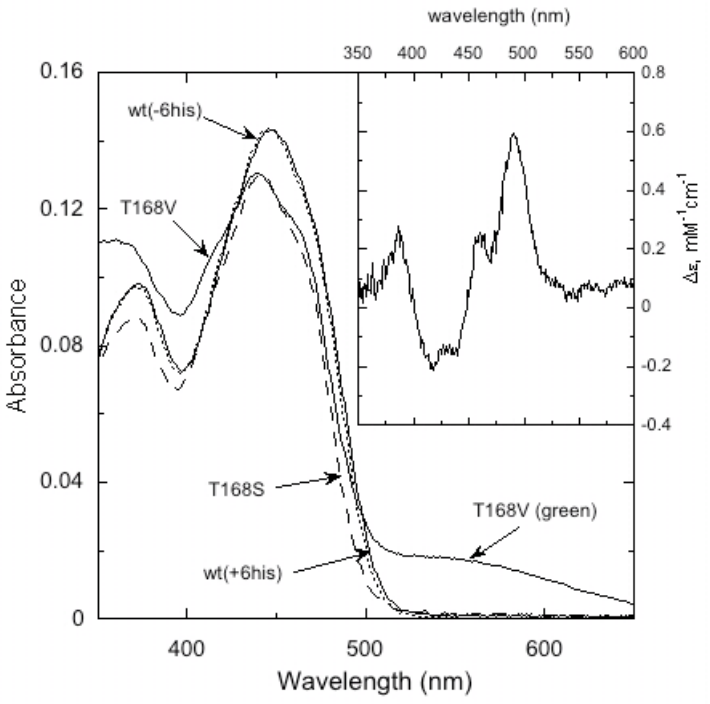

Figure 2. Visible absorbance spectra of His-Tag MCAD and its mutants and comparison with "normal" enzyme The spectra of wt-MCAD (with or without His-Tag) were recorded at 25 °C and pH 8.0. Absorbance spectra of the mutants were measured in the same buffer (pH 7.0). The insert shows the difference spectra between His-Tag-MCAD and "normal" recombinant MCAD.

Both of the mutants exhibit two distinct shoulders (at approx. 460 and 415 nm) and a blue shift from 447 to 439 in the λ_{max} in the visible region. Noticeably T168V-MCAD was

isolated in a green form (broad absorbtion band at 500-600 nm) attributed to tightly bound CoA-S-persulfide (Williamson et al., 1982). In contrast, the spectrum of the Thr168Ser mutant is similar to that of Thr168-MCAD (see Figure 2).

Activity parameters of "normal" wt-MCAD and His-Tag-wt-MCAD, as well as those of T-, V-, and S168-MCAD are compared in Table 1. First it appears that the insertion of the His-Tag at the C-terminal of MCAD has little if any effect on these properties. The only relevant difference is in Km for octanoyl-CoA (Table 1). With T168S-MCAD the activity is 60-70 % that of His-Tag-wt-MCAD (at pH 7 using the same buffer – see Figure 3), while with both Thr168Val- and Thr168Ala-MCAD it is reduced to approx 15% (Table 1). Direct comparison is not feasible since the different proteins have also different pH dependencies of the activity (Figure 3).

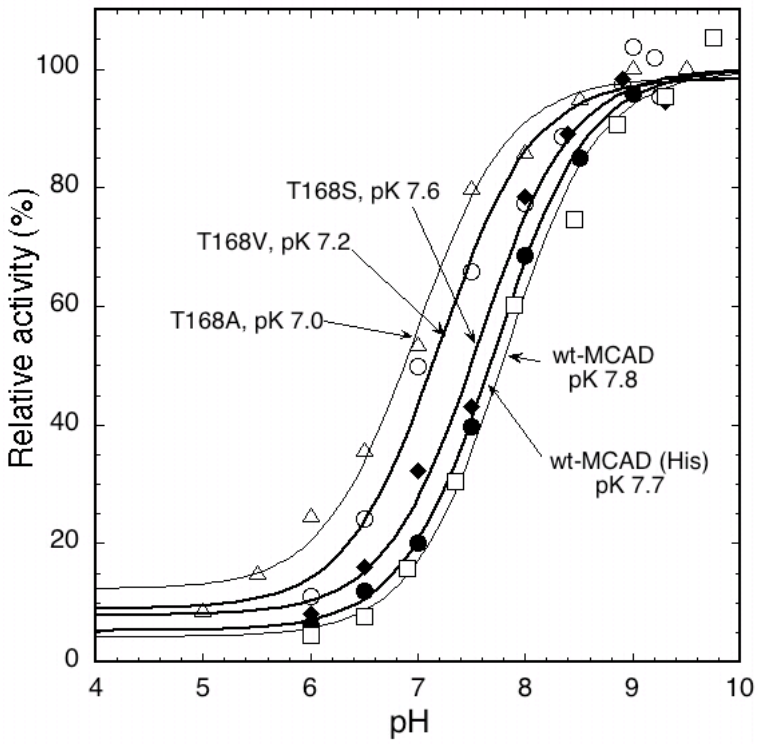

Figure 3. pH dependence of the activity for wt-, T168S- and T168V-MCAD (His-Tag enzymes) and comparison with wt- and T168A-MCAD. The activity was measured using C_8CoA as substrate and in „mixed buffer" containing 250 mM KCl at 25 °C. For wt-MCAD (60 nM) the data points are the result of a Michaelis Menten analysis. For T168S (100 nM) and T168V-MCAD (150-250 nM depending on pH) the value were obtained using 200 μM C_8CoA, a concentration that ensures saturation. The curve for T168A-MCAD is shown for comparison and was taken from Küchler et al (Küchler et al., 1999). The activity values have been normalized to 100 % for the purpose of comparison. The same figure was used to describe the pH dependence of activity in chapter 3.1.3 (Figure 8).

In this context it is intriguing that at low pH the mutants appear to be more active than wt-MCAD. A further, sensitive parameter for comparison is the pH dependence of the activities that reflects the apparent pK's (Figure 3). These pK's are assumed to reflect the polarity at the active center of MCAD (Ghisla & Thorpe, 2004). The identity of the pK in the case of normal, vs His-Tag-wt-MCAD is compatible with little or no changes induced

by this modification, and in agreement with the absorbance spectra. With the T168S mutant the pK is slightly lowered suggesting a minor effect at the active center. However, with the Ala and Val mutants the pKs are lowered significantly (Figure 3, Table 1)

Table 1. **Selected properties of T168-MCAD mutants and comparison with wt-MCAD**

Enzyme / Parameter	Wt-MCAD	Wt-His MCAD	T168A (Küchler 1999)	T168S	T168V
V_{max} (min^{-1}), pH 8.0, C_8CoA	1570	1600	200	1240	164
K_m (μM)	16	5.5	8.0	-	4.6
pK_{app} (see Fig. 1)	7.8	7.7	7.0	7.6	7.2
k_{red} (s^{-1}), pH 7.0, C_{14}CoA	6.8	6.1	nd	3.3	nd

3.5.3. Reductive Half-Reaction

Comparison of His-Tag- and "normal" MCAD and of wt-MCAD with T168X-mutants was extended to the study of the reductive half reaction with the stopped-flow technique. Since the reaction with the best substrate C_8CoA is too fast to be followed (k_{obs} > 500 s^{-1} (Nandy et al., 1996)), C_{14}CoA was selected as alternative substrate. With His-Tag- and "normal" MCAD the reaction proceeds very similarly, and as described earlier (Pohl et al., 1986). The rates for the reaction corresponding to enzyme flavin reduction (Scheme 1) are similar (6.1 s^{-1} for His-Tag- and 6.8 s^{-1} for "normal" enzyme). This suggests that the presence of the His-Tag "tail" does not interfere with substrate binding and dehydrogenation.

For the T168S-mutant the course of enzyme flavin reducton is depicted in Fig. 4. In contrast to the reaction of wt-MCAD, with the mutant there appears to be an initial rapid increase of absorbance of the 450 band with a rate $k_{obs} \approx 300\ s^{-1}$. This can be attributed to formation of the enzyme-substrate complex (Scheme 1). Upon this dehydrogenation ensues that is accompanied by the decrease of the oxidized flavin band in the 450 nm region, which occurs with a rate $k_{red} \approx 3.3\ s^{-1}$ (Figure 4).

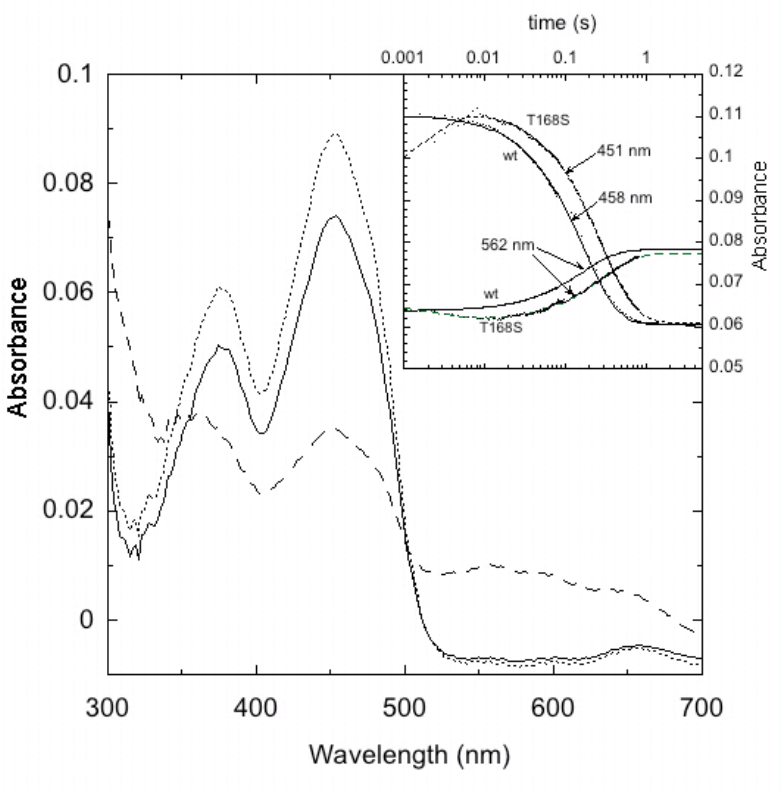

Figure 4. Spectral course of the reaction of oxidized His-Tag-T168S-MCAD (≈ 5 μM) with C_{14}CoA (50 μM) at pH 7 („mixed buffer", Figure 3) and 25 °C. Curve (—) represents the first spectrum obtained at 0.8 ms upon mixing. Curve (·····) was recorded after 7.5 ms and curve (□□□) approx. 1s. The insert shows the comparison of the time course of the reaction at the indicated wavelength for wt- and T168S-MCAD.

Scheme 1 represents a minimal set-up for the reactions just described.

$$\text{E-Fl}_{ox} + SH_2 \underset{k_{-1}}{\overset{k_1}{\rightleftharpoons}} \text{E-Fl}_{ox} \sim SH_2 \underset{k_{-2}}{\overset{k_2}{\rightleftharpoons}} \text{E-Fl}_{red} \sim S + 2H^+ + 2e^-$$

Scheme 1. Simplified kinetic scheme describing the steps involved in the reaction of His-Tag-T168S-MCAD with the substrate C_{14}CoA. E-Fl_{ox}~SH_2 is substrate complex of oxidized enzyme. E_{red}~S is the complex of reduced enzyme with trans-tetradec-2enoyl-CoA.

3.5.4. Interaction of 3-thia-octanoyl-CoA with MCAD

The identity of "normal" with His-Tag-MCAD is reflected also in the reaction with 3S-C_8CoA that deprotonates to its anionic form upon binding (Vock et al., 1998) and induced a strong charge transfer band (Figure 5). A minor difference is observed in the K_d for ligand binding that is approx. twofold weaker for the His-Tag enzyme.

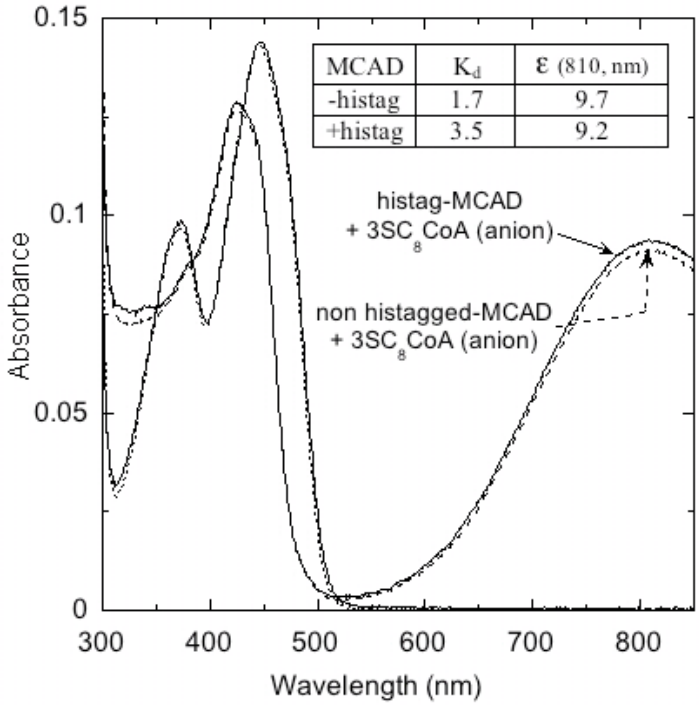

Figure 5. Interaction of MCAD with 3S-C_8CoA. Curve (---): spectrum of the uncomplexed or complexed "normal" MCAD, curve (—): spectrum of the uncomplexed or complexed His-Tag-MCAD. Conditions: 9-10 μM enzyme in "mixed buffer" containing 250 mM KCl and 10 % glycerol, pH 8, 25 °C. The spectra of complexed enzymes were obtained after adition of 80 μM (for "normal" enzyme) respectively 200 μM ligand (for His-Tag-MCAD). The absorbance values have been normalized for the purpose of comparison. The interaction constants (apparent Kd's) were estimated from experiments carried out at the same pH. The extinction coefficient values were resulted from extrapolation using Michaelis-Menten equation.

3.5.5. DISCUSSION

The method described here allows the production in good yield of soluble, active human His-Tag-MCAD (C-terminal) and of mutants (T168S and T168V) in *E. Coli* cells. As we demonstrate in the Figure 3 the activity/pH dependence of the "normal" and His-Tag- MCAD leads to similar pK values. Reduction of the MCAD was measured using C_{14}CoA as a substrate by stopped-flow method. His-Tag tail has a very small influence on the reduction rate of the enzyme. We have compared the ability of the His-Tag- and "normal"-wt-MCAD to form the charge transfer complex. The interactions of oxidized flavin with the ligand are very similar to those observed with "normal" enzyme. In conclusion the C-terminal His-Tag does have a significant influence on the enzymatic activity and kinetic properties of MCAD. The information gained by these studies generates new perspectives for faster purification and characterization of MCAD.

Two mutants were generated to elucidate the function of 168-OH···N(5) H-bond in MCAD catalysis. As described earlier, the T168 mutants revealed some differences in UV-Vis absorbtion spectra of the noncovalently bound chromophore (suggesting different environment of the FAD) (Küchler et al., 1999). The replacement of Thr-168 to serine slightly reduce the enzyme activity, but the T168V mutant was less active (at higher pH the activity of the mutant is approx. 10 % of that wt-His-Tag-MCAD) indicating that this 168-OH···N(5) H-bond is significant for catalysis. We have investigated reduction of His-Tag-T168S-MCAD with the same substrate by stopped flow method. This mutant retains the ability to produce a mutual orientation of the flavin with the substrate. In the first step (binding step), the oxidized enzyme rapidly forms a complex with the substrate (Scheme 1). In the slower second step (rate-limiting step or reduction step), the cofactor is partially reduced by the substrate and reduction rate of the mutant is two-fold lower. Moreover, for the wt-His-Tag-MCAD case the binding step seems to be much faster. Our findings are in concordance with earlier study regarding the role 168-OH···N(5) H-bond in MCAD catalysis (Küchler et al., 1999). Thus, both of the catalytical steps (proton and hydride transfer) are accompanies by preliminary hydrogen bonds formation.

4. REFERENCES

Abdel Ghany, A.G., Küchler, B., Bross, P., & Ghisla, S., *Medium Chain Acyl-CoA Dehydrogenase Genetic Defects: Identification and Partial Characterisation of two New Patient Mutants*, in *Flavins and Flavoproteins*, B. Agency for Scientific Publ., Editor. 1999, Ghisla, S., Kroneck, P., Macheroux, P., and Sund, H.: Konstanz, Germany. p. 535-538.

Adkins, S. & Burmeister, M. *Visualization of DNA in agarose gels as migrating colored bands: applications for preparative gels and educational demonstrations.* Anal Biochem, 1996. **240**(1): p. 17-23.

Al-Arif, A. & Blecher, M., *Synthesis of fatty acyl CoA and other thiol esters using N-hydroxysuccinimide esters of fatty acids.* J. Lipid Res., 1969. **10**: p. 344-345.

Amyes, T. L. & Richard, J. P., *Generation and stability of a simple thiol ester enolate in aqueous solution.* J.Am.Chem.Soc., 1992. **114**: p. 10297-10302.

Andresen, B. S. et al., *The molecular basis of medium-chain acyl-CoA dehydrogenase (MCAD) deficiency in compound heterozygous patients: is there correlation between genotype and phenotype?* Hum Mol Genet, 1997. 6(5): p. 695-707.

Andresen, B. S. et al., *Isolated 2-methylbutyrylglycinuria caused by short/branched-chain acyl-CoA dehydrogenase deficiency: identification of a new enzyme defect, resolution of its molecular basis, and evidence for distinct acyl-CoA dehydrogenases in isoleucine and valine metabolism. Am J Hum Genet*, 2000. **67**: p. 1095-1103.

Ankele, K., et al., *On the Role of Glu376 in Catalysis of Acyl-CoA Dehydrogenases*, in *Flavins and Flavoproteins 1990*, B. Curt, S. Ronchi, and G. Zanetti, Editors. 1991, Walter de Gruyter: Berlin. p. 325-328.

Ausubel, F. M., Brent, R., Kingston, R. E., Moore, D., Seidman, J. G., Smith, J. A., & Struhl K., *Schort Protocols in Molecular Biology*, ed. I. John Wiley & Sons. 2001. 1-29-1-30.

Bach, R., Thorpe, C. & Dmitrenko, O., *C-H.carboxylate oxygen hydrogen bonding in substrate activation by acyl-CoA dehydrogenases: Synergy between the H-bonds.* J. Phys. Chem. B, 2002. **106**: p. 4325-4335.

Battaile, K. P., Nguyen, T. V., Vockley, J. & Kim, J. J., *Structures of isobutyryl-CoA dehydrogenase and enzyme-product complex: comparison with isovaleryl- and short-chain acyl-CoA dehydrogenases.* J Biol Chem, 2004. **279**: p. 16526-16534.

Battaile, K. P., Mohsen, A-W., A. & Vockley, J., *Functional Role of the Active Site Glutamate-368 in Rat Short Chain acyl-CoA Dehydrogenase.* Biochemistry, 1996. 35: p. 15356-15363.

Becke, A. D. J., *Density-Functional Thermochemistry.3. the Role of Exact Exchange.* J. Chem. Phys., 1993. **98**: p. 5648.

Beckman, J. D. & Frerman., F. E., *The Effect of pH, ionic Strength, and Chemical Modifications on the Reaction of Electron Transfer Flavoprotein with Acyl Coenzyme A Dehydrogenase. J. Biol. Chem.*, 1983. **258**: p. 7563-7569.

Beckmann, J. D., Frerman, F. E. & McKean, M. C, *Inhibition of general acyl CoA dehydrogenase by electron transfer flavoprotein semiquinone. Biochem. Biophys. Res. Commun.*, 1981. **102**: p. 1290-1294.

Beckmann, J. D. & Frerman, F. E., *Reaction of electron-transfer flavoprotein with electron-transfer flavoprotein-ubiquinone oxidoreductase.. Biochemistry*, 1985. **24**: p. 3913-3921.

Beinert, H., *Acyl Coenzyme A Dehydrogenases and Electron-Transferring Flavoprotein*, in *The Enzymes*, P.D. Boyer, Lardy, H., & Myrback, K., Editor. 1963, Academic Press: New York. p. 447-476.

Bergman, E. N., Reid, R. S., Murray, M. G., Brockway, J. M. & Whitelaw, F, *Interconversions and production of volatile fatty acids in relation to the gut. Biochem. J.*, 1965. **97**: p. 53-58.

Bernert, J. T. & Sprecher, H., *An Analysis of Partial Reactions in the Overall Chain Elongation of Saturated and Unsaturated Fatty Acids by Rat Liver Microsomes.* J. Biol. Chem., 1977. **252**: p. 6736-6744.

Bertrand, C., Largilliere, C., Zabot, M. T., Mathieu, M., Vianey, & Saban C., *Very long chain acyl-CoA dehydrogenase deficiency: identification of a new inborn error of mitochondrial fatty acid oxidation in fibroblasts.* Biochim Biophys Acta, 1996. 1180: p. 327-329.

Bhattacharya, A.A., Grüne, T., & Curry, S., *Crystallographic Analysis Reveals Common Modes of Binding of Medium and Long-Chain Fatty Acids to Human Serum Albumin*. *J. Mol. Biol.*, 2000. **303**: p. 721-732.

Biemann, M., et al., *Oxidation of 2-thioflavins by peroxides. Formation of flavin 2-S-oxides.* J Biol Chem, 1983. **258**(9): p. 5440-5448.

Bisswanger, H., *Enzymkinetik. Theorie und Methoden.* 1994, Weinheim: VCH Verlagsgesellschaft mbH.

Bisswanger, H., *Enzyme Kinetics. Principles and Methods.*, ed. Weinheim. 2002: Wiley-VCH. 10-22.

Bloxam, W. P., *Die Analyse des Indigos.* Chemisches Zentralblatt, 1906. **II**(2): p. 1532-1533.

Bornhorst, J. A. & Falke, J. J., *Purification of proteins using polyhistidine affinity tags.* Methods Enzymol., 2000. **326**: p. 245-254.

Bowers, P. M. & Klevitt, R. E., *Hydrogen bond geometry and $^{2}H/^{1}H$ fractionation in proteins.* J Am Chem Soc, 2000. **122**: p. 1030-1033.

Bross, P., Engst, S., Strauss, A. W., Kelly, D. P., Rasched, I., & Ghisla, S., *Characterization of wild-type and an active site mutant of human medium chain acyl-CoA dehydrogenase after expression in Escherichia coli. J Biol Chem***.**, 1990. **265**: p. 7116-7119.

Bross, P. et al., *Effects of two mutations detected in medium chain acyl-CoA dehydrogenase (MCAD)-deficient patients on folding, oligomer assembly, and stability of MCAD enzyme.* J Biol Chem, 1995. **270**(17): p. 10284-10290.

Brown, N. F., Esser, V., Foster D. W., & McGarry, J. D., *Expression of a cDNA for rat liver carnitine palmitoyltransferase I in yeast establishes that catalytic activity and malonyl-CoA sensitivity reside in a single polypeptide. J. Biol. Chem.*, 1994. **269**: p. 26438-26442.

Buznikov, G. A., Lambert, H. W. & Lauder, J. M., *Serotonin and serotonin-like substances as regulators of early embryogenesis and morphogenesis. Cell Tissue Res.*, 2001. **305**(**2**): p. 177-186.

Carpenter, K., Wiley, V., Sim, K., G., Heath, D., & Wilcken, B., *Evaluation of newborn screening for medium chain acyl-CoA dehydrogenase deficiency in 275,000 babies. Arch Dis Child Fetal Neonatal Ed*, 2001. **85**: p. 105-109.

Chace, D. H., Hillman, S. L., Van Hove, J. L., & Naylor, E. W. (*Rapid diagnosis of MCAD deficiency: quantitatively analysis of octanoylcarnitine and other acylcarnitines in newborn blood spots by tandem mass spectrometry. Clin Chem*, 1997. **43**: p. 2106-2113.

Chace, D. H., Kalas, T. A., & Naylor, E. W., *The application of tandem mass spectrometry to neonatal screening for inherited disorders of intermediary metabolism. Annu Rev Genomics Hum Genet*, 2002. **3**: p. 17-45.

Chance, B., Eisenhardt, R. M., Gibson, Q. H. & Lonberg-Holm, K. K., *Rapid mixing and sampling techniques in biochemistry*. 1964, New York: Academic Press.

Charrow, J., Goodman, S. I., McCabe, E. R., & Rinaldo, P., *Tandem mass spectrometry in newborn screening. Genet. Med.*, 2000. **2**: p. 267-269.

Cho, Y.-K., Rebhonz, K. L., & Northrop, D. B., *Solvent isotope effects on the onset of Inhibition of porcine pepsin by pepstatin.* Biochemistry, 1994. **33**: p. 9637-9642.

Cleland, W. W., *The use of isotope effects to determine enzyme mechanisms.* J Biol Chem, 2003. **278**(52): p. 51975-51984.

Crane, F. L., et al., *On the mechanism of dehydrogenation of fatty acyl derivatives of coenzyme A.* J. Biol. Chem., 1956. **218**: p. 701-716.

Dixon, M. & Webb, E. C., ed. *Enzymes*. third ed. 1979, Longman Group Limited: London. 138-164.

Djordjevic, S., et al., *Three-dimensional structure of butyryl-CoA dehydrogenase from Megasphaera elsdenii.* Biochemistry, 1995. **34**(7): p. 2163-2171.

Djordjevic, S., et al., *Identification of the catalytic base in long chain acyl-CoA dehydrogenase.* Biochemistry, 1994. **33**(14): p. 4258-4264

Dmitrenko, O., Thorpe, C. & Bach, R. D., *Effect of a Charge-Transfer Interaction on the Catalytic Activity of Acyl-CoA Dehydrogenase: A theoretical study of the Role of Oxidized Flavin.* J. Phys. Chem. B., 2003. **107**: p. 13229-13236.

Dommes, V., & Kunau, W. H., *A convenient assay for acyl-CoA-dehydrogenases.* Anal Biochem., 1976. 71(2): p. 571-578.

DuPlessis, E. R., Pellett, J., Stankovich, M. T. & Thorpe, C., *Oxidase activity of the acyl-CoA dehydrogenases.* Biochemistry, 1998. **37**: p. 10469-10477.

Duran, M., et al., *Sudden child death and "healthy" affected family members with medium-chain acyl-Coenzyme A Dehydrogenase deficiency.* 1986. **78**: p. 1052-1057.

Dutton, P. L., *Redox potentiometry: Determination of Midpoint Potentials of Oxidation-Reduction Components of Biological Electron-Transfer Systems*, in *Meth. Enzym*. 1978, Academic Press, Inc. p. 411-435.

Eder, M., Kräutle, F.-G., Dong, Y., Vock, P., Kieweg, V., Kim, J.-J., Strauss, A., W. & Ghisla, S., *Characterization of human and pig kidney long-chain-acyl-CoA dehydrogenase and their role in ß-oxidation.* Eur. J. Biochem., 1997. 245: p. 600-607.

Engel, P. C., *Acyl-coenzyme A dehydrogenases.*, in *Chemistry and Biochemistry of Flavoenzymes*, F. Müller, Editor. 1992, Boca Raton. p. 597-655.

Engel, P. C. & Massey, V., *Green Butyryl-Coenzyme A Dehydrogenase.* Biochem. J., 1971. **125**: p. 889-902.

Engst, S., Vock, P., Wang, M., Kim, J.-J. & Ghisla, S., *Mechanism of activation of acyl-CoA substrates by medium chain acyl-CoA dehydrogenase: interaction of the thioester carbonyl with the flavin adenine dinucleotide ribityl side chain.* Biochemistry, 1999. **38**: p. 257-267.

Engst, S., *Untersuchungen zum Struktur-Wirkungsgefüge im Aktivzentrum der mittelkettigen Acyl-CoA Dehydrogenase*. 1993, Universität Konstanz.

Engst, S., Bross, P., Stiemke, J., Schieber, A., Strauss, A. W., Kelly, D. P., Rached, I. & Ghisla, S., *Some properties of Glu-376-Gln active site mutant of human medium-chain acyl-CoA dehydrogenase*, in *Flavins and Flavoproteins*. 1990, Walter de Gruyter & Co: Berlin & New York. p. 319-323.

Engst, S. & Ghisla, S., *Aromatic Substrate Analogues as Mechanistic Probes for Medium-Chain Acyl-CoA Dehydrogenases.*, in *Flavins and Flavoproteins 1990*, B. Curti, S. Ronchi, and G. Zanetti, Editors. 1991, Walter de Gruyter & Co.: Berlin. p. 311-314.

Felig, P. & Wahren, J., *Fuel homeostasis in exercise. N. Engl. J. Med*., 1975. **293**: p. 1078-1084.

Fendrich, G. & Abeles, R. H., *Mechanism of Action of Butyryl-CoA Dehydrogenase: Reaction with Acetylenic, Olefinic, and Fluorinated Substrate Analogues. Biochemistry*, 1982. **21**: p. 6685-6695.

Fenoll, L. G., et al., *Deuterium isotope effect on the oxidation of monophenols and o-diphenols by tyrosinase.* Biochem J, 2004. **380**(Pt 3): p. 643-650.

Fersht, A., *Enzyme. Structure and Mechanism*. 1985, New York: W. H. Freeman & Co.

Fox, K. M. & Karpus, P. A., *Old yellow enzyme at 2 A resolution: overall structure, ligand binding, and comparison with related flavoproteins. Structure*, 1994. **2**: p. 1089-1105.

Frerman, F. E. & Turnbull, D., *Interaction of medium chain acyl-CoA dehydrogenase with substrate and electron transfer flavoprotein.* Prog Clin Biol Res, 1990. **321**: p. 79-89.

Fu, Z., et al., *Crystal structures of human glutaryl-CoA dehydrogenase with and without an alternate substrate: structural bases of dehydrogenation and decarboxylation reactions.* Biochemistry, 2004. **43**(30): p. 9674-9684.

Furuta, S., Miyazawa, S. & Hashimoto, T., *Induction of acyl-CoA dehydrogenases and electron transfer flavoprotein and their roles in fatty acid oxidation in rat liver mitochondria. J. Biochem*. (Tokyo), 1981. **90**: p. 1751-1756.

Gerland, P. B., Shepherd, D. & Yates, D. W., *Biochem. J*., 1965. **97**: p. 587-594.

Gerlt, J. A., & Gassman, P. G., *An Explanation for Rapid Enzyme-Catalyzed Proton Abstraction from Carbon Acids: The Importance of Late Transition States in Concerted Mechanisms. J. Am. Chem. Soc.*, 1993. **115**: p. 11552-11568.

Ghisla, S. & Thorpe, C., *Acyl-CoA dehydrogenases. A mechanistic overview.* Eur J Biochem, 2004. **271**: p. 494-508.

Ghisla, S. et al., Prog Clin Biol Res: New Dev. Fatty Acid Oxid., 1994. 375: p. 283-292.

Ghisla, S., Engst, S., Vock, P., Kieweg, V., Bross, P., Nandy, A., Rasched, I. & Strauss, A.W., in *Flavins and Flavoproteins*, K. Yagi, Editor. 1993: New York. p. 283-292.

Ghisla, S., Engst, S., Vock, P., Kieweg, V., Bross, P., Nandy, A., Rasched, I., & Strauss, A., *Mechanism of □,□-Dehydrogenation by Acyl-CoA Dehydrogenases*. Flavins and Flavoproteins, ed. K. Yagi. Vol. 11. 1994, Nagoya: W. de Gruyter & Co., Berlin, New York.

Ghisla, S. & Massey, V., *Mechanisms of Flavoprotein-catalyzed Reactions. Eur. J. Biochem*, 1989. **181**: p. 1-17.

Ghisla, S., Thorpe, C. & Massey, V., *Mechanistic Studies with General Acyl-CoA Dehyrogenase and Butyryl-CoA Dehyrogenase: Evidence for the Transfer of the ß-Hydrogen To Flavin N(5)-Position as a Hydride.* Biochemistry, 1984. **23**: p. 3154-3161.

Gibson, K. M. et al. *2-Methylbutyryl-coenzyme A dehydrogenase deficiency: a new inborn error of L-isoleucine metabolism. Pediatr Res*, 2000. **47**: p. 830-833.

Goodman, S. I., et al., *Molecular cloning and expression of a cDNA encoding human electron transfer flavoprotein-ubiquinone oxidoreductase.* Eur J Biochem, 1994. **219**(1-2): p. 277-286.

Gopalan, K. V., & Strivastava, D. K., *Beyond the Proton Abstracting Role of Glu-376 in Medium-Chain Acyl-CoA Dehydrogenase: Influence of Glu-376 Gln Substitution on Ligand Binding and Catalysis.* Biochemistry, 2002. **41**: p. 4638-4648.

Gradinaru, R. V., Kieweg, V., Dmitrenko, O., Bach, R. D., & Ghisla, S, *Mechanisms and properties of medium-chain acyl-CoA dehydrogenase: Role of the active center Thr168-flavinN(5) H-bond in catalysis.* Biochemistry, 2005.

Gradinaru, R. V., Kieweg, V., Küchler, B. & Ghisla, S, *On the role of the 376-functional group in catalysis by medium chain acyl-CoA dehydrogenase*, in *Flavins and Flavoproteins*, S. Chapman, Perham, R. & Scrutton, N., Editor. 2002, Rudolf Weber: Cambridge, UK, p. 193-198.

Green, D. E., Mii, S., Mahler, H. R. & Bock, R. M., *Studies on the fatty acid oxidizing system of animal tissues.III. Butyryl CoA-Dehydrogenase.* J. Biol. Chem., 1954. 206: p. 1-12.

Gregersen, N., et al., *Molecular characterization of medium-chain acyl-CoA dehydrogenase (MCAD) deficiency: identification of a lys329 to glu mutation in the MCAD gene, and expression of inactive mutant enzyme protein in E. coli.* Hum Genet, 1991. **86**(6): p. 545-551.

Hall, C. L. & Kamin, H., *The Purification and Some Properties of Electron Transfer Flavoprotein and General Fatty Acyl Coenzyme A Dehydrogenase from Pig Liver Mitochondria.* J. Biol. Chem., 1975. **250**: p. 3476-3486.

Halliwell C. M., Morgan, G., Ou C. P. & Cass, A. E., *Introduction of a (poly)histidine tag in L-lactate dehydrogenase produces a mixture of active and inactive molecules.* Anal Biochem., 2001. **295(2)**: p. 257-261.

Hanahan, D., Jessee J & Bloom, F. R., *Techniques for transformation of E. coli. (2nd ed.)*, in *DNA Cloning: A Practical Approach*, D.M. Glover, Hames, B. D., Editor. 1998, Oxford University Press: England.

Hartridge, H. & Roughton, F. J. W., *The velocity with which carbon monoxide displaced oxygen from combination with haemoglobin.* Proceedings the Royal Society of London, 1923. **94**(Series B): p. 336-367.

Hauge, J. G., Crane, F. L. & Beinert, H., *The mechanism of dehydrogenation of fatty acyl derivatives of coenzyme A. III. Palmityl CoA dehydrogenase. J. Biol. Chem.*, 1956. **219**: p. 727-733.

Hazekawa, I., Nishina, Y., Sato, K., Shichiri, M., Miura, R., & Shiga, K., *A Raman study on the C(4)=O stretching mode of flavins in flavoenzymes: hydrogen bonding at the C(4)=O moiety. J Biochem* (Tokyo), 1997. **121**(**6**): p. 1147-1154.

Hazekawa, I., et al., *Substrate Activating Mechanism of Short-Chain Acyl-CoA, Medium-Chain Acyl-CoA, Long-Chain Acyl-CoA, and Isovaleryl-CoA Dehydrogenases from Bovine Liver: A Resonance Raman Study on the 3-Ketoacyl-CoA Complexes.* J. Biochem., 1995. **118**: p. 900-910.

Hemmerich, P., Massey, V. & Fenner, H., *Flavin and 5-deazaflavin: A chemical evaluation of „modified" flavoproteins with respect to the mechanisms of redox biocatalysis. FEBS Lett.*, 1977. **84**: p. 5-21.

Hesler, C., Olymbios, C. & Haldar, D., *Transverse-plane topography of long-chain acyl-CoA synthetase in the mitochondrial outer membrane. J. Biol. Chem*, 1990. **265**: p. 6600-6605.

Hoessel, R., Leclerc, S., Endicott, J. A., Nobel, M. E., Lawrie, A., Tunnah, P., Leost, M., Damiens, E., Marie, D., Marko, D., Niederberger, E., Tang, W., Eisenbrand, G., Meijer, L., *Indirubin, the active constituent of a Chinese antileukaemia medicine, inhibits cyclin-dependent kinases.* Nat Cell Biol, 1999. **1**(1): p. 60-67.

Iafolla, A. K., Thompson, R. J. Jr., & Roe, C. R., *Medium-chain acyl-coenzyme A dehydrogenase deficiency: clinical course in 120 affected children. J. Pediatr.*, 1994. **124**: p. 409-415.

Ikeda, Y., Okamura-Ikeda, K. & Tanaka, K., *Purification and Characterisation of Short-chain,Medium-chain,and Long-chain Acyl-CoA Dehydrogenases from Rat Liver Mitochondria.* J. Biol. Chem., 1985a. **260**: p. 1311-1325.

Ikeda, Y., et al., *Mechanisms of Action of Short-chain, Medium-chain, and Long-chain Acyl-CoA Dehydrogenases.* J. Biol. Chem., 1985b. **260**: p. 1326-1337.

Indiveri, C., Tonazzi, A. & Palmieri, F. *Characterization of the unidirectional transport of carnitine catalyzed by the reconstituted carnitine carrier from rat liver mitochondria.* Biochim Biophys Acta, 1991. **1069**(1): p. 110-116.

Itoh, Y. et.al, *Free fatty acids regulate insulin secretion from pancreatic ß cells through GPR40. Nature*, 2003. **422**: p. 173-176.

Izai, K., Uchida, Y., Orii, T., Yamamoto, S. & Hashimoto, T. (1992). Novel fatty acid beta-oxidation enzymes in rat liver mitochondria. I. Purification and properties of very-long-chain acyl-coenzyme A dehydrogenase. *J. Biol. Chem*. **267**, 1027-1033.

Jia, Y., Kappock, T. J., Frick, T., Sinskey, A. J. & Stubbe, J., *Lipases Provide a New Mechanistic Model for Polyhydroxybutyrate (PHB) Synthases: Characterization of the Functional Residues in Chromatium vinosum PHB Synthase.* Biochemistry, 2000. 39: p. 3927-3936.

Johnson, B. D., Mancini-Samuelson, G. J., & Stankovich M. T., *Effect of transition-state analogues on the redox properties of medium -chain acyl-CoA dehydrogenase. Biochemistry*, 1995. **34**: p. 7047-7055.

Johnson, B. D. & Stankovich, M. T., *Thermodynamic studies of medium-chain acyl-CoA dehydrogenase complexed to thioether-CoA ligands. Prog Clin Biol Res*, 1992. ***375***: p. 63-68.

Johnson, J. K., Wang, Z. X., & Strivastava, D. K., *Mechanistic Investigation of Medium Chain Fatty Acyl-CoA Dehydrogenase.Utilizing 3-Indolepropionyl/Acryloyl-CoA as Chromophoric Substrate Analogues. Biochemistry*, 1992. **31**: p. 10564-10575.

Karpefors, M., Ädelroth., P., & Brzezinski, P., *Localized Control of Proton Transfer through the D-Pathway in Cytochrome c Oxidase: Application of the Proton-Inventory Technique.* Biochemistry, 2000. **39**: p. 6850-6856.

Kelly, D. P., et al., *Molecular characterization of inherited medium-chain acyl-CoA dehydrogenase deficiency.* Proc Natl Acad Sci U S A, 1990. **87**(23): p. 9236-9240.

Kieweg, V., Krautle, F. G., Nandy, A., Engst, S., Vock, P., Abdel-Ghany, A. G., Bross, P., Gregersen, N., Rasched, I., Strauss, A., & Ghisla, S., *Biochemical characterization of purified, human recombinant Lys304-->Glu medium-chain acyl-CoA dehydrogenase containing the common disease-causing mutation and comparison with the normal enzyme.* Eur J Biochem, 1997. **246**: p. 548-556.

Killenberg, P. G., Davidson, E. D. & Webster, Jr. L., *Evidence for a medium-chain fatty acid: coenzyme A ligase (adenosine monophosphate) that activates salicylate. Mol. Pharmacol.*, 1971. **7**: p. 260-268.

Kim, J.-J. P. & Miura, R., *Acyl-CoA dehydrogenase and Acyl-CoA oxidases. Structural basis for mechanistic similarities and differences.* Eur. J. Biochem., 2004. **271**: p. 483-493.

Kim, J.-J. P. & Paschke, W. R., *Evolution of an Active Site: The Three-Dimensional Structures of Acyl-CoA Dehydrogenases*, in *Flavins and Flavoproteins*, S. Ghisla, Kroneck, P., Macheroux, P., and Sund H., Editor. 1999, Agency for Scientific Publ., Berlin: Konstanz, Germany. p. 491-498.

Kim, J.-J. P.., et al., *Three Dimensional Structures of Acyl-CoA Dehydrogenases: Structural Basis of Substrate Specificity*, in *Flavins and Flavoproteins 1993*, K. Yagi, Editor. 1994, Walter de Gruyter & Co.: Berlin. p. 274-282.

Kim, J.-J. P., Wang, M. & Paschke, R., *Crystal structures of medium-chain acyl-CoA dehydrogenase from pig liver mitochondria with and without substrate.* Proc. Natl. Acad. Sci. USA, 1993. **90**: p. 7523-7527.

Kim, J.-J. P. & Wu, J., *Structure of the medium-chain acyl-Co A dehydrogenase from pig liver mitochondria at 3-Å resolution.* Proc. Natl. Acad. Sci. USA, 1988. **85**: p. 6677-6681.

Kinney, H. C. et al. (2003). " Serotonergic brainstem abnormalities in Northern Plains Indians with the sudden infant death syndrome." *J Neuropathol Exp Neurol.* **62**(**11**): 1178-1191.

Kleman, G. L. & Strohl, W. R., *Developments in high cell density and high productivity microbial fermentation.* Curr Opin Biotechnol, 1994. **5**(2): p. 180-1806.

Kolodziej, M. P., Crilly, P. J., Corstorphine, C. G. & Zammit, V. A., *Development and characterization of a polyclonal antibody against rat liver mitochondrial overt carnitine palmitoyltransferase (CPT I). Distinction of CPT I from CPT II and of isoforms of CPT I in different tissues. Biochem*. J., 1992. **282**: p. 415-421.

Kumar, N. R., Srivastava, D. K., *Reductive half-reaction of medium-chain fatty acyl-CoA dehydrogenase utilizing octanoyl-CoA/octenoyl-CoA as a physiological substrate/product pair: similarity in the microscopic pathways of octanoyl-CoA oxidation and octenoyl-CoA binding.* Biochemistry, 1994. **33**: p. 8833-8841.

Küchler, B., Abdel-Ghany, A. G., Bross, P., Nandy, A., Rasched, I., & Ghisla, S., *Biochemical characterization of a variant human medium-chain acyl-CoA dehydrogenase with a disease-associated mutation localized in the active site.* Biochem J., 1999. **337**: p. 225-230.

Küchler, B., Nandy, A., Ghany, A., & Ghisla, S., *Substrate chain length specificity of acyl-CoA dehydrogenases: Studies on different mutants*, in *Flavins and Flavoproteins*, S. Ghisla, Kroneck, P., Macheroux, P., & Sund H., Editor. 1999, Weber, R.: Berlin. p. 523-526.

Laemmli, U. K., *Cleavage of structural proteins during the assembly of the head of bacteriophage T4.* Nature, 1970. **227**(5259): p. 680-685.

Lau, S.-M. & Thorpe, C., *Substrate Complexes in the Acyl-Coenzyme A Dehydrogenase.* Arch. Biochem. Biophys., 1988. **262**: p. 293-297.

Lau S.-M., Brantley, R. K., & Thorpe, C., *The reductive half-reaction in acyl-CoA dehydrogenase from pig kidney: studies with thiaoctanoyl-CoA and oxaoctanoyl-CoA analogues. Biochemistry*, 1988. **27**: p. 5089-5095.

Lau, S. M., et al., *Medium-Chain Acyl Coenzyme A Dehydrogenase from Pig Kidney Has Intrinsic Enoyl Coenzyme A Hydratase Activity.* Biochemistry, 1986. **25**: p. 4184-4190.

Lehman, T. C. & Thorpe, C., *Alternate Electron Acceptors for Medium-Chain Acyl-CoA Dehydrogenase: Use of Ferricenium Salts.* Biochemistry, 1990. **29**: p. 10594-10602.

O'Leary, M. H., Yamada, H., & Yapp, C. J., *Multiple isotope effect probes of glutamate decarboxylase.* Biochemistry, 1981. **20**: p. 1476-1481.

Lemasters, J. J., Chacon, E., Ohata, H., Harper, I. S., Nieminen, A.-L., Tesfal, S. S. & Herman. B., *Measurement of electrical potential, pH, and free calcium ion concentration in Mitochondria of living cells by laser scanning confocal microscopy.* Meth. Enzym., 1995. 260: p. 428-444.

Leslie, A. G. W., Moody, P. C. E. & Shaw, W. V., *Structure of chloramphenicol acetyltransferase at 1.75-A resolution. Proc. Natl. Acad. Sci* USA, 1988. **85**: p. 4133-4137.

LiWang, A. C. & Bax, A., *Equilibrium protium/deuterium fractionation of backbone amides in U-$^{13}C/^{15}N$ labeled human ubiquitin by triple resonance NMR.* J. Am. Chem. Soc., 1996. **118**: p. 12864-12865.

Mahler, H. R., Wakil, S. J. & Bock, R. M., *Studies on Fatty acid oxidation. Enzymatic activation of fatty acids. J. Biol. Chem.*, 1953. **204**: p. 453-468.

Mancini-Samuelson, G. J., Kieweg, V., Sabaj, K. M., Ghisla, S. & Stankovich, M. T., *Redox properties of Human Medium Chain Acyl-CoA Dehydrogenase, Modulation by Charged Active-Site Amino Acid Residues*. Biochem, 1998. **37**(41): p. 14605-14612.

Maniscalco, S .J., Tally, J. F. & Ficher, H. F., *The interpretation of multiple-step transient-state kinetic isotope effects*. Arch Biochem Biophys, 2004. **425**: p. 165-172.

Manstein, D. J., Pai, E. F., Schopfer, L. M. & Massey, V., *Absolute stereochemistry of flavins in enzyme-catalyzed reactions.* J. Biol. Chem., 1986. **261**: p. 16169-16173.

Massey, V., *A simple method for the determination of redox potentials*, in *Flavins and Flavoproteins*, B. Curti, Ronchi, S. & Zanetti, G., Editor. 1991, Walter de Gruyter: Berlin, Germany. p. 59-66.

Mast, N., Andersson, U., Nakayama, K., Bjorkhem, I. & Pikuleva, I. A., *Expression of human cytochrome P450 46A1 in Escherichia coli: effects of N- and C-terminal modifications.* Arch Biochem Biophys, 2004. **428**(1): p. 99-108.

Matern, D., *Tandem mass spectrometry in newborn screening. Endocrinologist*, 2002. **12**: p. 50-57.

Matsubara, V., Narisawa, K., Miyabayaschi, S., Tada, K., & Coates, P. M., *Molecular lesion in patients with medium-chain acyl-CoA dehydrogenase deficiency. Lancet*, 1990. **335**: p. 1589.

Matsubara, Y., Indo, Y., Naito, E., Ozasa, H., Glassberg, R., Vockley, J., Ikeda, Y., Kraus, J. & Tanaka, K., *Molecular cloning and nucleotide sequence of cDNAs encoding the precursors of rat long chain acyl-coenzyme A, short chain acyl-coenzyme A, and isovaleryl-coenzyme A dehydrogenases. Sequence homology of four enzymes of the acyl-CoA dehydrogenase family. J. Biol. Chem.*, 1989. **264**: p. 16321-16331.

Matsubara, Y., et al., *Identification of a common mutation in patients with medium chain acyl-coA dehydrogenase deficiency.* Biochem. Biophys. Res. Comm., 1990. **171**: p. 498-505.

Matthews, R. G., Massey, V. & Sweeley, C. C., *Identification of p-hydroxybenzaldehyde as the ligand in the green form of old yellow enzyme.* J Biol Chem, 1975. **250**(24): p. 9294-9298.

Melde, K., Jackson, S., Barlett, K., Sherratt, H. S. A. & Ghisla, S., *Metabolic consequences of methylenecyclopropylglycine poisoning in rats. Biochem. J.*, 1991. **274**: p. 395-400.

Millington, D. S., Terada, N., Chace, D. H., Chen, Y. T., Ding, J. H., Kodo, N., & Roe, C. R., *The role of tandem mass spectrometry in the diagnosis of fatty acid oxidation disorders. Prog Clin Biol Res*, 1992. **375**: p. 339-354.

Minnaert, K., *Measurement of the equilibrium constant of the reaction between cytochrome c and cytochrome a.* Biochim. Biophys. Acta, 1965. **110**: p. 42-56.

Mohsen, A. W. & Vockley, J., *Identification of the active site catalytic residue in human isovaleryl-CoA dehydrogenase.* Biochemistry, 1995. **34**(32): p. 10146-10152.

Molla, G., et al., *Role of arginine 285 in the active site of Rhodotorula gracilis D-amino acid oxidase. A site-directed mutagenesis study.* J Biol Chem, 2000. **275**(32): p. 24715-24721.

Muller, F., Mayhew, S. G., & Massey, V., *On the effect of temperature on the absorption spectra of free and protein-bound flavines . Biochemistry*, 1973. ***12***: p. 4654-4662.

Muller-Newen, G., Janssen, U., & Stoffel, W., *Enoyl-CoA hydratase and isomerase form a superfamily with a common active-site glutamate residue.* Eur. J. Biochem., 1995. 228(1): p. 68-73.

Murfin, W. W. , 1974, Washington University, St. Louis, MO.

Nandy, A., *Acyl-CoA-Dehydrogenasen. Substratspecificität, molekulare Evolution und Plötzlicher Kindstod*. 1996, Universität Konstanz. p. 29-31.

Nandy, A et al., *Medium/Long Chain Chimeric Human Acyl-CoA Dehydrogenase: Medium Chain Enzyme with the Active Center Base Arrangement of Long Chain Acyl-CoA Dehydrognase.* Biochemistry, 1996. **35**: p. 12402-12411.

Nakajima, Y., et al., *Three-Dimensional Structure of the Flavoenzyme Acyl-CoA Oxidase-II from Rat Liver, the Peroxisomal Counterpart of Mitochondrial Acyl-CoA Dehydrogenase.* J Biochem (Tokyo), 2002. **131**(3): p. 365-374.

Nandy, A. et al., *Medium/Long Chain Chimeric Human Acyl-CoA Dehydrogenase: Medium Chain Enzyme with the Active Center Base Arrangement of Long Chain Acyl-CoA Dehydrognase.* Biochemistry, 1996. **35**: p. 12402-12411.

Nattie, E. E., Li, A., Richerson, G. B., & Lappi, D. A., *Medullary serotonergic neurons and adjacent neurons that express neurokinin-1 receptors are both involved in chemoreception in vivo. J Physiol.*, 2004. **Jan 14**: p. 235-253.

Nguyen, T. et al., *Identification of isobutyryl-CoA dehydrogenase and its deficiency in humans. Mol Genet Metab*, 2002. **77**: p. 68.

Nieslanik, B. S., et al., *Stopped-flow kinetic analysis of the ligand-induced coil-helix transition in glutathione S-transferase A1-1: evidence for a persistent denatured state.* Biochemistry, 1999. **38**(21): p. 6971-6980.

Nishina, Y., Sato, K., Tamaoki, H., Tanaka, T., Setoyama, C., Miura, R. & Shiga, K., *Molecular mechanism of the drop in the pKa of a substrate analog bound to medium-chain acyl-CoA dehydrogenase: implications for substrate activation.* J Biochem (Tokyo), 2003. **134**: p. 835-842.

Nishina, Y., et al., *Structural Modulation of 2-Enoyl-CoA Bound to Reduced Acyl-CoA Dehydrogenases: A Resonance Raman Study of a Catalytic Intermediate*. J. Biochem., 1995. **117**: p. 800-808.

Nishina, Y., et al., *Resonance Raman study on complexes of medium-chain acyl-CoA dehydrogease.* J. Biochem., 1992. **111**: p. 699-706.

Parker, A. & Engel, P., C., *Preliminary evidence for the existence of specific functional assemblies between enzymes of the -oxidation pathway and the respiratory chain. Biochem. J.*, 2002. **345**: p. 429-435.

Parkash, O. & Bhatia, I. S., *Graphical determination of pK values of the active-site groups of enzymes. An analysis of the bell-shaped curves.* Biochem J, 1980. **185**(3): p. 609-610.

Peterson, K. M., Gopalan, K. V., & Srivastava, D. K., *Influence of alpha-CH-->NH substitution in C8-CoA on the kinetics of association and dissociation of ligands with medium chain acyl-CoA dehydrogenase. Biochemistry*, 2000. **39**: p. 12659-12670.

Pohl, B., Raichle, T. & Ghisla, S., *Studies on the reaction mechanism of general acyl-CoA dehydrogenase. Determination of selective isotope effects in the dehydrogenation of butyryl-CoA. Eur. J. Biochem*, 1986. **160**: p. 109-115.

Pollard-Knight, D., & Cornish-Bowden, *Solvent isotope effects on the glucokinase reaction.* Eur J Biochem., 1984. **141**: p. 157-163.

Pollegioni, L., Porrini, D., Moll, G. & Pilone, M. S., *Redox potentials and their pH dependence of D-amino-acid oxidase of Rhodotorula gracilis and Trigonopsis variabilis.* Eur J Biochem, 2000. **267**: p. 6624-6632.

Powell, P. J., Lau, S. M., Killian, D. & Thorpe, C., *Interaction of Acyl-CoA Substrates and Analogs with Pig Kidney Medium Chain Acyl-CoA Dehydrogenase. Biochemistry*, 1987. **26**: p. 3704-3710.

Powell, P. J. & Thorpe, C., *2-Octynoyl-CoA Is a Mechanism-Based Inhibitor of Pig Kidney Medium Chain Acyl-CoA Dehydrogenase: Isolation of the Target Peptide. Biochemistry*, 1988. **27**: p. 8022-8028.

Raymond, K., Bale, A. E., Barnes, C. A., & Rinaldo, P., *Sudden adult death and medium-chain acyl-CoA dehydrogenase deficiency. Genet. Med.*, 1999. **1**: p. 293-294.

Qin, L. & Srivastava, D. K., *Energetics of two-step binding of a chromophoric reaction product, trans-3-indoleacryloyl CoA, to medium-chain acyl-coenzyme-A dehydrogenase. Biochemistry*, 1998. ***37***: p. 3499-3508.

Reinsch, J. et al., *The Deuterium Isotope Effect upon the Reaction of Fatty Acyl-CoA Dehydrogenase and Butyryl-CoA*. J. Biol. Chem., 1980. **255**: p. 9093-9097.

Reinsch, J. W., Feinberg, B. A. & McFarland, J. T., *Intermediates during the Fatty Acyl CoA Dehydrogenase Catalyzed Reduction of Electron Transfer Flavoprotein (ETF) by Fatty Acyl CoA Esters*. Biochem. Biophys. Res. Comm., 1980. **94**: p. 1409-1416.

Remington, S., Wiegand, G. & Huber, R., *Crystallographic Refinement and Atomic Models of Two Different Forms of Citrate synthase at 2.7 and 1.7 Å. J. Mol. Biol.*, 1982. **158;** p. 111-152.

Richard, J. P., *The enhancement of enzymatic rate accelerations by Bronsted acid-base catalysis*. Biochemistry, 1998. **37**(13): p. 4305-4309.

Rinaldo, P., O'Shea, J. J., Coates, P. M., Hale D. E., Stanley, C. A., & Tanaka, K., *Medium-chain acyl-CoA dehydrogenase deficiency. Diagnosis by stable-isotope dilution measurement of urinary n-hexanoyl-glycine and 3-phenylpropionylglycine. N Engl J Med*, 1988. **319**: p. 1308-1313.

Roberts, D. L., Frerman, F. E. & Kim, J. J. P., *Three dimensional structure of human electron transfer flavoprotein to 2.1 A resolution. Proc Nat Acad Sci*, 1996. **93**: p. 14355-14360.

Rudik, I., Ghisla, S. & Thorpe, C., *Protonic equilibria in the reductive half-reaction of the medium-chain acyl-CoA dehydrogenase.* Biochemistry, 1998. **37**(23): p. 8437-8445.

Ruzicka, F. J. & Beinert, H., *A new iron–sulfur flavoprotein of the respiratory chain. A component of the fatty acid beta oxidation pathway. J. Biol. Chem.*, 1977. **252**: p. 8440–8445.

Saijo, T., Kim, J. J., Kuroda, Y. & Tanaka, K., *The roles of threonine-136 and glutamate-137 of human medium chain acyl-CoA dehydrogenase in FAD binding and peptide folding using site-directed mutagenesis: creation of an FAD-dependent mutant, T136D.* Arch Biochem Biophys, 1998. 358(1): p. 49-57.

Sambrook, J., Fritsch, E. F. & Maniatis, T., *Molecular Cloning: A Laboratory Manual*, ed. C.S. Harbor. Vol. 1. 1989, NY: Laboratory Press. 1.82-1.83.

Sander, S., Janzen, N., Janetzky, B., Scholl, S., Steuerwald, U., Schafer, J., & Sander, J., *Neonatal screening for medium chain acyl-CoA deficiency: high incidence in Lower Saxony (northern Germany). Eur. J. Pediatr.*, 2001. **160**: p. 318-319.

Sastry, S., Debenedetti, P. G., & Stillinger, F. H., *Signature of distinct dynamical regimes in the energy landscape of a glass-forming liquid. Nature (Letters to Nature)*, 1998. **393** : p. 554-557.

Satoh, A., Nakajima, Y., Miyahara, I., Hirotsu, K., Tanaka, T., Nishina, Y., Shiga, K., Tamaoki, H., Setoyama, C. & Miura, R., *Structure of the Transition State Analog of Medium-Chain Acyl-CoA Dehydrogenase. Crystallographic and Molecular Orbital Studies on the Charge-Transfer Complex of Medium-Chain Acyl-CoA Dehydrogenase with 3-Thiaoctanoyl-CoA.* J Biochem (Tokyo), 2003. **134**: p. 297-304.

Schan, S., Loh, S. & Herschlag, D., *The Energetics of Hydrogen Bonds in Model Systems: Implications for Enzymatic Catalysis. Science*, 1996. **272**: p. 97-101.

Shaw, L., & Engel, P. C., *CoA-persulphide: a possible in vivo inhibitor of mammalian short-chain acyl-CoA dehydrogenase.* Biochim Biophys Acta, 1987. 919(2): p. 171-174.

Schopfer, L. M., Massey, V., Ghisla, S. & Thorpe, C., *Oxidation-Reduction of General Acyl-CoA Dehydrogenase by the Butyryl-CoA/Crotonyl-CoA Couple. A New Investigation of the Rapid Reaction Kinetics. Biochemistry*, 1988. **27**: p. 6599-6611.

Schowen, R. L., *Hydrogen bonds, transition-state stabilization, and enzyme catalysis*, in *Isotope Effects in Chemistry and Biology*, A. Kohen, Limbach, H.-H., Editor. 2004: in press, Marcel Dekker: New York.

Schowen, K. B., Limbach, H.-H., Denisov, G. S., & Schowen, R. L., *Hydrogen bonds and proton transfer in general-catalytic transition-state stabilization in enzyme catalysis*. Biochim Biophys Acta, 2000. **1458**: p. 43-62.

Schowen, K. B. & Schowen, R. L., *Solvent Isotope Effects on Enzyme Systems*, in *Methods in Enzymology*. 1982, Academic Press. p. 551-606.

Setoyama, C., Nishina, Y., Tamaoki, H., Mizutani, H., Miyahara, I., Hirotsu, K., Shiga, K., Miura, R., *Effects of hydrogen bonds in association with flavin and substrate in flavoenzyme D-amino acid oxidase. The catalytic and structural roles of Gly313 and Thr317.* J Biochem (Tokyo), 2002. 131(1): p. 59-69.

Smith, P. K., et al., *Measurement of protein using bicinchoninic acid.* Anal Biochem, 1985. **150**(1): p. 76-85.

Staack, H., Binstock, J. F. & Schulz, H., *Purification and properties of a pig heart thiolase with broad chain length specificity and comparison of thiolases from pig heart and Escherichia coli. J. Biol. Chem*., 1978. **253**: p. 1827-1831.

Stern, J. R., *Optical properties of aceto-acetyl-S-coenzyme A and its metal chelates.* J Biol Chem, 1956. **221**(1): p. 33-44.

Steyn-Parve, E. P. & Beinert, H., *On the mechanism of dehydrogenation of fatty acyl derivatives of coenzyme A. VII. The nature of the green color of butyryl dehydrogenase.* J Biol Chem, 1958. **233**(4): p. 853-861.

Strickland, S., Palmer, G. & Massey, V., *Determination of Dissociation Constants and Specific Rate Constants of Enzyme-Substrate (or Protein-Ligand) Interactions from Rapid Reaction Kinetic Data.* J. Biol. Chem., 1975. **250**: p. 4048-4052.

Sullivan, M. X., Cohen, B. & Clark, W. M., U.S. Pub. Health. Rep., 1923. **38**: p. 1669.

Tanaka, K. et al., *A survey of the newborn populations in Belgium, Germany, Poland, Czech Republic, Hungary, Bulgaria, Spain, Turkey, and Japan for the G985 variant allele with haplotype analysis at the medium chain Acyl-CoA dehydrogenase gene locus: clinical and evolutionary consideration. Pediatr. Res*., 1997. **41**: p. 201-209.

Tanaka, K. & Indo, Y., *Evolution of the acyl-CoA dehydrogenase/oxidase superfamily.* Prog Clin Biol Res, 1992. **375**: p. 95-110.

Tanaka, K., et al., *Mutations in the medium chain acyl-CoA dehydrogenase (MCAD) gene.* Hum Mutat, 1992. **1**(4): p. 271-279.

Theorell, H., *Reindarstellung der Wirkungsgruppe des gelben Ferments. Biochem. Z.*, 1935. **275**: p. 344-346.

Thorpe, C., *Electron transferring flavoproteins*, in *Chemistry and Biochemistry of Flavoenzyme*, F. Müller, Editor. 1990, RCR Press: Boca Raton. p. 472-479.

Thorpe, C., & Kim, J.-J., P., *Structure and Mechanism of Action of the Acyl-CoA Dehydrogenases. FASEB J*., 1988. **9**: p. 718-725.

Thorpe, C. & Massey, V., *Flavin Analogue Studies of Pig Kidney General Acyl-CoA Dehydrogenase.* Biochemistry, 1983. **22**: p. 2972-2978.

Thorpe, C., Matthews, R. G.& Williams, C.H.Jr. *Acyl-Coenzyme A Dehydrogenase from Pig Kidney. Purification and Properties.* Biochemistry, 1979. **18**: p. 331-337.

Tiffany, K. A., Roberts, D. L., Wang, M., Paschke, R., Mohsen, A. W., Vockley, A. W. & Kim, J. J., *Structure of human isovaleryl-CoA dehydrogenase at 2.6 A resolution: structural basis for substrate specificity.* Biochemistry, 1997. **36**: p. 8455-8464.

Toogood, H. S., van Thiel, A., Basran, J., Sutcliffe, M. J., Scrutton, N. S. & Leys, D, *Extensive Domain Motion and Electron Transfer in the Human Electron Transferring Flavoprotein-Medium Chain Acyl-CoA Dehydrogenase Complex.* The Journal of Biological Chemistry, 2004. **279**(30): p. 32904-32912.

Towbin, H., Staehelin, T. & Gordon, J., *Electrophoretic transfer of proteins from polyacrylamide gels to nitrocellulose sheets: procedure and some applications.* Proc Natl Acad Sci U S A, 1979. **76**(9): p. 4350-4354.

Trievel, R. C., Wang, R., Anderson, V. E., & Thorpe, C. (1995). "The Role of the Carbonyl Group in Thioester Chain Length Recognition by Medium Chain Acyl-CoA Dehydrogenase." *Biochemistry* **34**: 8597-8605.

Uchida, Y., Izai, K., Orii, T. & Hashimoto, *T., Novel fatty acid beta-oxidation enzymes in rat liver mitochondria. II. Purification and properties of enoyl-coenzyme A (CoA) hydratase/3-hydroxyacyl-CoA dehydrogenase/3-ketoacyl-CoA thiolase trifunctional protein*. J. *Biol. Chem*., 1992. **267**: p. 1034-1041.

Veglia, G., et al., *Deuterium/hydrogen exchange factors measured by solution nuclear magnetic resonance spectroscopy as indicators of the structure and topology of membrane proteins.* Biophys J, 2002. **82**(4): p. 2176-2183.

Venkatasubban, K. S. & Schowen, R. L., *The proton inventory technique. CRC Crit Rev Biochem*, 1984. ***17***: p. 1-44.

Vock, P., Engst, S., Eder, M., & Ghisla, S., *Substrate Activation by Acyl-CoA Dehydrogenases: Transition-State Stabilization and pKs of Involved Functional Groups. Biochemistry*, 1998. **37**: p. 1848-1860.

Wang, R. & Thorpe, C., *Reactivity of Medium-chain Acyl-CoA Dehydrogenase toward Molecular Oxygen.* Biochemistry, 1991. **30**: p. 7895-7901.

Wang, S. S., Bross, P., Fernhoff, P. M., Hannon, W. H., & Khoury, M. J., *Medium Chain acyl-coA dehydrogenase deficiency (MCADD). Genet. Med.*, 1999. **1**(**7**): p. 332-339.

Wenz, A., Ghisla, S. & Thorpe, C., *Studies with general acyl-CoA dehydrogenase from pig kidney.* Eur. J. Biochem., 1985. **147**: p. 553-560.

Whitby, L. G., *A new method for preparing flavin-adenine dinucleotide.* Biochem. J., 1953. **54**: p. 437-442.

Wilson, G. S., *Determination of Oxidation-Reduction Potentials*, in *Meth. Enzym.* 1978, Academic Press, Inc. p. 396-410.

Williamson, G., Engel, P., Mizzer, J. P.,Thorpe, C. & Massey, V., *Evidence That the Greening Ligand in Native Butyryl-CoA Dehydrogenase Is a CoA Persulfide.* J. Biol. Chem., 1982. **257**: p. 4314-4320.

Yee, L. & Blanch, H. W., *Recombinant protein expression in high cell density fed-batch cultures of Escherichia coli.* Biotechnology (N Y), 1992. **10**(12): p. 1550-1556.

Yokota, I., et al., *Molecular basis of medium chain acyl-coenzyme A dehydrogenase deficiency. An A to G transition at position 985 that causes a lysine-304 to glutamate substitution in the mature protein is the single prevalent mutation.* J. Clin. Invest., 1990. **86**: p. 1000-1003.

Zeng, J. & Li, D., *Expression and purification of His-tagged rat mitochondrial medium-chain acyl-CoA dehydrogenase wild-type and Arg256 mutant proteins.* Protein Expr Purif, 2004. **37**(2): p. 472-478.

Zhang, J. et al., *Cloning and functional characterization of ACAD-9, a novel member of human acyl-CoA dehydrogenase family. Biochem Biophys Res Commun*, 2002. **297**: p. 1033-1042.

Ziadeh, R., Hoffman, E. P., Finegold, D. N., Hoop, R. C., Brackett, J. C., Strauss, A. W., & Naylor, E. W., *Medium chain acyl-CoA dehydrogenase deficiency in Pennsylvania: neonatal screening shows high incidence and unexpected mutation frequencies. Pediatr. Res.*, 1995. **37**: p. 675-678.

Zytkovicz, T. H. et. al., *Tandem mass spectrometric analysis for amino, organic, and fatty acid disorders in newborn dried blood spots: a two-year summary from the New England Newborn Screening Program. Biochemistry*, 2001. **18**: p. 331-337.